HYPORHEIC EXCHANGE AND BIOGEOCHEMICAL PROCESSING IN ARCTIC TUNDRA STREAMS

A Thesis Presented

by

Morgan Johnston Greenwald

to

The Faculty of the Graduate College

of

The University of Vermont

In Partial Fulfillment of the Requirements
for the Degree of Master of Science
Specializing in Natural Resources

May, 2007

Accepted by the Faculty of the Graduate College, The University of Vermont, in partial fulfillment of the requirements for the degree of Master of Science specializing in Natural Resources.

Thesis Examination Committee:

_____Advisor
William Breck Bowden, Ph.D.

_____
Suzanne Levine, Ph.D.

_____Chairperson
Andrea Lini, Ph.D.

_____Vice President for
Frances E. Carr, Ph.D. Research and Dean
of Graduate Studies

Date: March 2, 2007

ABSTRACT

The North Slope of Alaska's Brooks Range is underlain by continuous permafrost, but an active layer of thawed sediments develops at the surface of the tundra and beneath streambeds during the summer. The thawed sediments facilitate hyporheic exchange. The hyporheic zone is an important site for organic matter decomposition and nutrient regeneration to the surface water. Information on the characteristics of hyporheic processes, both physical and biogeochemical, is limited in arctic stream systems.

The goal of the first study was to understand how hyporheic exchange patterns and biogeochemical processes are influenced by stream geomorphology and the extent of the thaw bulb. Two second-order arctic tundra streams of contrasting geomorphology were studied. The first was a high-gradient, cobble-bottomed alluvial stream characterized by distinct riffle-pool sequences (average thaw depth: 157 cm). The second was a low-gradient, peat-bottomed, beaded stream characterized by large deep pools connected by deep runs (average thaw depth: 67 cm). The degree of surface-subsurface exchange decreased with depth in the subsurface in both streams, but was substantial at depths >50 cm in the alluvial stream, whereas all surface-subsurface exchange in the peat stream occurred within the top ~10 cm of the streambed sediments. While the surface waters of the two streams were not significantly different from one another in terms of biogeochemistry, their subsurface waters were significantly different from one another in every biogeochemical constituent measured. In the alluvial stream, subsurface concentrations of nitrate, ammonium, soluble reactive phosphorus (SRP) and DOC were not significantly different from the surface water at any depth. Dissolved oxygen (DO) concentration decreased significantly with depth, yet remained sufficiently oxic at the deepest depth sampled. In the peat stream, however, DO and nitrate concentrations decreased significantly with depth to a point where they were not detectable at ~30 cm, while ammonium, SRP and DOC concentrations increased exponentially with depth in the subsurface. The physical differences in the geomorphology of the streams led to differences in their hyporheic exchange characteristics, which then influenced the biogeochemistry of the subsurface water. In turn, the stream ecosystems were influenced differently by nutrient regeneration from their hyporheic zones. The hyporheic zone served as a source of ammonium and SRP to the surface water in both streams. The hyporheic zone served as a net nitrate sink in the peat stream and as a net nitrate source in the alluvial stream.

In the second study, physical water movement and subsurface biogeochemistry were examined in a network of well-defined subsurface flow paths through a natural gravel bar. The most utilized subsurface flow paths were approximately 1 m beneath the surface of the gravel bar. These flow paths exhibited high dissolved oxygen concentrations due to their high degree of connection to the surface water and also had lower ammonium and SRP concentrations than less-connected regions, where inorganic nutrient concentrations tend to build up. The gravel bar served as a net source of ammonium (18.01 $\mu M\ m^{-1}\ d^{-1}$) and SRP (0.37 $\mu M\ m^{-1}\ d^{-1}$) to the surface water and as a net nitrate sink (-0.99 $\mu M\ m^{-1}\ d^{-1}$).

ACKNOWLEDGEMENTS

I would like to thank my advisor, Breck Bowden, for his continued guidance, knowledge, insight and support throughout this project. I would also like to thank the other members of the Arctic Hyporheic Team, including Mike Gooseff, Jay Zarnetske, Jim McNamara, John Bradford and Troy Brosten for their collaboration and support with this research. Julia Larouche, Ken Turner and Joel Homan provided valuable field assistance. Adrian Green, Alan Howard, Donna Rizzo and Lael Rogan provided helpful advice with laboratory analysis, statistical analyses and geospatial data. Helpful comments were provided by members of my thesis committee, Suzanne Levine and Andrea Lini. Finally, I would also like to thank my family members for their unending love and support, especially my husband, Andrew, who has witnessed the good and the bad and continued to offer his encouragement and praise.

TABLE OF CONTENTS

Page

ACKNOWLEDGEMENTS..... ii

LIST OF FIGURES..... vii

LIST OF TABLES..... x

CHAPTER 1: COMPREHENSIVE LITERATURE REVIEW.....1

1.1. Introduction.....2

1.2. Hyporheic Exchange Hydrology.....3

1.3. Influence of Geomorphology on Hyporheic Exchange.....4

1.4. Methods for Quantifying Transient Storage.....7

1.5. Hyporheic Biogeochemistry.....13

1.5.1. Dissolved Oxygen and Dissolved Organic Carbon Dynamics..... 13

1.5.2. Importance of Nutrient Regeneration in the Hyporheic Zone.....17

1.5.3. Nitrogen Dynamics..... 18

1.5.4. Phosphorus Dynamics..... 23

1.6. Arctic Tundra Streams..... 24

1.6.1. Description of the North Slope of the Brooks Range, Alaska.....24

1.6.2. Hyporheic Zones in Arctic Tundra Streams..... 27

1.6.3. Potential Reponses of Arctic Tundra Streams to Climate Change…….. 28

1.6.4. Research Goals……...31

LITERATURE CITED……... 32

CHAPTER 2: HYPORHEIC BIOGEOCHEMICAL PROCESSES IN ARCTIC TUNDRA STREAMS: A COMPARISON OF TWO STREAMS OF DIFFERING GEOMORPHOLOGY..... 42

2.1. Introduction……..... 43

2.2. Methods……..……..... 47

2.2.1. Study Area……..47

2.2.2. Hyporheic Sampling…….. 48

2.2.3. Extent of Hyporheic Exchange……. 50

2.2.4. Biogeochemical Sampling and Analysis……...51

2.2.5. Calculation of Nutrient Regeneration Rates……... 53

2.2.6. Statistical Analysis……. 54

2.3. Results……...……...……..... 55

2.3.1. Extent of Hyporheic Exchange……. 55

2.3.2. Biogeochemical Comparisons between the Two Streams.. 56

2.3.2.1. Dissolved Oxygen…… 57

2.3.2.2. Nitrate…….…… 58

2.3.2.3 Ammonium……. 58

2.3.2.4 Soluble Reactive Phosphorus……59

2.3.2.5. Dissolved Organic Carbon…… 60

2.3.3. Estimates of Nutrient Regeneration Rates…… 60

2.4. Discussion..... 61

2.4.1. Extent of Hyporheic Exchange……61

2.4.2. Biogeochemical Comparisons between the Two Streams 64

2.4.3. Estimates of Nutrient Regeneration……66

2.5. Conclusions……69

2.6. Implications……... 71

LITERATURE CITED……... 73

CHAPTER 3: HYPORHEIC FLOW AND BIOGEOCHEMICAL PROCESSING IN AN ARCTIC RIVER GRAVEL BAR……... 94

3.1. Introduction……...95

3.2. Methods……..98

3.2.1. Study Site…… 98

3.2.2. Solute Injection Experiments……99

3.2.3 Subsurface Water Sampling Technique……... 100

3.2.4. Geostatistical Methods……...101

3.2.5. Biogeochemical Sampling and Analysis…… 103

3.3. Results…… 106

3.3.1. Tracer Concentration Estimates…….. 106

3.3.2. Biogeochemical Concentration Estimates……107

3.4. Discussion…….. 108

3.4.1. Tracer Concentration Estimates…….. 108

3.4.2. Biogeochemical Concentration Estimates……..... 110

3.4.3 Conclusions……..……...…… 112

LITERATURE CITED…….. 114

COMPREHENSIVE LITERATURE CITED…… 132

LIST OF FIGURES

Page

Figure 1.1. A cross-sectional diagram of a typical temperate stream, showing hyporheic exchange and potential groundwater interaction…… 38

Figure 1.2. Common vertical, lateral and longitudinal patterns of hyporheic exchange; shaded area is hyporheic zone (taken from *Findlay* [1995])…….. 39

Figure 1.3. A model simulation of a solute breakthrough curve highlighting the regions of sensitivity attributed to each of the model parameters (taken from *Harvey and Wagner* [2000])…… 40

Figure 1.4. The observed solute pulse data of a solute addition experiment in a second-order stream in Oregon simulated by (A) exponential RTD model and (B) general (power-law) RTD model (taken from *Gooseff et al.* [2003])……... 41

Figure 2.1. A cross-sectional diagram of a typical temperate stream, showing hyporheic exchange and potential groundwater interaction…… 83

Figure 2.2. Arctic tundra stream cross section showing the active layer and thawbulb within the continuous permafrost. The hyporheic zone exists within the thawbulb…… 84

Figure 2.3. (A) Location of the Toolik Field Station on the North Slope of the Brooks Range in Alaska (credit: A. Balser) and (B) an illustration of the Inlet Series to Toolik Lake taken from *Kling et al.* [2000]. The alluvial stream location is indicated by the number 14 on this illustration and the peat stream location is indicated by the number 16…… 85

Figure 2.4. Median P_C values at (A) distinct subsurface depths, (B) stream features and (C) two time periods in the alluvial and peat stream types (error bars indicate first and third quartile values)…… 86

Figure 2.5. Median dissolved oxygen concentration at (A) distinct subsurface depths, (B) stream features and (C) two time periods in the alluvial and peat stream types (error bars indicate first and third quartile values)……. 87

Figure 2.6. Subsurface dissolved oxygen concentration vs. degree of surface-subsurface connection in the alluvial and peat streams. The Spearman's correlation coefficient between the two variables is 0.74 ($p < 0.001$) for the alluvial stream and 0.78 ($p < 0.001$) for the peat stream……. 88

Figure 2.7. Median nitrate concentration at (A) distinct subsurface depths, (B) stream features and (C) two time periods in the alluvial and peat stream types (error bars indicate first and third quartile values)…….. 89

Figure 2.8. Median ammonium concentration at (A) distinct subsurface depths, (B) stream features and (C) two time periods in the alluvial stream and at (D) distinct subsurface depths, (E) stream features and (F) two time periods in the peat stream (error bars indicate first and third quartile values)……... 90

Figure 2.9. Median soluble reactive phosphorus concentration at (A) distinct subsurface depths, (B) stream features and (C) two time periods in the alluvial and peat stream types (error bars indicate first and third quartile values)……... 91

Figure 2.10. Median dissolved organic carbon concentration at (A) distinct subsurface depths, (B) stream features and (C) two time periods in the alluvial and peat stream types (error bars indicate first and third quartile values)……... 92

Figure 2.11. Estimated net regeneration rates for (A) nitrate, (B) ammonium and (C) soluble reactive phosphorus in the alluvial and peat stream types; a negative value indicates that the subsurface served as a sink for a given nutrient, while a positive value indicates that the subsurface served as a source for a given nutrient……. 93

Figure 3.1. Location of the Toolik Field Station on the North Slope of Alaska's Brooks Range. Credit: A. Balser (2004)…… 120

Figure 3.2. A representation of the gravel bar (shown in dark grey) with all subsurface sampling locations marked to scale (as solid black dots). Arrow indicates general direction of subsurface flow through the bar. Note that channels A (peat) and B (alluvial) used to come together to form channel C, but channel A has been truncated by the deposit of the gravel so that all of its flow became subsurface when it reached the gravel bar……. 121

Figure 3.3. Example of a tracer breakthrough curve from the gravel bar SIE. Tracer dripper was started at 0 h and stopped at 4 h. Dotted lines indicate the four time periods for which variograms were constructed and [RWT] estimates were made…… 122

Figure 3.4. Variograms developed for the four SIE time points chosen (A-D). Solid dots represent the mean semivariance for mean lag distances. Open dots represent the model chosen to fit the data. Solid lines represent $\pm$ 1 standard deviation around the plotted means……. 123

Figure 3.5. Estimated RWT concentrations over the gravel bar throughout the SIE. Plots from top to bottom show the concentrations in the shallow, medium and deep layers of the subsurface. Plots from left to right show the movement of RWT through the gravel bar at each of the four time points during the SIE. Black points represent sampling locations…….. 124

Figure 3.6. Variograms developed for each of the biogeochemical parameters (A-E). Solid dots represent mean lag distances and semivariances for binned data. Lines represent $\pm$ 1 standard deviation around the plotted means. Open circles represent the linear model chosen to fit the data…….. 125

Figure 3.7. Estimated dissolved oxygen (DO) concentrations for the (A) shallow, (B) medium and (C) deep layers of the gravel bar subsurface. Black dots represent actual sampling locations for each layer…….. 126

Figure 3.8. Estimated nitrate concentrations for the (A) shallow, (B) medium and (C) deep layers of the gravel bar subsurface. Black dots represent actual sampling locations for each layer…… 127

Figure 3.9. Estimated ammonium concentrations for the (A) shallow, (B) medium and (C) deep layers of the gravel bar subsurface. Black dots represent actual sampling locations for each layer……. 128

Figure 3.10. Estimated soluble reactive phosphorus concentrations for the (A) shallow, (B) medium and (C) deep layers of the gravel bar subsurface. Black dots represent actual sampling locations for each layer…….. 129

Figure 3.11. Estimated dissolved organic carbon (DOC) concentrations for the (A) shallow, (B) medium and (C) deep layers of the gravel bar subsurface. Black dots represent actual sampling locations for each layer…… 130

Figure 3.12. Linear regressions for (A) dissolved oxygen, (B) nitrate, (C) ammonium, (D) soluble reactive phosphorus and (E) dissolved organic carbon against RWT concentration at SIE Plateau (2.63-hour mark)……. 131

LIST OF TABLES

Page

Table 2.1. Location of each of the minipiezometers installed in the alluvial subsurface. The letter indicates the location of the nest along the thalweg of the stream and the number indicates its depth layer beneath the streambed……. 77

Table 2.2. Location of each of the minipiezometers installed in the peat subsurface. The letter indicates the location of the nest along the thalweg of the stream and the number indicates its depth layer beneath the streambed……. 78

Table 2.3. Median concentrations of DO, NO_3, NH_4, SRP and DOC in the surface and subsurface water of the alluvial and peat streams (* indicates statistically significant difference between stream types)…… 79

Table 2.4. The set of p-values resulting from Mann-Whitney comparisons of P_C, DO, NO_3, NH_4, SRP and DOC among subsurface depths, stream features and time in the alluvial stream (* indicates a statistically significant difference for a given comparison; $\alpha' = 0.017$ for depth and feature and $\alpha' = 0.05$ for time)…….. 80

Table 2.5. The set of p-values resulting from Mann-Whitney comparisons of P_C, DO, NO_3, NH_4, SRP and DOC among subsurface depths, stream features and time in the peat stream (* indicates a statistically significant difference for a given comparison; $\alpha' = 0.025$ for depth; $\alpha' = 0.017$ for feature; $\alpha' = 0.05$ for time)……. 81

Table 2.6. Estimated net nutrient regeneration rates for the Kuparuk River, AK [*Edwardson et al.*, 2003] and the alluvial and peat streams in the current study… 82

Table 3.1. Location of each of the mini-piezometers installed in the gravel bar. The letter in the mini-piezometer identification indicates its position on the bar and the number indicates its subsurface depth layer…… 116

Table 3.2. Variogram model parameters (nugget, sill and range) for each of the linear models created for the RWT concentrations at four separate time periods and the biogeochemical concentrations……... 117

Table 3.3. Linear regression results for dissolved oxygen, nitrate, ammonium, soluble reactive phosphorus and dissolved organic carbon against RWT concentration at SIE Plateau (2.63-hour mark). R-squared values, linear equations and p-values are given for each parameter…….. 118

Table 3.4. Estimated net NO_3, NH_4 and SRP regeneration rates for the gravel bar…… 119

CHAPTER 1: COMPREHENSIVE LITERATURE REVIEW

ABSTRACT

The hyporheic zone is a region of subsurface transient storage in streams. As water moves through the hyporheic zone, its transport downstream is delayed and it is in close contact with sediment biofilms for a relatively long period of time. Significant organic matter decomposition occurs in the hyporheic zone and inorganic nutrients are regenerated to the surface water. Organic matter and nutrient dynamics are dependent on the physical exchange of water between the surface and subsurface. Physical exchange patterns are highly influenced by stream geomorphic characteristics. For example, some geomorphic factors that influence surface-subsurface exchange include stream slope, degree of streambed complexity, degree of channel constraint and sediment particle size. While much is known about hyporheic processes in temperate streams, information is limited in arctic tundra streams. The hyporheic zone is an important component of these stream systems, but the pattern and extent of hyporheic exchange in streams of differing geomorphology are not known. These streams are underlain by permafrost and are dependent on annual freeze-thaw cycles. Therefore, they are very susceptible to climate change and it is important to understand the current role of the hyporheic zone in arctic tundra streams so that we may predict how that role might change with global climate change.

1.1 Introduction

Hyporheic exchange occurs when stream water flows into near-stream sediments, carrying with it dissolved organic carbon, dissolved oxygen and other solids [*Valett et al.*, 1990; *Jones and Holmes*, 1996]. The water moves into and through the saturated subsurface sediments in response to pressure gradients and typically reenters the stream channel after moving relatively slowly through the interstitial spaces between subsurface sediment particles [*De Wiest*, 1969; *Harvey and Bencala*, 1993] (Figure 1.1). This region of exchange beneath the stream is known as the hyporheic zone. It includes sediments beneath the stream, but can also extend laterally into the parafluvial and riparian zones [*Dent et al.*, 2000]. In many cases, groundwater and stream water actively mix in the hyporheic zone, which serves as an ecotone between stream water and groundwater systems [*Boulton et al.*, 1998]. Water flowing through the hyporheic zone serves as one form of transient storage. Transient storage is any mechanism by which a portion of the water moving downstream is temporarily retained in regions of stagnant or slowly moving water [*Packman and Bencala*, 2000]. Transient storage can include surface water flow (i.e., backwaters and eddies) and subsurface water flow (i.e., through the hyporheic zone).

The surfaces of sediments in the hyporheic zone are often covered with a biofilm layer, which contains a diverse population of microorganisms suspended in a polysaccharide matrix [*Findlay and Sobczak*, 2000; *Cushing and Allan*, 2001; *Battin et al.*, 2003]. Since the hyporheic zone offers the water passing through it a relatively long residence time in an environment with a high sediment surface area to water volume

ratio, hyporheic exchange promotes many important microbially-mediated biogeochemical transformations that are vital to the stream ecosystem [*Harvey and Wagner*, 2000]. The hyporheic zone can serve as either a source or sink of limiting nutrients in the stream ecosystem. The importance of the hyporheic zone to stream ecosystems depends on the proportion of stream flow interacting with it and the types and magnitude of metabolic activity occurring there [*Findlay*, 1995].

The overall purpose of this chapter is to introduce the hyporheic zone and its contributions to arctic tundra stream ecosystem functioning. Information currently known about hyporheic zone characteristics and processes will be presented, including the physical factors that control hyporheic exchange and current methods used to describe the transient storage aspects of individual streams. The important biogeochemical reactions that take place in the hyporheic zone will also be reviewed. Lastly, arctic tundra streams and the role of hyporheic processes in these unique systems will be described.

1.2 Hyporheic Exchange Hydrology

To understand the ecological connections that the hyporheic zone provides, it is essential to understand the hydrology of the water flowing into and out of the hyporheic zone. Hyporheic flow occurs in three dimensions: vertically, laterally and longitudinally [*Jones and Holmes*, 1996]. An example of lateral flow occurs in meandering streams, where hyporheic water may flow laterally underneath channel bars, taking a more direct path than the surface water does from one meander crest to the next. The vertical

component of hyporheic flow determines whether water is moving from the stream to the hyporheic zone (downwelling) or from the hyporheic zone to the stream (upwelling). The direction of flow can be determined by measuring the vertical hydraulic gradient (VHG) at a given point in the hyporheic zone. The VHG is calculated as the difference between the water level inside a piezometer (hyporheic sampling device) and the water level outside the piezometer (ΔH) divided by the depth of the piezometer beneath the streambed surface (ΔL). A negative VHG indicates downwelling and a positive VHG indicates upwelling. The heads of riffles tend to be downwelling zones, while the tails of riffles tend to be locations of upwelling [*Harvey and Bencala*, 1993; *Valett et al.*, 1994; *Jones et al.*, 1995b]. This characteristic of water exchanging between the surface and subsurface with a net downstream travel is considered longitudinal flow. Examples of hyporheic exchange patterns are shown in Figure 1.2 (taken from *Findlay* [1995]).

1.3 Influence of Geomorphology on Hyporheic Exchange

Hyporheic exchange is controlled by the geomorphology of streams. Many factors act to control hyporheic exchange rates and residence times, but the primary driver is abrupt changes in channel gradient, which create head gradients that drive surface-subsurface exchange of water [*Harvey and Bencala*, 1993]. Streams with more complex bed topography offer more elevation differences and, thus, more opportunity for exchange. Other geomorphic factors affecting hyporheic exchange include the degree of channel constraint and the presence of secondary channels or channel splits [*Kasahara and Wondzell*, 2003], stream size and discharge [*D'Angelo et al.*, 1993] and channel

sinuosity [*Wroblicky et al.*, 1998; *Kasahara and Wondzell*, 2003]. Factors other than geomorphology may also affect hyporheic exchange, including the parent material of the stream catchment, sediment size and hydraulic conductivity [*Morrice et al.*, 1997; *Storey et al.*, 2003], stream channel friction and channel vegetative cover [*Harvey et al.*, 2003] and seasonal changes in stream discharge, head gradients and local groundwater recharge [*Wroblicky et al.*, 1998; *Storey et al.*, 2003]. *Battin et al.* [2003] suggested that the presence of microbial biofilms on the streambed surface can also increase the transient storage capacity of a stream reach.

Morrice et al. [1997] studied the influence that the parent material of the alluvium and sediment size have on hydrological retention, which quantifies storage zone residence time of water per unit of stream reach traveled. Hydrological retention was compared in three alluvial streams in New Mexico with very different lithologies and sediment sizes. Hydrologic exchange rate, hyporheic extent and hydrological retention increased as particle size and hydraulic conductivity of the stream sediment increased.

Morrice et al. [1997] also found that hydrological retention decreased with a seasonal increase in discharge. The site with the highest hydraulic conductivity also exhibited the greatest degree of connectivity between the stream and alluvial aquifer and had the fastest travel times of water through the sediments [*Valett et al.*, 1996]. Through a study employing two-dimensional groundwater modeling and particle tracking methods, *Wroblicky et al.* [1998] determined that the area of the lateral hyporheic zone in a volcanic tuff stream was approximately twice that in a sandstone-siltstone stream. In both streams, lateral hyporheic area decreased by about 50% during high flows.

Kasahara and Wondzell [2003] examined the relative effects of various stream and valley-floor geomorphologic features on hyporheic exchange in mountain stream systems in Oregon, including stream size, degree of channel constraint, step-pool or riffle-pool sequences, channel sinuosity, and presence of secondary channels or channel splits. They found that hyporheic exchange in small headwater streams was dominated by lateral hyporheic flow paths extending around step-pool sequences formed by large boulders or woody debris in the channel. These hyporheic exchanges were induced by channel gradient and generally had rapid hyporheic exchange rates and relatively short hyporheic residence times. In these small streams, abrupt changes in channel elevation at step-pool transitions produced the principal hyporheic exchange flows, regardless of the degree of channel constraint. *D'Angelo et al.* [1993] also found that the ratio of transient storage cross-sectional area to stream cross-sectional area (A_S/A) was highest in small, headwater streams and decreased with increasing stream size and discharge.

Kasahara and Wondzell [2003] found that in larger streams, the degree of channel constraint played a more important role in determining hyporheic exchange and flow patterns. In higher-order, unconstrained stream reaches, lateral exchange flows between main and secondary channels dominated the hyporheic exchange flows and produced much longer hyporheic flow paths and residence times. However, unlike the unconstrained fifth-order stream, the higher-order, constrained stream had a relatively narrow valley and was unable to develop complex channel patterns with multiple channels, high sinuosity and channel bars and islands. As a result, little hyporheic exchange occurred in the constrained stream.

1.4 Methods for Quantifying Transient Storage

Quantifying and describing hyporheic storage and exchange has traditionally been done using a combination of stream solute additions and mathematical modeling. Monitoring the concentration of a solute in a stream over time can provide information regarding the physical characteristics of a stream reach. In this type of stream solute addition, a detectable, biologically conservative tracer is added to the stream at the top of a reach at a known rate and concentration. The tracer can be a component of a salt such as chloride, sodium or magnesium, or an organic dye such as Rhodamine WT (RWT). The concentration of the tracer in the stream water is monitored over time at some known distance downstream. The resulting concentration data are plotted and models are used to simulate the transport of the solute through the stream reach over time [*Stream Solute Workshop*, 1990].

Models, such as the popular OTIS model described in the following paragraphs, estimate the concentration of solute in the water over time based on several parameters, which are introduced below. Each of the model parameters are iteratively estimated until the model simulation curve matches the observed data curve. Each parameter in the model is responsible for a certain characteristic of the curve's shape, so the successful resulting parameter values can explain a number of physical characteristics of the stream reach [*Harvey and Wagner*, 2000]. Solute additions can also be used to study biological characteristics of a stream reach such as nutrient uptake and retention rates by adding a biologically reactive tracer along with the conservative tracer and by including a model parameter corresponding to first-order decay [*Stream Solute Workshop*, 1990].

Bencala and Walters [1983] presented a transient storage model to simulate solute transport in small mountain streams. Their model describes the change in solute concentration over time using four main terms: advection, dispersion, lateral inflow and transient storage. Advection describes the downstream transport of the solute within the channel at a mean velocity and dispersion describes the spreading and diffusion of the solute due to shear stress [*Runkel*, 2000]. These two terms describe only the movement of solutes downstream within the main channel. Due to the irregular shape of stream channels and other local environmental influences, however, two additional terms are included to make the description more realistic. The lateral inflow term takes into account the dilution effect that lateral inputs of surface and subsurface water have on solute transport. Lastly, and most importantly to the study of hyporheic zone processes, is the transient storage term.

Transient storage zones can include the hyporheic zone, eddies created behind channel obstructions such as logs or boulders and regions of relatively slowly moving water at the edges or bottoms of pools [*Bencala and Walters*, 1983]. These transient storage zones exist as the result of a variety of physical stream features and, therefore, also exhibit a variety of water and solute residence times. As the solute moves through the stream reach, a portion of it fills the transient storage zones, is held up for a period of time and is released again, producing the characteristic shape of the solute response curve. The transient storage terms of the model, α and A_S, are important in describing the curvature of the shoulder of the rising limb of the solute response curve and the drawn out tail at the end of the solute response curve [*Stream Solute Workshop*, 1990].

A mathematical model based on the concepts put forth by *Bencala and Walters* [1983] has been widely used in conjunction with solute additions to learn more about the physical characteristics of solute transport in streams. This model is called the one-dimensional transport with inflow and storage (OTIS) model. One-dimensional refers to the assumption that solute concentration varies only in the longitudinal direction. OTIS uses solute mass balance equations to describe the solute concentrations in the two different conceptual compartments of the stream: (1) the channel and (2) the collective transient storage zone [*Runkel*, 1998]. The two equations initially put forth by *Bencala and Walters* [1983] have become the base of the OTIS model. The two mass balance equations used to describe the transport of a conservative tracer are listed below:

Advection *Dispersion* *Lateral Inflows* *Transient Storage*

$$\frac{\delta C}{\delta t} = -\frac{Q}{A}\frac{\delta C}{\delta x} + \frac{1}{A}\frac{\delta}{\delta x}\left(AD * \frac{\delta C}{\delta x}\right) + \frac{Q_{LIN}}{A}(C_L - C) + \alpha(C_S - C) \quad (1)$$

$$\frac{dC_S}{dt} = -\alpha \frac{A}{A_S}(C_S - C) \quad (2)$$

where,

- **A – main channel cross-sectional area [L^2]**
- **A_S – storage zone cross-sectional area [L^2]**
- **C – main channel solute concentration [M/V^{-1}]**
- **C_L – lateral inflow solute concentration [M/V^{-1}]**
- **C_S – storage zone solute concentration [M/V^{-1}]**
- **D – longitudinal dispersion coefficient [L^2T^{-1}]**
- **Q – stream discharge [L^3T^{-1}]**
- **Q_{LIN} – lateral inflow rate per unit length of stream [$L^3T^{-1}L^{-1}$]**
- **t – time [T]**
- **x – distance [L]**
- **α – storage zone exchange coefficient [T^{-1}]**

[*Stream Solute* Workshop, 1990; *Runkel*, 1998]

Equation (1) shows that the change in solute concentration over time in the stream channel is a function of advection, dispersion, lateral inflows and transient storage. Equation (2), which describes the solute concentrations in the transient storage zone, indicates that the processes of advection, dispersion and lateral inflows and outflows are negligible in the transient storage zone. Again, the terms in this equation most important to hyporheic study are the storage zone exchange coefficient, α, and the storage zone cross-sectional area, A_S. Information about the transient storage characteristics of a stream can be estimated using the resulting OTIS parameter values. Specific regions of the curve are influenced by specific parameter values (see Figure 1.3., taken from *Harvey and Wagner* [2000]). Other information that can be gleaned from the model and used to compare streams includes [*Harvey et al.*, 1996; *Morrice et al.*, 1997]:

$1/\alpha$ = hydraulic residence time of solute in the stream
$A\alpha$ = storage exchange flux (average water flux through storage zone per unit length)
$A_S/A\alpha$ = hydraulic residence time of solute in transient storage
$Q/A\alpha$ = hydraulic uptake length (average distance a water molecule travels before entering transient storage)
A_S/A = standardized storage zone area (A_S normalized to stream cross-sectional area)
A_S/Q = hydrological retention factor (A_S normalized to discharge)

The stream-tracer method combined with OTIS modeling has been widely used, but it has some shortcomings. For instance, the model treats transient storage as a single, lumped zone for a given reach, but transient storage is actually a collection of multiple storage zones, each with unique physical characteristics and residence times. This poses a problem in hyporheic research. It is difficult to separate transient storage into its

hyporheic and in-channel components using the stream tracer and modeling approach [*Harvey and Wagner*, 2000].

Choi and Harvey [2000] examined the validity of this lumped transient storage zone by comparing the basic OTIS model to a variation of the OTIS model that included two distinct transient storage zones instead of one. Using a Monte Carlo approach, datasets were created using the two-zone model for 500 hypothetical streams. The single-zone model was then used to attempt to characterize the transient storage features of the hypothetical two-storage-zone streams.

In 91% of the cases, the traditional single-zone model accurately described the transient storage characteristics of the streams with two distinct storage zones. *Choi and Harvey* [2000] noted that the 9% of streams that were not accurately characterized by the traditional model were streams that had two very different storage zones. In this case, the storage zones were labeled "competitive", which means that one of the two zones encompassed a relatively large area but had slower exchange rates, while the other zone was smaller, but had faster exchange rates. Both zones were key contributors to total transient storage, but for different reasons.

Many researchers [*Harvey and Bencala*, 1993; *Harvey and Wagner*, 2000; *Gooseff et al.*, 2003] have found that the stream tracer and simulation modeling approach tends to be biased toward short hyporheic flowpaths exhibiting relatively rapid exchange with the channel, while often not properly detecting the hyporheic exchange flows that occur over larger spatial and temporal scales. *Harvey et al.* [1996] also showed that the stream tracer and modeling approach was more reliable at low flows than at high flows

and that it was only able to properly characterize short-timescale (6-hour travel time) hyporheic flowpaths with relatively rapid exchange rates. Longer flowpaths through poorly sorted alluvium located farther from the stream exhibited much longer travel times (84 hours) and had a very different residence time distribution than the shorter hyporheic flowpaths.

Haggerty et al. [2002] and *Gooseff et al.* [2003] challenged the OTIS model with an alternative model called STAMMT-L (Solute Transport and Multirate Mass Transfer). The major difference between the two models lies in their residence time distributions (RTD). The residence time distribution can be thought of as a simple probability density function of transient storage residence times and is defined by *Haggerty et al.* [2002] as "the probability density that a tracer molecule entering the hyporheic zone at time = 0 will still be in the hyporheic zone at time = t". OTIS assumes that all transient storage residence times are distributed exponentially, which implies that all exchange between stream and transient storage zones can be modeled as a simple, first-order mass transfer function and does not allow for multiple storage zones with different first-order rate constants [*Harvey et al.*, 1996]. *Haggerty et al.* [2002] and *Gooseff et al.* [2003] found this assumption to be limiting and took the approach of a power-law RTD with STAMMT-L, wherein the RTD could be more flexible and more than one type of transient storage flowpath could be modeled.

In comparing the two models, *Gooseff et al.* [2003] found that the OTIS model tended to fit the observed data well in the early part of the curve, but did not accurately predict the solute tail. Therefore, the OTIS model may be adequate for predicting short-

term storage zone residence times, but not for relatively longer residence times. The power-law RTD model (STAMMT-L) predicted the shape of the tail end of the solute pulse much more accurately than the exponential RTD model (OTIS). OTIS underestimated the time it took for the solute in the stream to return to baseline concentration (see Figure 1.4., taken from *Gooseff et al.* [2003]). This conclusion is important because the tail end of the solute pulse contains information about the transient storage zones with the longest residence times, which tend to foster important biogeochemical reactions in the hyporheic zone. Being able to describe and quantify the physical traits of a stream reach is very important to understanding its biogeochemical aspects. Since stream geomorphology and hydrology influence surface-subsurface exchange rates and travel times and paths of water in a stream reach, they also govern the biogeochemistry of the hyporheic zone.

1.5 Hyporheic Biogeochemistry

1.5.1. Dissolved Oxygen and Dissolved Organic Carbon Dynamics

The hyporheic zone acts as a transitional zone between two very different flow environments. Stream water flow is characterized by fast-moving, often turbulent, unidirectional, open-channel flow, whereas groundwater flows much more slowly through porous media and moves in response to pressure gradients. Groundwater exhibits significantly longer residence times than stream water does. Stream ecosystems are well lit and provide habitat for both autotrophs and heterotrophs, while groundwater ecosystems are dark and dominated by respiration rather than photosynthesis [*Boulton et*

al., 1998]. Because the hyporheic zone is a heterotrophic system, two important consequences exist. The first of these is that any interaction of stream water with the heterotrophic hyporheic zone will tend to reduce the P/R ratio of the whole stream. Several studies [*Grimm and Fisher*, 1984; *Naegeli and Uehlinger*, 1997; *Fellows et al.*, 2001] have highlighted the contribution of hyporheic respiration to whole-stream respiration.

Grimm and Fisher [1984] combined measurements of whole-stream metabolism with isolated benthic surface chamber metabolism measurements as well as with measurements of respiration in deep sediment cores (10-30 cm). They found that deep sediment respiration rates were approximately equal to benthic surface respiration rates. Comparing these rates to rates of whole-stream respiration, they determined that even a highly productive stream ecosystem can be considered heterotrophic ($P/R < 1$) when respiration rates of both benthic surface and deeper hyporheic sediments are included in the whole-stream metabolism balance. Using a combination of whole-stream metabolism and benthic chambers, *Fellows et al.* [2001] estimated that the contribution of hyporheic respiration to whole-stream respiration rates ranged from 40-93% in two headwater streams in New Mexico. *Naegeli and Uehlinger* [1997] estimated a hyporheic contribution to whole-stream respiration of 74-92% in a large gravel bed river.

The second consequence of the heterotrophic nature of hyporheic zone is that there is a limited oxygen budget. Since the dissolved oxygen (DO) supply depends on incoming stream water and because sediment particle size and arrangement are highly heterogeneous, it is not uncommon for DO concentration gradients and localized

anaerobic patches to occur along hyporheic flowpaths, particularly where aerobic metabolic activity is high or hydraulic conductivity is low. Hydraulic conductivity influences the development of DO concentration gradients because hyporheic residence time tends to increase as the hydraulic conductivity of the subsurface sediments decreases. Smaller sediment particles such as clay and silt have relatively low hydraulic conductivities, resulting in longer residence times of water moving through the sediments, which can lead to a depletion of DO [*Baker et al.*, 2000].

Rates of metabolic activity in the hyporheic zone are controlled largely by the supply of organic carbon, as it is the fuel for respiration. Furthermore, the decomposition of this organic matter can be nutrient limited [*Dent et al.*, 2000]. Organic carbon can enter the hyporheic zone in dissolved or particulate form. POC is usually buried in the hyporheic zone as the result of episodic disturbance events that cause rearrangement of streambed particles [*Findlay*, 1995].

Jones et al. [1995b] found that only 15% of the hyporheic respiration observed in Sycamore Creek, Arizona, could be supported by the POC buried after flooding events. The other 85% of the respiration was supported by DOC released regularly by algae in the surface stream. This highly labile organic matter enters the hyporheic zone at downwelling points, is taken up immediately by microbes and is subsequently rapidly mineralized and the nutrients are returned to the algae in the stream in inorganic form. This cycle is ongoing and highlights the importance of the interconnectedness of the surface and subsurface environments to stream ecosystem function. *Jones* [1995] also

found that respiration rates were highest when more sediment surface area was available (i.e., smaller sediment diameter).

Holmes et al. [1998] reported that microbial activity in the parafluvial zone of a desert stream was most likely supported by DOC in the form of algal exudates. However, following a flood disturbance that scoured out algae and rearranged the streambed structure, bacterial functioning in the parafluvial zone remained high, indicating that a carbon source other than algal DOC was supporting parafluvial bacterial activity at that point. They attributed this carbon source to terrestrial DOC transported into the stream and parafluvial zone from overland runoff during the storm.

It is common to see a decrease in the concentration of DOC along a hyporheic flowpath in concert with a decrease in DO and an increase in dissolved inorganic carbon (DIC), all of which are indicators of aerobic respiration. In addition to observing these traits, *Findlay et al.* [1993] noted a higher abundance of interstitial bacteria in the presence of water with high DOC content than in water with low DOC content, supporting the importance of DOC as a carbon source. *Findlay and Sobczak* [2000] noted that bacterial abundance in the hyporheic zone was greater in shallow hyporheic sediments than in deeper sediments and greater in sediments of downwelling zones than upwelling zones. They found bacterial production to be positively correlated with sediment organic matter content.

The development of DO concentration gradients is one of the most important features of the hyporheic zone in terms of biogeochemical transformations. This is because as anaerobic regions develop in the hyporheic zone and aerobic respiration is no

longer supported, other microbially mediated metabolic reactions supported by the reduction of alternative electron acceptors take over. Many of these reactions influence the abundance and speciation of important nutrients in the ecosystem. The transition between these reactions occurs in a predictable sequence, which is dictated by redox potential. Each of the reactions in the series is a less energy-yielding metabolic process than the one before it, with aerobic respiration being the most efficient process [*Stumm and Morgan*, 1996].

1.5.2. Importance of Nutrient Regeneration in the Hyporheic Zone

Inorganic nutrient concentrations tend to be substantially higher in the hyporheic zone than in surface water [*Valett et al.*, 1990; *Pepin and Hauer*, 2002]. It has been shown that nutrient concentrations in the surface water at upwelling zones are higher than in other areas in the surface stream [*Dent et al.*, 2001]. Benthic algal abundance and chlorophyll *a* accrual rates have also been shown to be higher in upwelling zones than in downwelling zones [*Valett et al.*, 1994; *Pepin and Hauer*, 2002]. *Valett et al.* [1994] also found that the supply of nitrogen from the hyporheic zone supported the rapid recovery of benthic algae after flooding in a desert stream.

In hyporheic sediments, nutrient transformations are dependent upon concentrations of dissolved oxygen (DO), dissolved organic carbon (DOC) and the relative abundance of the various nutrient species present [*Dent et al.*, 2000]. The variable redox conditions in the hyporheic zone facilitate a variety of microbially-mediated biogeochemical reactions that are dependent on a particular redox potential.

Many of these reactions influence nutrient concentrations and speciation in surface and subsurface environments.

Inorganic nutrients are very important to primary producers in streams, but they are also typically the limiting factor to primary production rates. Therefore, the nutrients that are regenerated to the surface water from the decomposition of organic matter in the hyporheic zone are very important to the stream ecosystem. The following sections describe the dynamics of specific nutrients in the hyporheic zone.

1.5.3. Nitrogen Dynamics

Streams, particularly headwater reaches, control the transport of nitrogen from upland ecosystems to larger bodies of water and they exert control over nitrogen transformations along the way [*Peterson et al.*, 2001]. In the stream ecosystem, most of the nitrogen present is immobilized in the form of dissolved organic nitrogen (DON). Primary producers in the stream ecosystem can only assimilate nitrogen in the form of dissolved inorganic nitrogen (DIN), which includes nitrate (NO_3), nitrite (NO_2) and ammonium (NH_4) [*Duff and Triska*, 2000].

Due to large inputs from the watershed, nitrate is typically present in higher concentrations in stream water than ammonium. Ammonium also tends to exhibit a much shorter uptake length than nitrate in headwater streams [*Peterson et al.*, 2001]. In a lotic inter-biome nitrogen experiment, *Peterson et al.* [2001] found that on average, 20-30% of the ammonium removal from stream water was due to nitrification, while the remaining 70-80% was assimilated by benthic organisms.

The major nitrogen processes of interest in the hyporheic zone are ammonification, nitrification and denitrification. Nitrification is an important aerobic process that is carried out by chemoautotrophic bacteria [*Duff and Triska*, 2000]. These nitrifying bacteria are often in competition with heterotrophic bacteria for ammonium. A study by *Verhagen and Laanbroek* [1991] used chemostats to explore this competition. By keeping the ammonium concentration constant in the chemostats and iteratively increasing the concentration of glucose, they determined that nitrification is inhibited by the addition of organic carbon to a system because the resulting increase in the C:N ratio creates a situation of nitrogen limitation for the heterotrophic bacteria. In the case of nitrogen limitation, the heterotrophic bacteria outcompete the nitrifying bacteria and nitrification is inhibited. Labile organic carbon has a greater inhibitory effect on nitrification than refractory organic matter, since it is a better substrate for heterotrophic bacteria [*Butturini et al.*, 2000; *Strauss and Lamberti*, 2000].

In addition to organic carbon, it appears that nitrate and ammonium concentrations also affect the occurrence and efficiency of nitrification. Following short-term nitrate and ammonium enrichment experiments in streams of the Hubbard Brook Experimental Forest, *Bernhardt et al.* [2002] determined that the percentage of ammonium uptake used in nitrification, although variable, was positively correlated with the nitrate concentration in the stream. When nitrate concentrations were higher, the heterotrophic bacteria were able to satisfy their nitrogen requirements with the relatively abundant nitrate, leaving more ammonium available for nitrification.

In a series of experiments involving sediment biofilm reactors (SBR), *Butturini et al.* [2000] showed that high ammonium concentrations in sediments taken from a Mediterranean stream tended to promote nitrification, exhibiting an average nitrification efficiency of 85%. However, when both glucose and ammonium were added to the SBRs in a short-term addition, the nitrification efficiency dropped to a range of 31-46%. In both of these situations, no ammonium was left in the water after it passed through the SBR, but nitrate concentrations increased, indicating that nitrification had occurred. Following a long-term glucose addition, a short-term ammonium addition yielded very poor nitrification efficiency, allowing 64% of the ammonium input to pass through the SBR. That the SBRs in this case did not produce any nitrate supports the notion that, under higher organic carbon concentrations, heterotrophic bacteria dominate.

Jones et al. [1995a], however, found a positive relationship between organic matter respiration in the hyporheic zone and nitrification. In a metabolism chamber study conducted with sediments from Sycamore Creek, Arizona, they found that nitrification rates were significantly higher in sediments from downwelling zones (13.1 μgNO_3-N•L sediments^{-1}•h^{-1}) than in those from upwelling zones (1.7 μgNO_3-N•L sediments^{-1}•h^{-1}). Organic matter respiration rates were significantly higher in downwelling sediments (1.12 mg O_2•L sediment^{-1}•h^{-1}) than those in upwelling sediments (0.46 mg O_2•L sediment^{-1}•h^{-1}) [*Jones*, 1995b]. As organic matter from the stream enters the hyporheic zone at downwelling points, respiration rates are high as organic matter is mineralized to ammonium. This flux of ammonium becomes available for nitrification and nitrate is supplied to the stream. There was not only a spatial correlation between nitrification and

organic matter respiration, but also a temporal correlation. Throughout the recovery of Sycamore Creek from large floods, both respiration and nitrification rates increased, suggesting the two processes are closely linked [*Jones et al.*, 1995a].

In pristine, high-gradient, alluvial streams with high hydraulic conductivity, the hyporheic zone is typically large and consists mainly of advected stream water. Hyporheic exchange is relatively rapid in these systems. As a result, anaerobic sites in the hyporheic zone are less common and nitrification is a common process, causing the interstitial water to be dominated by nitrate rather than ammonium. In lower-gradient streams with a strong groundwater influence, however, the hyporheic zone is smaller and the chemistry of the water entering the stream is controlled by the concentration of nutrients in the incoming groundwater. Conditions in the hyporheic zone are often reducing in those situations and ammonium dominates the nitrogen presence in the porewater [*Duff and Triska*, 2000]. While coarse, well-oxygenated sediments support nitrification, fine, organic-rich sediments promote denitrification [*Dent et al.*, 2001].

If organic matter and DIN inputs to the shallow hyporheic zone are high, oxygen can be rapidly depleted through aerobic respiration, creating a strong oxic-anoxic boundary where groundwater and streamwater mix or where oxygen depletion occurs due to high rates of aerobic metabolism. This interface provides an opportunity for rapid nitrogen cycling and efficient nitrogen removal from the system. This is because organic matter in the hyporheic zone is mineralized to ammonium, which can be transformed into nitrate by nitrification in aerobic zones. If the aerobic zone is close to an anaerobic zone,

the nitrate can be reduced and exported from the system as a gas to the atmosphere through the process of denitrication [*Duff and Triska*, 2000].

Denitrification removes nitrogen from a system by reducing dissolved nitrate into nitrogen gases, including nitrous oxide (N_2O) and dinitrogen gas (N_2). In nitrogen-enriched streams, this is an efficient method to improve water quality [*Martin et al.*, 2001]. *Martin et al.* [2001] incubated sediments from two streams of differing nitrate concentrations and measured their denitrification potentials. Denitrification rates in unamended sediments from the stream with the higher nitrate concentration were much higher (300-1231 ng N_2O $gAFDM^{-1}h^{-1}$) than those in the sediments from the low-nitrate stream (12.1-152 ng N_2O $gAFDM^{-1}h^{-1}$). When the sediments were amended with nitrate alone or nitrate and labile organic carbon, the sediments from the low-nitrate stream responded with increased rates of denitrification, but the sediments from the high-nitrate streams showed no significant difference. The microbes in the sediments from the low-nitrate stream appeared to be nitrate limited.

In a study of ammonium retention in Brazilian savannah streams of four different geomorphologies, *Gücker and Boëchat* [2004] found that the relative transient storage zone size (A_S/A) and transient storage residence times associated with the different stream morphotypes were the principle predictors of ammonium retention potential. Streams of swamp and step-pool morphologies were the most retentive and also exhibited the largest A_S/A values and transient storage residence times. Interestingly, in both of these streams, a large proportion of the transient storage occurred in the stream channel.

In meandering and run reaches, however, ammonium retention potentials and residence times were lower and advection and dispersion played a larger role in solute transport than transient storage did. Based on reactive and conservative tracer concentration ratios in the falling limbs of the solute curves, ammonium retention was deemed to be biological rather than abiotic (i.e., adsorption to sediments) [*Gücker and Boëchat*, 2004].

1.5.4. Phosphorus Dynamics

Phosphorus dynamics in streams are driven by both biotic and abiotic processes. Abiotic processes include the sorption of phosphorus onto ferric and aluminum hydroxides, clay minerals and humic compounds [*Schlesinger*, 1997]. Under high redox and low pH conditions, phosphorus is often bound to inorganic particles. If conditions are reducing or pH increases, however, phosphorus can be released from the complexes and become soluble in interstitial waters [*Hendricks and White*, 2000]. *Carlyle and Hill* [2001] found high concentrations (>50 μg L^{-1}) of soluble reactive phosphorus (SRP) in the floodplain groundwaters leading into a fifth-order Ontario stream to be associated with low DO concentrations (<3 mg L^{-1}) and high Fe^{2+} concentrations (>1 mg L^{-1}) and lower SRP concentrations to be associated with high DO and low Fe^{2+} concentrations. Phosphorus dynamics are influenced by biota through the mineralization of organic matter and subsequent release of inorganic phosphorus [*Hendricks and White*, 2000] as well as phosphorus uptake. Much of the phosphorus requirement of aquatic primary producers is satisfied by internal recycling of organic matter [*Schlesinger*, 1997].

In a study of two streams in the southeastern United States, *Mulholland et al.* [1997] emphasized the connection between hyporheic zone processes and stream phosphorus dynamics. They found that phosphorus uptake rates were five times higher and phosphorus uptake lengths were five times shorter in a stream with a relatively large transient storage zone volume ($A_S/A = 1.49$) than in a stream with a much smaller transient storage zone volume ($A_S/A = 0.9$). In the stream with the larger storage volume, an estimated 57% of the total phosphorus uptake was performed by the surface community, while 43% was performed by the transient storage community. In both streams, heterotrophic P uptake rates were higher than autotrophic P uptake rates.

1.6 Arctic Tundra Streams

1.6.1. Description of the North Slope of the Brooks Range, Alaska

Although studies over the past ten to twenty years have contributed greatly to the growing knowledge base of surface-subsurface exchange and transient storage characteristics of streams, many of the streams that have been studied are located in temperate or desert [*Valett et al.*, 1990; *Valett et al.*, 1994] ecosystems. Information regarding hyporheic processes in arctic streams is lacking. This section will introduce arctic tundra streams and discuss what is known and unknown about the role of hyporheic exchange in those ecosystems.

The North Slope of the Brooks Range in Alaska is located about 180 km south of the Arctic Ocean [*Hobbie et al.*, 1999]. There are no trees in this region. It is dominated

by tussock tundra vegetation. The region is underlain by continuous permafrost and is covered with snow for 7 to 9 months out of the year. *Craig and* McCart [1975] classified the streams in this region into three main stream types: mountain streams, spring streams and tundra streams. Mountain streams originate in the Brooks Range and receive water from both springs and surface runoff. Springs are the only source of flow to mountain streams in the winter, but snowmelt creates high flows in the spring of the year. Discharge can be highly variable in the summer and is dependent on the degree of surface runoff produced by heavy rains. The silt load is proportional to discharge in these streams. Spring streams are the spring-fed tributaries to mountain streams and they originate in the mountains. Because of their spring source, their discharge and temperature remain quite stable and their suspended sediment concentrations are very low. Tundra streams drain the tundra-covered foothills of the Brooks Range. These streams freeze to the bottom in the winter and there is a spring flood event caused by snowmelt in late May to early June. Discharge and suspended sediment levels are more stable in tundra streams than in mountain streams because the surface runoff that feeds tundra streams passes through the surrounding absorbent tundra before entering the stream and also because there are many lakes and wetlands on the tundra surface that provide storage and attenuation. Because of these patterns of water movement, water temperatures in tundra streams tend to be higher than in mountain or spring streams. Two common morphologies within the tundra stream classification are alluvial streams with riffle pool sequences and peat-bottomed streams with a "beaded" structure consisting of round, deep pools connected by deep, narrow runs.

The spring flooding event is one of the most hydrologically important events of the year. While the ice breakup and outflow period often lasts just a few days to a week in May, it is responsible for 75% of the annual flow of Arctic streams and rivers [*McBean*, 2005]. *McNamara et al.* [1998] estimate that 70% of the annual runoff at the mouth of the Kuparuk River in Alaska could be attributed to snowmelt. The North Slope region experiences short, cool summers with 24-hour daylight at the summer solstice. In the summer months, as air temperatures and day length increase, a region of thawed sediments called the active layer develops at the surface of the tundra. Active layer depths can vary from tens of centimeters to one or two meters [*Walsh*, 2005]. *Hinzman et al.*, [1991] found that typical active layer depths on the North Slope of the Brooks Range in Alaska were about 25-40 cm, but that some were as deep as a meter. Active layer depths were greater on ridgetops and slopes than in valley bottoms.

According to *Hinzman et al.* [1991], much of the water flowing downslope into the streams flows through this active layer, which exists in the organic layer of soil, because the permeability is high. Meanwhile, the deeper mineral layers of soil remain saturated with much less movement of water. *McNamara et al.* [1998] also indicated that permafrost and the active layer have a unique effect on storm hydrographs in streams on the North Slope. The storm hydrograph of the Kuparuk showed a quick initial response, but also a long, drawn out recession. This is because the water moves quickly through water tracks in the shallow subsurface active layer and reaches the stream relatively early. As the storm wanes, this organic layer can hold its moisture for a long period of time and it continues to slowly supply the stream with water.

The active layer of thawed sediments that develops on the surface of the tundra extends beneath streambeds and is referred to as the thaw bulb. *Bradford et al.* [2005] demonstrated that ground penetrating radar (GPR) is a useful tool for estimating thaw bulb depth beneath peat streams in arctic Alaska. *Brosten et al.* [2006] used GPR to compare seasonal thaw bulb development patterns in streams of contrasting geomorphology and found that high-energy, cobble-lined streams responded more quickly to temperature changes than lower-energy, peat-lined streams. They suggested that low-energy streams are better insulated than high-energy streams in this region and, therefore, are slower to respond to temperature changes.

1.6.2. Hyporheic Zones in Arctic Tundra Streams

The presence of permafrost imposes a constraint that restricts connection of the stream with deep groundwater. Initially, it was thought that permafrost may restrict the development of hyporheic zones in arctic tundra streams. However, *Edwardson et al.* [2003] found that an active layer that develops beneath streambeds in the summer months, creating thawed sediments through which hyporheic exchange can occur. They were the first to study hyporheic processes in arctic streams in detail. Through a series of conservative tracer additions and concurrent hyporheic and channel sampling, they found that the hyporheic zone was indeed important to stream ecosystem functioning. Transient storage and hyporheic exchange characteristics in these arctic streams were similar in most ways to temperate streams of similar size. Hyporheic zones in the streams in their study served as sites for the mineralization of organic matter, often followed by rapid

nitrification. Ammonium, phosphate and carbon dioxide were all produced in the hyporheic zone and upwelling from the hyporheic zone to the stream channel supplied the stream with important nutrients. In fact, they determined that the equivalent of 14-162% of the nitrogen demands and up to 13% of the phosphorus demands of benthic organisms were supplied to the streams by the hyporheic zone.

1.6.3. Potential Responses of Arctic Tundra Streams to Climate Change

In a given year, there are four hydrologic periods in the Arctic: a snowmelt period, an outflow ice breakup period, a summer period with no ice cover and a winter period in which water bodies are covered by ice. The Intergovernmental Panel on Climate Change (IPCC) has predicted that, due to its dependence on climate-driven annual freeze-thaw cycles, the Arctic will experience some of the largest and most rapid responses to global climate change on Earth. In fact, as reported in the Arctic Climate Impact Assessment (ACIA) Scientific Report composed by the Arctic Council and the International Arctic Science Committee, it has been estimated that Arctic regions have seen an average land-surface air temperature increase of 0.09ºC per decade from 1900-2003 and 0.40ºC per decade from 1966-2003. According to the IPCC, precipitation has increased by 0.5 to 1.0% per decade during the twentieth century [*McBean*, 2005].

Climate change is predicted to continue and the ACIA predicts an average air temperature increase of 3.7ºC from the 1981-2000 baseline temperature record to the time period of 2071-2090 [*Wrona et al.*, 2005]. Such significant changes in the air temperature and overall climate regime are likely to have considerable effects on the

structure and function of Arctic ecosystems. The main effects of increasing air temperature on stream ecosystems in the arctic include earlier and less intense snowmelt and ice breakup, later freeze-up and snow accumulation and an increase in the depth of the permafrost active layer during the warm months [*Wrona et al.*, 2005].

An increase in active layer depth would affect streams physically and biogeochemically. Arctic tundra ecosystems are generally characterized by low primary productivity and low nutrient availability, particularly phosphorus. Due to the permafrost and the otherwise moist, cool tundra soils that are present as the active layer develops in the warm months, microbial soil decomposition rates are typically quite low and there is a large, long-term accumulation of organic matter [*Bunnell et al.*, 1975]. Therefore, arctic tundra ecosystems serve as major carbon (C) and nutrient sinks. However, because soil microbial decomposition rates are limited primarily by temperature and secondarily by moisture content of the soil, predicted increases in temperature and moisture may promote the decomposition of stored organic matter, thus releasing more CO_2 and mineralized nutrients and drawing down the tundra C stores.

As a result of the melting permafrost, erosion, slumping and thermokarsts are also probable, which will increase sediment loading into streams and lakes [*Rouse et al.*, 1997; *Callaghan*, 2005]. These episodic events would not only add to the carbon pool of streams in the form of particulate organic carbon, but would also increase sediment and phosphorus loading to streams. *Hobbie et al.* [1999] found that after 7 or 8 years of experimental phosphorus addition to the Kuparuk River, the dominant primary producers shifted from diatoms and filamentous algae to nutriophilic bryophyte species. This

bottom-up effect changed not only the primary producer community, but also increased insect abundance and fish production. Climate change can have far reaching effects on Arctic tundra streams due to the interconnectedness of the physical and biogeochemical variables of the tundra and stream systems.

Specifically, in the context of arctic stream hyporheic functioning, the potential concerns regarding climate change are: (1) an increase in the length of the warm season (2) increased extent of the thaw bulb (3) increased carbon and nutrient loading and (4) any changes in sediment loading, temperature, precipitation, runoff patterns that could potentially change stream geomorphology. An increase in the length of the warm season would increase the annual magnitude of hyporheic processing and nutrient regeneration to streams. If average temperatures of thawed sediments increase, rates of microbial metabolic reactions which drive the biogeochemical processing in the hyporheic zone could increase, thus increasing the annual magnitude of hyporheic processing. If the thaw bulb increases in depth, the extent of the hyporheic zone may increase as well, possibly changing the nature and magnitude of influence that the hyporheic zone has on stream ecosystem functioning. Changes in the geomorphology of a stream can lead to changes in the surface-subsurface exchange characteristics of a stream, which can have significant implications for the microbial metabolic activity and biogeochemical cycling in the hyporheic zone [*Holmes et al.*, 1998]. Therefore, changes in stream geomorphology due to climate change may considerably alter the hydrologic and biogeochemical functions of the hyporheic zone in the context of the stream ecosystem.

1.6.4. Research Goals

The studies described in Chapters 2 and 3 of this thesis were carried out within a larger project called the Arctic Hyporheic Project (AHP). The goals of the AHP were to determine the current extent of hyporheic exchange within the thaw bulb of arctic streams with contrasting geomorphic characteristics and to understand how hyporheic exchange patterns and hyporheic extent differ with stream geomorphology. The goal of my portion of this research was to identify the biogeochemical patterns within the subsurface environments of the two geomorphically distinct stream reaches, so that we could predict how biogeochemical processing differs in streams with different physical characteristics and hyporheic exchange patterns. If climate warming alters the geomorphology of arctic streams, as we expect, then this information will provide a critical basis to predict how these geomorphological changes might influence biogeochemical processing in arctic streams.

LITERATURE CITED

Baker, M.A., C.N. Dahm, and H.M. Valett, (2000), Anoxia, anaerobic metabolism, and biogeochemistry of the stream-water-ground-water interface, in *Streams and Groundwaters*, edited by J.B. Jones, and P.J. Mulholland, p. 259, Academic Press, San Diego, California.

Battin, T.J., L.A. Kaplan, J.D. Newbold, and C.M.E. Hansen (2003), Contributions of microbial biofilms to ecosystem processes in stream mesocosms, *Nature*, *426*, 439-442.

Bencala, K.E., and R.A. Walters (1983), Simulation of solute transport in a mountain pool-and-riffle stream: A transient storage model, *Water Resources Research*, *19*, 718-724.

Bernhardt, E.M., R.O. Hall, and G.E. Likens (2002), Whole-system estimates of nitrification and nitrate uptake in streams of the Hubbard Brook Experimental Forest, *Ecosystems*, *5*, 419-430.

Boulton, A.J., S. Findlay, P. Marmonier, E.H. Stanley, and H.M. Valett, (1998), The functional significance of the hyporheic zone in streams and rivers, *Annual Review of Ecology and Systematics*, *29*, 59-81.

Bradford, J.H., J.P. McNamara, W.B. Bowden, and M.N. Gooseff (2005), Measuring thaw depth beneath peat-lined arctic streams using ground-penetrating radar, *Hydrological Processes*, *19*, 2689-2699.

Brosten, T.R., J.H. Bradford, J.P. McNamara, J.P. Zarnetske, M.N. Gooseff, and W.B. Bowden (2006), Profiles of temporal thaw depths beneath two arctic stream types using ground-penetrating radar, *Permafrost and Periglacial Processes*, *17*, 341-355.

Bunnell, F.L., S.F. Maclean, Jr., and J. Brown (1975), Barrow, Alaska, USA., in *Structure and function of tundra ecosystems, Ecol. Bull., 20, 73-124,* edited by T. Rosswall, and O.W. Heal, Stockholm: Swedish Natural Science Research Council.

Butturini, A., T.J. Battin, and F. Sabater (2000), Nitrification in stream sediment biofilms: The role of ammonium concentration and DOC quality, *Water Research, 34,* 629-639.

Callaghan, T.V. (2005), Arctic tundra and polar desert ecosystems, in *Arctic Climate Impact Assessment*, Cambridge University Press, New York, New York.

Carlyle, G.C., and A.R. Hill (2001), Groundwater phosphate dynamics in a river riparian zone: Effects of hydrologic flowpaths, lithology and redox chemistry, *Journal of Hydrology*, *247*, 151-168.

Choi, J., J.W. Harvey, and M.H.Conklin (2000), Characterizing multiple timescales of stream and storage zone interaction that affect solute fate and transport in streams, *Water Resources Research*, *36*, 1511-1518.

Craig, P.C., and P.J. McCart (1975), Classification of stream types in Beaufort Sea drainages between Prudhoe Bay, Alaska, and the Mackenzie Delta, N.W.T., Canada, *Arctic and Alpine Research*, *7*, 183-198.

Cushing, C.E., and J.D. Allan (2001), *Streams: Their ecology and life*, Academic Press, San Diego, California.

D'Angelo, D.J., J.R. Webster, S.V. Gregory, and J.L. Meyer (1993), Transient storage in Appalachian and Cascade mountain streams as related to hydraulic characteristics, *Journal of the North American Benthological Society*, *12*, 223-235.

De Wiest, R.J.M. (1969), *Flow through porous media*, Academic Press, New York, New York.

Dent, C.L., J.D Schade, N.B. Grimm, and S.G. Fisher (2000), *Subsurface influences on surface biology*, in *Streams and Groundwaters*, edited by J.B. Jones, and P.J. Mulholland, p. 381, Academic Press, San Diego, California.

Dent, C.L., N.B. Grimm, and S.G. Fisher (2001), Multiscale effects of surface-subsurface exchange on stream nutrient concentrations, *Journal of the North American Benthological Society, 20,* 162-181.

Duff, J.H., and F.J. Triska (2000), Nitrogen biogeochemistry and surface-subsurface exchange in streams, in *Streams and Groundwaters*, edited by J.B. Jones, and P.J. Mulholland, pp. 197, Academic Press, San Diego, California.

Edwardson, K.J., W.B. Bowden, C. Dahm, and J. Morrice (2003), The hydraulic characteristics and geochemistry of hyporheic and parafluvial zones in Arctic tundra streams, North Slope, Alaska, *Advances in Water Resources*, *26*, 907-923.

Fellows, C.S., H.M. Valett, and C.M. Dahm (2001), Whole-stream metabolism in two montane streams: Contribution of the hyporheic zone, *Limnology and Oceanography, 46*, 523-531.

Findlay, S., D. Strayer, C. Goumbala, and K. Gould (1993), Metabolism of streamwater dissolved organic carbon in the shallow hyporheic zone, *Limnology and Oceanography, 38*, 1493-1499.

Findlay, S. (1995) Importance of surface-subsurface exchange in stream ecosystems: The hyporheic zone, *Limnology and Oceanography*, *40*, 159-164.

Findlay, S., and W.V. Sobczak (2000), Microbial communities in hyporheic sediments, in *Streams and Groundwaters*, edited by J.B. Jones, and P.J. Mulholland, p. 287, Academic Press, San Diego, California.

Gooseff, M.N., S.M. Wondzell, R. Haggerty, and J. Anderson (2003), Comparing transient storage modeling and residence time distribution (RTD) analysis in geomorphically varied reaches in the Lookout Creek Basin, Oregon, USA, *Advances in Water Resources*, *26*, 925-937.

Grimm, N.B., and S.G. Fisher (1984), Exchange between interstitial and surface water: Implications for stream metabolism and nutrient cycling, *Hydrobiologia*, *111*, 219-228.

Gücker, B., and I.G. Boëchat (2004), Stream morphology controls ammonium retention in tropical headwaters, *Ecology*, *85*, 2818-2827.

Haggerty R., S.M. Wondzell, and M.A. Johnson (2002), Power-law residence time distribution in the hyporheic zone of a 2nd order mountain stream, *Geophysical Research Letters*, *29*(13), doi:10.1029/2002GL014743.

Harvey, J.W., and K.E. Bencala (1993), The effect of streambed topography on surface-subsurface exchange in mountain catchments, *Water Resources Research*, *29*, 89-98.

Harvey, J.W., B.J. Wagner, and K.E. Bencala (1996), Evaluating the reliability of the stream tracer approach to characterize stream-subsurface water exchange, *Water Resources Research, 32*, 2441-2451.

Harvey, J.W., and B.J. Wagner (2000), Quantifying hydrologic interactions between streams and their subsurface hyporheic zones, in *Streams and Groundwaters*, edited by J.B. Jones, and P.J. Mulholland, p. 41, Academic Press, San Diego, California.

Harvey, J.W., M.H. Conklin, and R.S. Koelsch (2003), Predicting changes in hydrologic retention in an evolving semi-arid alluvial stream, *Advances in Water Resources*, *26*, 939-950.

Hendricks, S.P., and D.S. White (2000), Stream and groundwater influences on phosphorus biogeochemistry, in *Streams and Groundwaters*, edited by J.B. Jones, and P.J. Mulholland, p. 221, Academic Press, San Diego, California.

Hinzman, L.D., D.L. Kane, R.E. Gieck, and K.R. Everett (1991), Hydrologic and thermal properties of the active layer in the Alaskan Arctic, *Cold Regions Science and Technology, 19*, 95-110.

Hobbie, J.E., B.J. Peterson, N. Bettez, L. Deegan, W.J. O'Brien, G.W. Kling, G.W. Kipphut, W.B. Bowden, and A.E. Hershey (1999), Impact of global change on the biogeochemistry and ecology of an Arctic freshwater system, *Polar Research*, *18*, 207-214.

Holmes, R.M., S.G. Fisher, N.B. Grimm, and B.J. Harper (1998), The impact of flash floods on microbial distribution and biogeochemistry in the parafluvial zone of a desert stream, *Freshwater Biology*, *40*, 641-654.

Jones, J.B., S.G. Fisher, and N.B. Grimm (1995a), Nitrification in the hyporheic zone of a desert stream ecosystem, *Journal of the North American Benthological Society*, *14*, 249-258.

Jones, J.B., S.G. Fisher, and N.B. Grimm (1995b), Vertical hydrologic exchange and ecosystem metabolism in a Sonoran Desert stream, *Ecology*, *76*, 942-952.

Jones, J.B. (1995), Factors controlling hyporheic respiration in a desert stream, *Freshwater Biology*, *34*, 91-99.

Jones, J.B., and R.M. Holmes (1996), Surface-subsurface interactions in stream ecosystems, *Trends in Ecology and Evolution*, *11*, 239-242.

Kasahara, T., and S.M. Wondzell (2003), Geomorphic controls on hyporheic exchange flow in mountain streams, *Water Resources Research*, *39*(1), 1005, doi:10.1029/2002WR001386.

Martin, L.A., P.J. Mulholland, J.R. Webster, and H.M. Valett (2001), Denitrification potential in sediments of headwater streams in the southern Appalachian Mountains, USA, *Journal of the North American Benthological Society*, *20*, 505-519.

McBean, G. (2005), Arctic climate: Past and present, in *Arctic Climate Impact Assessment*, Cambridge University Press, New York, New York.

McNamara, J.P., D.L. Kane, and L.D. Hinzman (1998), An analysis of stream flow hydrology in an Arctic drainage basin: a nested watershed approach, *Journal of Hydrology*, *206*, 39-57.

Morrice, J.A., H.M. Valett, C.N. Dahm, and M.E. Campana (1997), Alluvial characteristics, groundwater-surface water exchange and hydrological retention in headwater streams, *Hydrological Processes*, *11*, 253-267.

Mulholland, P.J., E.R. Marzoff, J.R. Webster, D.R. Hart, and S.P. Hendricks (1997), Evidence that hyporheic zones increase heterotrophic metabolism and phosphorus uptake in forest streams, *Limnology and Oceanography*, *42*, 443-451.

Naegeli, W.M., and U. Uehlinger (1997), Contribution of the hyporheic zone to ecosystem metabolism in a prealpine gravel-bed river, *Journal of the North American Benthological Society*, *16*, 794-804.

Packman, A.I. and K.E. Bencala (2000), Modeling surface-subsuface hydrological interactions, in *Streams and Groundwaters*, edited by J.B. Jones, and P.J. Mulholland, p. 45, Academic Press, San Diego, California.

Pepin, D.M., and F.R. Hauer., (2002), Benthic responses to groundwater-surface water exchange in 2 alluvial rivers in northwestern Montana, *Journal of the North American Benthological Society, 21*, 370-383.

Peterson, B.J., W.M. Wollheim, P.J. Mulholland, J.R. Webster, J.L. Meyer, J.L. Tank, E. Marti, W.B. Bowden, H.M. Valett, A.E. Hershey, W.H. McDowell, W.K. Dodds, S.K. Hamilton, S. Gregory, and D.D. Morrall (2001), Control of nitrogen export from watersheds by headwater streams, *Science*, *292*, 86-90.

Rouse, W.R., M.S.V. Douglas, R.E. Hecky, A.E. Hershey, G.W. Kling, L. Lesack, P. Marsh, M. McDonald, B.J. Nicholson, N.T. Roulet, and J.P. Smol (1997), Effects of climate change on the freshwaters of Arctic and Subarctic North America, *Hydrological Processes*, *11*, 873-902.

Runkel, R.L. (1998), One-dimensional transport with inflow and storage (OTIS) - A solute transport model for streams and rivers, in U.S. *Geological Survey Water-Resources Investigations Report 98–4018*, 73 pp.

Runkel, R.L. (2000), Using OTIS to model solute transport in streams and rivers, in *U.S. Geological Survey Fact Sheet FS-138-99*. 4 pp.

Schlesinger, W.H. (1997), *Biogeochemistry: An analysis of global change*, Academic Press, San Diego, California.

Storey, R.G., K.W.F. Howard, and D.D. Williams (2003), Factors controlling riffle-scale exchange flows and their seasonal changes in a gaining stream: A three-dimensional groundwater flow model, *Water Resources Research*, *39*(2), 1034, doi:10.1029/2002WR001367.

Strauss, E.A., and G.A. Lamberti (2000), Regulation of nitrification in aquatic sediments by organic carbon, *Limnology and Oceanography*, *45*, 1854-1859.

Stream Solute Workshop (1990), Concepts and methods for assessing solute dynamics in stream ecosystems, *Journal of the North American Benthological Society*, *9*, 95-119.

Stumm, W., and J.J. Morgan (1996), *Aquatic chemistry: Chemical equilibria and rates in natural waters*, John Wiley & Sons, Inc., New York, New York.

Valett, H.M., S.G. Fisher, and E.H. Stanley (1990), Physical and chemical characteristics of the hyporheic zone of a Sonoran Desert stream, *Journal of the North American Benthological Society*, *9*, 210-215.

Valett, H.M., S.G. Fisher, N.B. Grimm, and P. Camill (1994), Vertical hydrologic exchange and ecological stability of a desert stream ecosystem, *Ecology*, *75*, 548-560.

Valett, H.M., J.A. Morrice, C.N. Dahm, and M.E. Campana (1996), Parent lithology, surface-groundwater exchange, and nitrate retention in headwater streams, *Limnology and Oceanography, 41*, 333-345.

Verhagen, F.J.M., and H.J. Laanbroek (1991), Competition for ammonium between nitrifying and heterotrophic bacteria in dual energy-limited chemostats, *Applied and Environmental Microbiology*, *57*, 3255-3263.

Walsh, J.E. (2005), Cryosphere and hydrology, in *Arctic Climate Impact Assessment,* Cambridge University Press, New York, New York.

Wroblicky, J.R., M.E. Campana, H.M. Valett, and C.M. Dahm (1998), Seasonal variation in surface-subsurface water exchange and lateral hyporheic area of two stream-aquifer systems, *Water Resources Research*, *34*, 317-328.

Wrona, F.J., T.D. Prowse, and J.D. Reist (2005), Freshwater ecosystems and fisheries, in *Arctic Climate Impact Assessment*, Cambridge University Press, New York, New York.

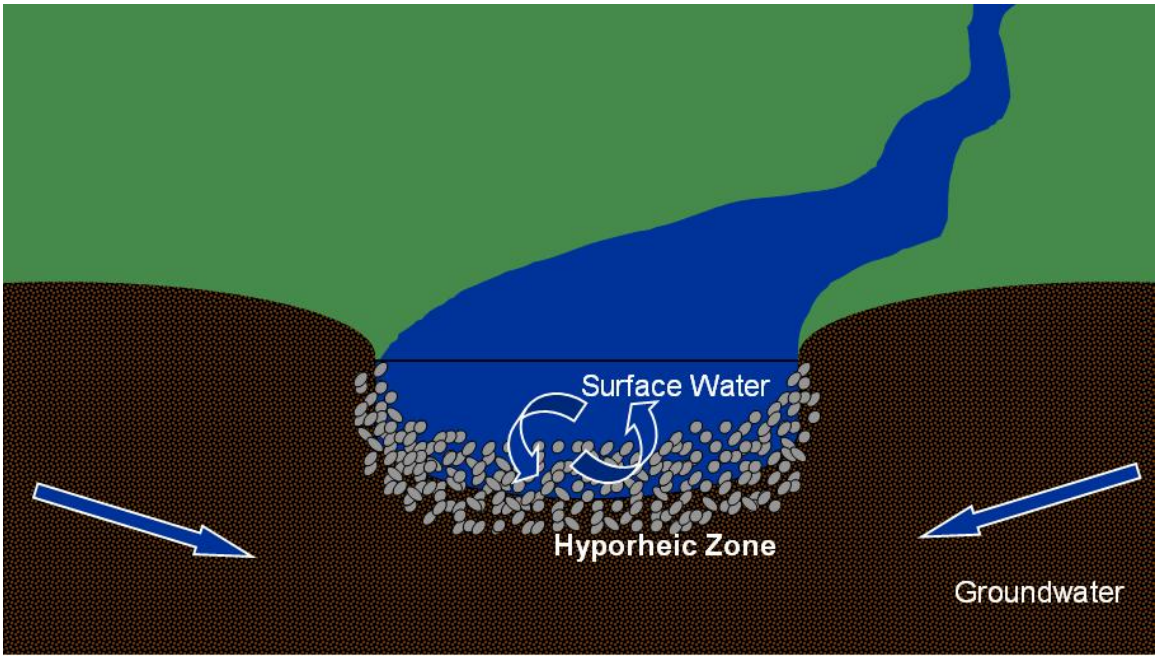

Figure 1.1. A cross-sectional diagram of a typical temperate stream, showing hyporheic exchange and potential groundwater interaction

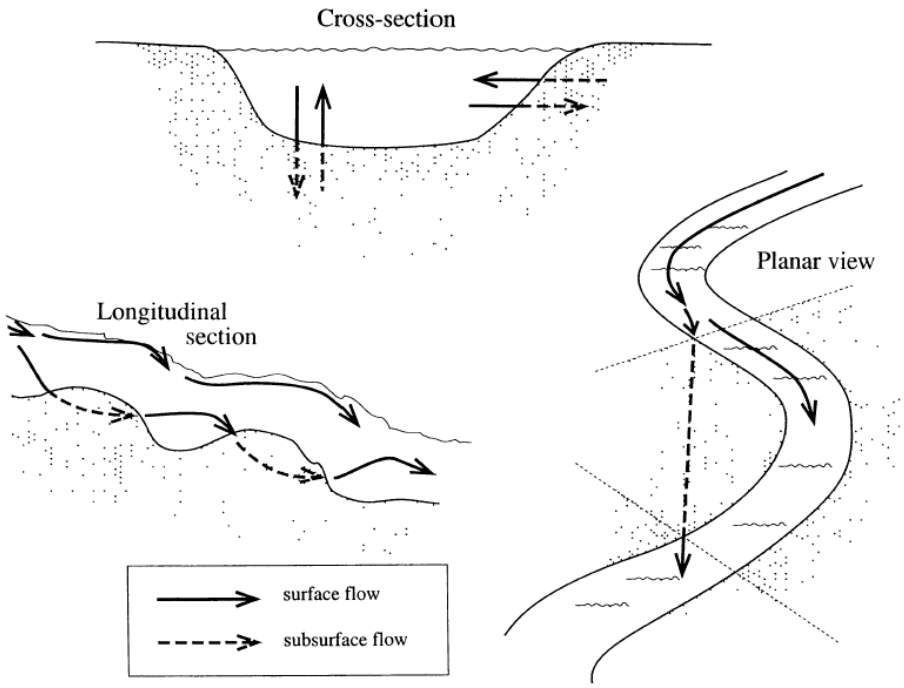

Figure 1.2. Common vertical, lateral and longitudinal patterns of hyporheic exchange; shaded area is hyporheic zone (taken from *Findlay* [1995])

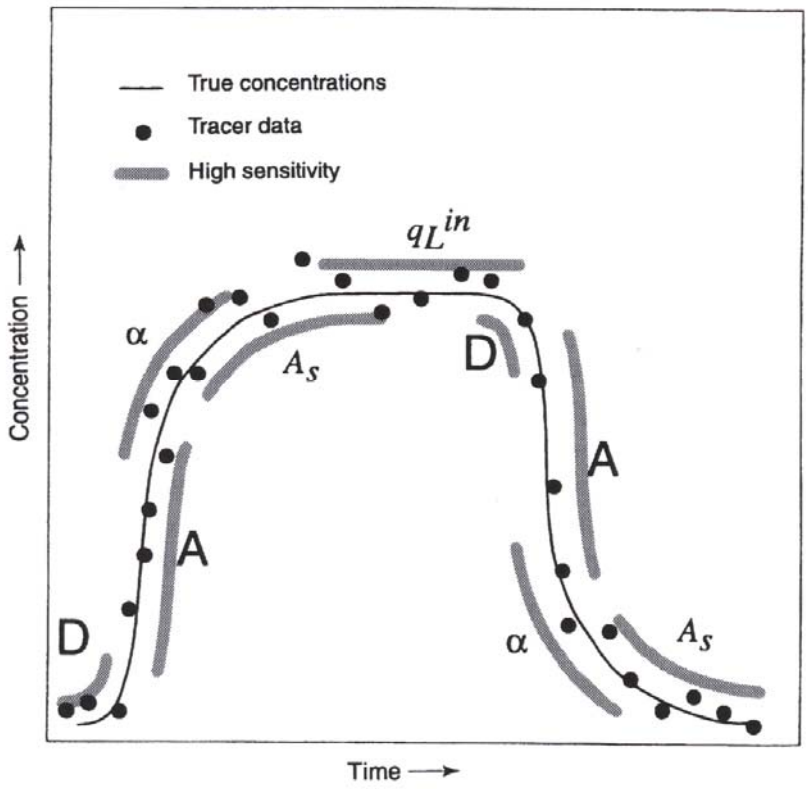

Figure 1.3. A model simulation of a solute breakthrough curve highlighting the regions of sensitivity attributed to each of the model parameters (taken from *Harvey and Wagner* [2000])

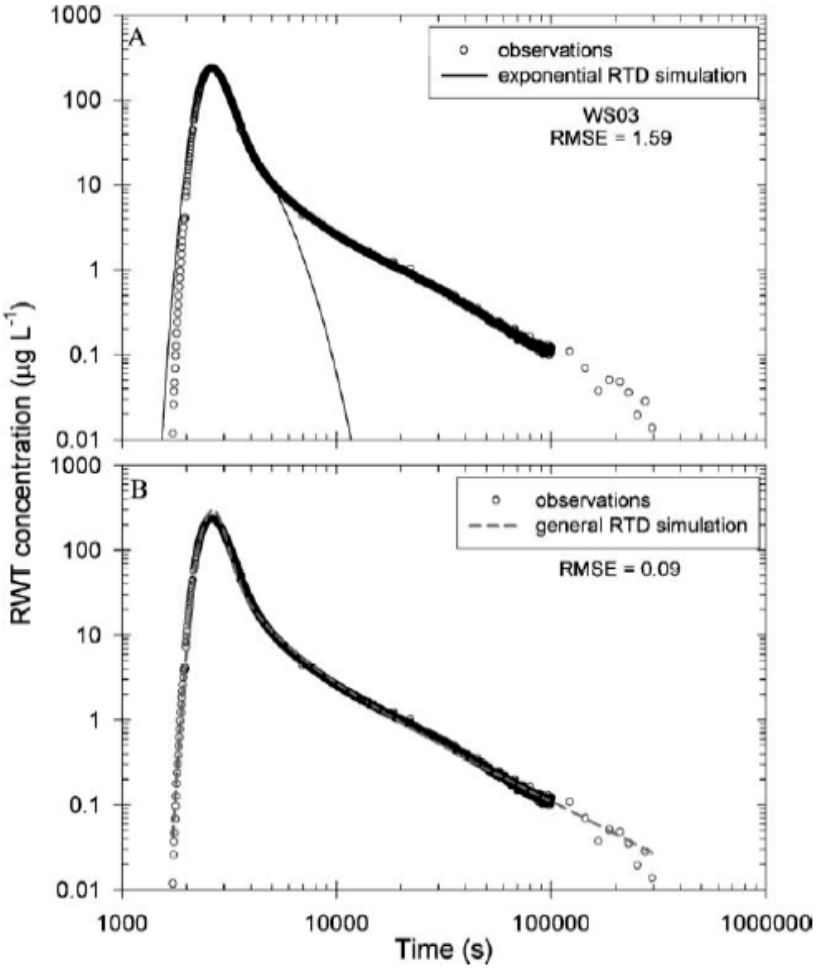

Figure 1.4. The observed solute pulse data of a solute addition experiment in a second-order stream in Oregon simulated by (A) exponential RTD model and (B) general (power-law) RTD model (taken from *Gooseff et al.* [2003])

CHAPTER 2: BIOGEOCHEMICAL CHARACTERISTICS OF THE HYPORHEIC ZONES OF TWO ARCTIC TUNDRA STREAMS OF CONTRASTING GEOMORPHOLOGY

ABSTRACT

The North Slope of Alaska's Brooks Range is underlain by continuous permafrost, but an active layer of thawed sediments develops at the surface of the tundra and beneath streambeds during the summer. This active layer facilitates hyporheic exchange and important biogeochemical processing, but information on the characteristics of hyporheic processes in arctic tundra streams is limited. The goal of this study was to understand how hyporheic exchange patterns and biogeochemical processes are influenced by stream geomorphology and the extent of the active layer. Two second-order arctic tundra stream types of contrasting geomorphology were studied. The first was a high-gradient, cobble-bottomed, alluvial stream characterized by distinct riffle-pool sequences (average thaw depth: 157 cm). The second was a low-gradient, peat-bottomed, beaded stream characterized by large deep pools connected by deep runs (average thaw depth: 67 cm).

In the alluvial stream, the degree of surface-subsurface exchange decreased with depth, but was active at depths >50 cm. In contrast, all surface-subsurface exchange in the peat stream occurred within the top ~10 cm of the streambed sediments. While the surface waters of the two streams were not significantly different from one another in terms of biogeochemistry, their subsurface waters were significantly different from one another in every biogeochemical constituent measured. In the alluvial stream, subsurface concentrations of nitrate, ammonium, soluble reactive phosphorus (SRP) and DOC were not significantly different from the surface water at any depth. Dissolved oxygen (DO) concentration decreased significantly with depth, yet remained sufficiently oxic at the deepest depth sampled (median: 4.13 mg/L). In the peat stream, however, surface water biogeochemical characteristics were significantly different from those in the subsurface at any depth. DO and nitrate concentrations decreased with depth to a point where they were not detectable at ~30 cm, while ammonium, SRP and DOC concentrations increased exponentially with depth in the subsurface. The physical differences in the geomorphology of the streams led to differences in their hyporheic exchange characteristics, which then influenced the biogeochemistry of the subsurface water. In turn, the stream ecosystem was influenced by nutrient regeneration from the hyporheic zone. The hyporheic zone served as a source of ammonium and SRP to the surface water in both streams. The alluvial hyporheic zone was a stronger source of SRP than the peat stream, but the peat stream was a stronger source of ammonium. The hyporheic zone served as a net nitrate sink in the peat stream and as a net nitrate source in the alluvial stream.

2.1 Introduction

The hyporheic zone is the region of saturated subsurface sediments with which water from the open channel of a stream interacts (Figure 2.1). Surface water enters the hyporheic zone, moves through the interstitial spaces of the sediments and returns to the open channel at a point downstream [*Harvey and Bencala*, 1993]. Any saturated subsurface region containing >10% surface water is considered hyporheic [*Triska et al.*, 1989]. Due to a heterogeneous distribution of sediment, hyporheic flow occurs through many different subsurface flow paths that exhibit a range of residence times, all of which are longer than the surface flow path through the thalweg of the stream [*Haggerty et al.*, 2000; *Gooseff et al.*, 2003]. Because of the increased residence time in the hyporheic zone and the close contact of the water with sediment biofilms, many important biogeochemical transformations that affect the stream ecosystem occur in the hyporheic zone.

The hyporheic zone is a critical site for the decomposition of organic matter, often accounting for a large proportion of whole-stream respiration [*Grimm and Fisher*, 1984; *Naegeli and Uehlinger*, 1997; *Fellows et al.*, 2001]. Once organic matter has been broken down into its inorganic constituents, those inorganic nutrients are transported back to the stream via hyporheic upwelling. *Dent et al.* [2001] found that nutrient concentrations in the surface water at upwelling zones are higher than in other areas in the surface stream. Benthic algal abundance and chlorophyll *a* accrual rates have also been shown to be higher in upwelling zones than in downwelling zones [*Valett et al.*, 1994; *Pepin and Hauer*, 2002].

Studies of hyporheic exchange in temperate streams have shown that it is strongly influenced by stream geomorphologic characteristics. Many physical factors act to control hyporheic exchange rates and residence times. They include abrupt changes in channel gradient due to streambed topography [*Harvey and Bencala*, 1993], degree of channel constraint, presence of secondary channels or channel splits [*Kasahara and Wondzell*, 2003], channel sinuosity [*Wroblicky et al.*, 1998] and degree of channel complexity due to land use [*Gooseff et al.*, 2007]. Other factors include stream size [*D'Angelo et al.*, 1993], parent material of the stream catchment, sediment size, hydraulic conductivity [*Morrice et al.*, 1997; *Storey et al.*, 2003], stream channel friction, channel vegetative cover [*Harvey et al.*, 2003] and seasonal changes in stream discharge, head gradients and local groundwater recharge [*Wroblicky et al.*, 1998; *Storey et al.*, 2003). All factors influencing the geomorphology of a stream may have an effect on its hyporheic exchange characteristics. In turn, hyporheic exchange patterns control the residence time of water in the hyporheic zone, which influences the biogeochemical transformations occurring there.

Most hyporheic studies have been carried out in temperate streams and only a handful of studies have focused on hyporheic dynamics in arctic [*Edwardson et al.*, 2003] or antarctic [*McKnight et al.*, 1999; *Gooseff et al.*, 2003] environments. *Edwardson et al.* [2003] found that, despite the presence of permafrost, the thaw bulb allows for significant hyporheic exchange and nutrient regeneration to occur in arctic tundra streams on the North Slope. They found that the hyporheic zones of arctic tundra streams served as sites for the mineralization of organic matter, often followed by nitrification. Upwelling from

the hyporheic zone to the surface water supplied the streams with nitrate, ammonium, phosphate and carbon dioxide. The nutrients supplied by hyporheic regeneration are very important to arctic tundra stream ecosystems because they are quite oligotrophic and nutrient supply is limited.

While the previously mentioned geomorphic influences on hyporheic exchange are very important in arctic streams, an additional control on exchange extent in arctic tundra streams may be the boundary condition imposed by the continuous permafrost present beneath these streams. The potential role of permafrost as a control on hyporheic zone dynamics in arctic streams was virtually unknown prior to this research.

The North Slope of the Brooks Range in Alaska, an arctic region underlain by continuous permafrost, exhibits three main stream types: mountain, spring and tundra [*Craig and McCart*, 1975]. Tundra streams, which drain the tundra-covered foothills of the North Slope, freeze solid in the winter, flood in late May or early June and flow for about four months of the year. They typically exhibit lower turbidity than mountain streams and warmer temperatures, lower pH and lower conductivity than both mountain and spring streams. Depending on stream slope, two common stream geomorphologic types occur within the tundra stream classification: (a) high-gradient, alluvial streams with alternating riffle-pool sequences and (b) low-gradient, peat-bottomed streams with a "beaded" morphology in which large, deep pools are connected by narrow, deep runs. *Huryn et al.* [2005] classified streams on the North Slope into five categories: mountain-spring, tundra-spring, tundra, mountain and glacier. They related physical stream

structure to biological function (i.e., macroinvertebrate assemblages) based on three factors: substratum freezing, substratum instability and nutrient supply.

Although tundra streams on the North Slope are underlain by continuous permafrost, an active layer of thawed soil develops to depths of about 25 to 40 cm deep as a result of increased air temperatures in the summer (June through August) [*Hinzman et al.*, 1991]. The active layer extends beneath stream beds where the energy of moving water creates a region of thawed sediments called the thaw bulb (Figure 2.2). *Bradford et al.* [2005] demonstrated that ground penetrating radar (GPR) is a useful tool for estimating thaw bulb depth beneath peat streams in arctic Alaska. *Brosten et al.* [2006] used GPR to compare seasonal thaw bulb development patterns in streams of contrasting geomorphology and found that high-energy, cobble-lined streams responded more quickly to seasonal temperature changes than lower-energy, peat-lined streams, which were better insulated.

The objective of our study was to compare hyporheic exchange patterns and biogeochemistry in two arctic tundra streams with contrasting geomorphologies (high-gradient, cobble-bottom and low-gradient, peat-bottom). The physical differences in these two streams are driven by their different slopes. We hypothesized that the differences in stream gradient that led to geomorphologic differences between the two steam types would affect the characteristics of hyporheic exchange in permafrost-controlled tundra streams on the North Slope. We also expected that the interaction between exchange depth and geomorphology would have important influences on biogeochemical dynamics in these streams. Specifically, we asked:

1. What portion of the thaw bulb participates in hyporheic exchange in the two stream types?
2. Are there differences in subsurface biogeochemical patterns (DO, NO_3, NH_4, SRP and DOC) in the two stream types?
3. Are there important differences in estimated average regeneration rates for NO_3, NH_4 and SRP in the two contrasting stream types?

2.2. Methods

2.2.1. Study Area

The study area is located near the Toolik Lake Field Station (68° 38'N, 149° 36'W) (Figure 2.3). Toolik Lake is located about 180 km south of the Arctic Ocean [*Hobbie et al.*, 1999]. The two second-order, clear-water streams in this study are a part of a series of lakes and connecting streams that flow north into Toolik Lake and eventually into the Arctic Ocean. This series of lakes and streams was described by *Kling et al.* [2000]. Before they enter Toolik Lake, the two streams flow parallel to each other, just a few hundred meters apart, and are separated by a small ridge. *Kling et al.* [2000] referred to these two stream reaches as the inlets to Lakes I-8 and I-Swamp (see Figure 2.3). Despite their close proximity to each other, the two study streams have very different physical characteristics.

These two streams were chosen to represent two geomorphically contrasting headwater, clear-water stream types on the North Slope of Alaska's Brooks Range. The first is a high-gradient, alluvial reach with pool-riffle sequences and cobble substrate and

the second is a low-gradient, peat-bottomed reach with large, deep pools connected by narrow, deep runs. These streams will be referred to as the alluvial stream and the peat stream, respectively. Both streams are underlain by permafrost, but also have a thaw bulb that develops beneath them throughout the summer months. Ground penetrating radar showed that the average depths of subsurface thaw are 157 cm in the alluvial stream and 67 cm in the peat stream [*T. Brosten*, unpublished data, 2006]. This difference in thaw depth occurs because the higher gradient, higher hydraulic conductivity and greater bed complexity of the alluvial stream promote deeper hyporheic flow paths, while the low thermal and hydraulic conductivity of the peat tend to insulate the permafrost.

2.2.2. Hyporheic Sampling

Hyporheic water samples were obtained from inexpensive, lightweight minipiezometers inserted into the streambed to known depths. Each minipiezometer was constructed from a 1.5-meter long tube of rigid Delrin plastic with a 6.3-mm outer diameter and 3.2-mm inner diameter. Five holes were drilled into the walls of the piezometers over the bottom 10 cm of its length and the bottom hole of each minipiezometer tube was left open (total open area = 68 mm^2). The drilled ends of the piezometers were covered with a geotextile sleeve to prevent sediment clogging.

The minipiezometers were bundled in sets of two (for the peat stream) or three (for the alluvial stream) so that the screened ends of the piezometers were a known distance apart. The installation of each bundle then provided 2 to 3 distinct sampling depths at one location in the streambed along the thalweg. The minipiezometer bundles

were arranged so that the deepest minipiezometer was installed at the deepest accessible point (i.e., depth of refusal). The shallowest minipiezometer was installed at approximately 10-20 cm beneath the streambed and the location of the mid-depth minipiezometer (in the alluvial sets) was placed roughly one third of the way between the shallow and deep minipiezometers. To span the respective depth ranges of thawed sediments in the two streams, piezometers were installed at average depths of 15 cm, 50 cm and 110 cm in the alluvial stream (Table 2.1) and at average depths of 12 cm and 33 cm in the peat stream (Table 2.2).

The nested bundles were installed into the streambed using a steel installation tool consisting of a hardened steel rod (19.0 mm diameter, 240 cm length) within a hardened steel tube (25.4 mm inner diameter, 235 cm length) similar to that described by *Baxter et al.* [2003]. The inner rod and sleeve were pounded into the streambed to the depth of refusal using a fencepost driver. The inner rod was removed from the sleeve and the minipiezometer bundle was inserted into the sleeve. The sleeve was then carefully removed, allowing the sediment to collapse around the minipiezometer bundle, securing its position within the thawed sediments.

Nine bundles were installed along a longitudinal transect in each of the two stream reaches (three replicates of three different stream features). In the alluvial stream the features were riffle heads, riffle tails and pools. In the peat stream, the analogous features were run heads, run tails and pools. Because the bundles consisted of three depths in the alluvial stream and two depths in the peat stream, the alluvial stream had a

total of 27 minipiezometers (Table 2.1) and the peat stream had a total of 18 minipiezometers (Table 2.2).

To take a hyporheic sample, a 60 ml disposable syringe (Becton-Dickenson, Franklin Lakes, NJ) was attached to each minipiezometer via a 3-way disposable syringe stopcock (Cole-Parmer, Vernon Hills, IL). A small volume of water (5-10 ml) was drawn into the syringe to clear the minipiezometer and was discarded via the open port of the 3-way stopcock without detaching the syringe from the minipiezometer. Fresh sample water was then drawn into the syringe and processed for analysis as described in the following sections. Between sampling events the syringes were removed from the minipiezometers, but the 3-way stopcocks were left in place in the off position, such that the minipiezometer was closed to the atmosphere.

2.2.3. Extent of Hyporheic Exchange

Conservative solute injection experiments (SIEs) using Rhodamine WT (RWT) were performed twice (June and August) during the summer season in each stream to determine the extent of hyporheic exchange within the thaw bulb. The alluvial SIEs were performed on 18-June-2005 (2.6-hour duration) and 8-August-2005 (2.3-hour duration). The peat SIEs were performed on 27-June-2005 (6.0-hour duration) and on 11-August-2005 (9.8 hour duration). During an SIE, the RWT was dripped into the stream water at a constant rate at the top of the reach until the surface water RWT concentration reached a plateau at the bottom of the reach. The peat stream SIEs were longer than the alluvial stream SIEs because it took longer to achieve a plateau in the peat stream due to its lower

stream gradient and discharge. Throughout the duration of the solute injection and for a period following the injection, surface and subsurface waters were sampled at regular intervals and samples were returned to the laboratory for analysis of RWT concentration using a Turner Designs 10-AU fluorometer. For each piezometer location, a tracer breakthrough curve (RWT concentration vs. time) was obtained for the surface water and each subsurface location sampled for each SIE.

From the surface and subsurface breakthrough curves at each location, the maximum concentrations were identified. Using the maximum stream water RWT concentrations ($Surface_{MAX}$) and the maximum subsurface water RWT concentrations ($Subsurface_{MAX}$), the percent connection to surface water (P_C) was calculated for each of the subsurface locations sampled using the following equation:

$$P_C = \frac{Subsurface_{MAX}}{Surface_{MAX}} \times 100$$

This metric was used to compare the degree of surface-subsurface water connection at each site.

2.2.4. Biogeochemical Sampling and Analysis

Four times during the summer, surface water and all subsurface locations in both streams were sampled and analyzed for concentrations of nitrate (NO_3), ammonium (NH_4), soluble reactive phosphorus (SRP), dissolved oxygen (DO) and dissolved organic carbon (DOC). For each stream, the results from the first two sampling dates were averaged and reported as June data and the results from the last two sampling dates were averaged and reported as August data.

DO was measured in the field (directly in the sampling syringe after carefully removing the plunger) with a WTW Oxi 340i handheld dissolved oxygen meter. The reported accuracy for this dissolved oxygen meter is ±0.01 mg/L (WTW, Weilheim, Germany). However, due to our modified use of the equipment (measuring concentration of water in syringe pulled from the subsurface), we estimate a more liberal accuracy of ±0.1 mg/L. All other biogeochemical samples were filtered through a 0.45 μm, 25 mm diameter, cellulose acetate syringe filter and kept on ice for transport to the laboratory. Ammonium and SRP analyses were done within 24-48 h at the Toolik Field Station. Ammonium analysis was performed using the orthophthaldialdehyde (OPA) method [*Holmes et al.*, 1999]. The minimum detection limit of Protocol A of the OPA Method is 0.03 μM and the relationship is linear up to a concentration of 6.2 μM [*Holmes et al.*, 1999]. SRP analysis was performed using the colorimetric molybdate blue method [*Hach Company*, 1997]. The reported minimum detection limit for this method is 0.004 mg/L and the reported precision is 1 RSD. Nitrate samples were immediately frozen at the field station then transported to the University of Vermont's Rubenstein Ecosystem Science Laboratory in Burlington, VT where they were analyzed within 6 months by the cadmium reduction technique [*Askew and Smith*, 2005, p. 123]. The cadmium reduction method has a reported detection limit of 0.01 mg NO_3-N/L. Reported standard deviations for standards at four concentrations (0.04 mg/L, 0.24 mg/L, 0.55 mg/L and 1.04 mg/L) were ±0.005, ±0.004, ±0.005 and ±0.01, respectively [*Askew and Smith*, 2005, p. 123]. DOC samples were preserved with 6N hydrochloric acid to a pH of 2, transported to the Ecosystems Center in Woods Hole, MA and analyzed by the persulfate-ultraviolet

method within 6 months [*Baird*, 2005, p. 23]. The reported minimum detection limit for this method is 0.01 mg/L and the reported single-operator precision (P) for a concentration range of 0.1 – 4000 mg/L is expressed as $P = 0.04x + 0.1$, where x = DOC concentration [*Baird*, 2005, p. 23]. All of the above analyses were based on standard calibration curves built each day before an analytical run. These response vs. concentration curves were fitted via linear regressions and r^2 values of ≥ 0.99 were ensured. In all analytical runs, check standards of a known, mid-range concentration were analyzed to ensure congruence with the day's standard calibration curve.

2.2.5. Calculation of Nutrient Regeneration Rates

Net nutrient regeneration rates (R_{NR}) were estimated for NO_3, NH_4 and SRP for the two stream reaches in both June and August. R_{NR} was calculated as the difference between the flux of a given nutrient into the subsurface (F_{IN}) and the flux of that nutrient out of the subsurface (F_{OUT}). In this way, a positive R_{NR} value indicates that the subsurface is a source of a given nutrient and a negative R_{NR} value indicates that it is a sink for that nutrient. F_{IN} was calculated by multiplying the average surface water nutrient concentration ($[N]_{SURF}$) by the reach-averaged rate of surface-subsurface water exchange (R_{EXCH}). Similarly, F_{OUT} was calculated by multiplying the connectedness-weighted, reach-averaged subsurface nutrient concentration ($[N]_{SUB}$) by R_{EXCH}. *Zarnetske* [unpublished data, 2006] used the SIE data in conjunction with MODFLOW and MODPATH modeling to estimate R_{EXCH} for each reach in June and August. Because the stream reaches were neither gaining nor losing in this study, the rate of exchange

from surface to subsurface ($R_{EXCH(IN)}$) was equal to the rate of exchange from subsurface to surface ($R_{EXCH(OUT)}$). The calculation of $[N]_{SUB}$ was less straightforward than that of $[N]_{SURF}$ due to the varying degree of surface-subsurface connection among the subsurface samples. Instead of simply averaging all of the subsurface nutrient concentrations in a reach to arrive at $[N]_{SUB}$, each individual subsurface nutrient concentration was multiplied by the P_C value at that subsurface location. All of those connectedness-weighted, subsurface nutrient concentrations were then summed for a reach and divided by the sum of the P_C values for that reach to arrive at a value of $[N]_{SUB}$ that accounted for the degree of surface-subsurface connection. The following equations summarize the procedures described above:

$$R_{NR} = F_{OUT} - F_{IN}$$

$$F_{IN} = R_{EXCH} \cdot [N]_{SURF}$$

$$F_{OUT} = R_{EXCH} \cdot [N]_{SUB}$$

In this case, $R_{EXCH}(IN) = R_{EXCH}(OUT)$

$$[N]_{SUB} = [N]_{SUB\text{-}W} = \frac{\Sigma ([N_{SUBij}] \cdot P_{Cij})}{\Sigma (P_{Cij})}$$

where i = depth and j = feature

2.2.6. Statistical Analysis

Non-parametric statistics were used to analyze these data because the total number of data points was relatively small and the majority of the RWT and biogeochemical data were not normally distributed, could not be transformed to

normality due to the large number of zero values, and may not have been independent (at least within a stream type). For each response variable in each stream type, separate Mann-Whitney tests were performed for each of the predictor variables: depth, feature and time. For depth comparisons, the median value for a given parameter at a particular subsurface depth was compared to the median value for that parameter in the surface water. The selected alpha value (α) for the Mann-Whitney comparison tests was 0.05, but because multiple comparisons were made in some cases, α was divided by the number of comparisons made for each response variable (n) to arrive at an adjusted alpha value (α') that was more conservative (see Tables 2.4 and 2.5 for p-values).

2.3. Results

2.3.1. Extent of Hyporheic Exchange

P_C decreased exponentially with depth in the subsurface in both streams to a point where the bottom subsurface locations in each had a median value of 0% connection to surface water (Fig. 2.4a). By definition, the surface water connection values in both streams were 100%. Median P_C values in the shallow subsurface (83%) and medium subsurface (7%) of the alluvial stream were not significantly different from the 100% P_C value of the surface water ($\alpha' = 0.017$, $p = 0.067$ (shallow), $p = 0.026$ (medium)). The median P_C value at the bottom subsurface depth of the alluvial stream (0%), however, was significantly lower than the surface water value ($p = 0.007$). In the peat stream, the median P_C value in the shallow subsurface (47%) was not significantly different from the

surface water P_C value of 100% ($\alpha' = 0.025$, $p = 0.027$), but the median P_C value at the bottom subsurface depth (0%) was significantly lower than the surface water P_C ($\alpha' = 0.025$, $p = 0.013$).

While P_C values at all features in both streams were variable, riffle head subsurface locations in the alluvial stream were more connected to the surface water than riffle tail or pool locations (Figure 2.4b). Riffle head locations had a median P_C value of 25%, while riffle tails and pools had median P_C values of 2% and 0%, respectively. There were no significant differences in P_C among features in the peat stream. All locations in the peat stream had median P_C values of $\leq$2%. There were no significant increases or decreases in P_C over time in either stream type.

2.3.2. Biogeochemical Comparisons between the Two Streams

There were no significant differences between the concentrations of DO, SRP, NH_4, NO_3 or DOC in the surface water of the two study streams (Table 2.3a). There were, however, significant differences in the biogeochemical composition of subsurface water in the two streams. All five parameters measured in the subsurface were significantly different between the two streams (Table 2.3b). The alluvial subsurface water exhibited significantly higher DO and NO_3 concentrations than the peat subsurface water, but significantly lower SRP, NH_4 and DOC concentrations than the peat subsurface water.

2.3.2.1. Dissolved Oxygen

In both streams, DO concentration decreased with depth in the subsurface (Figure 2.5a). DO was depleted much more steeply with depth in the peat subsurface than in the alluvial subsurface. In the alluvial stream, the median DO concentration in the shallow subsurface (8.3 mg/L) was not significantly different ($p = 0.131$) from the surface water (9.7 mg/L). Median DO concentrations at medium and bottom subsurface locations were moderate (4.7 mg/L and 4.1 mg/L, respectively) and were both significantly lower than the median alluvial surface water ($p = 0.008$ and $p = 0.003$, respectively). In the peat stream, median DO concentration in the shallow subsurface (4.2 mg/L) was significantly lower ($p = 0.002$) than the median peat surface water DO concentration (9.2 mg/L). Median DO concentration in the bottom subsurface of the peat stream (1.0 mg/L) was also significantly lower than that of the surface water ($p = 0.002$).

In the alluvial stream, subsurface pool locations had a lower median DO concentration (2.5 mg/L) than riffle tail (median: 6.7 mg/L) or head (median: 8.1 mg/L) subsurface locations (Figure 2.5b). The difference between median subsurface DO concentrations at pool and riffle head locations was statistically significant ($p = 0.001$). There were no significant differences in subsurface DO concentration among features within the peat stream. Median subsurface DO concentrations were consistently significantly higher in the alluvial subsurface than in the peat subsurface. Median subsurface DO concentration increased significantly from June (4.2 mg/L) to August (7.3

mg/L) in the alluvial stream ($p = 0.026$). There was no significant difference in median subsurface DO concentration over time in the peat stream.

In each stream, there was a positive correlation between subsurface DO concentration and P_C. The Spearman's correlation coefficient for these two variables was 0.74 ($p < 0.001$) in the alluvial stream and 0.78 ($p < 0.001$) in the peat stream (Figure 2.6).

2.3.2.2. Nitrate

Patterns of subsurface nitrate concentration with depth were very different in the two stream types. Nitrate concentrations increased with depth in the subsurface of the alluvial stream and decreased with depth in the subsurface of the peat stream (Figure 2.7a). Although the increase with depth was not statistically significant in the alluvial subsurface, median nitrate concentrations increased progressively from 5.75 μM in the surface water to 9.64 μM in the bottom subsurface. Median nitrate concentration decreased significantly in the peat stream from 7.49 μM in the surface water to 2.25 μM ($p = 0.008$) in the shallow subsurface and to below detection in the bottom subsurface ($p < 0.001$). There were no significant differences in median subsurface nitrate concentration with feature or time in either stream (Figures 2.7b and 2.7c).

2.3.2.3 Ammonium

There were no significant differences in median ammonium concentration with depth in the alluvial subsurface, but there were significant increases in ammonium

concentration with depth in the peat subsurface (Figures 2.8a and 2.8d). Median ammonium concentration increased significantly from 0.52 μM in the surface water of the peat stream to 6.78 μM in the shallow subsurface ($p = 0.018$) and to 101.40 μM in the bottom subsurface ($p = 0.002$).

There were no significant differences in subsurface ammonium concentration in the alluvial stream with respect to stream feature (Figure 2.8b). In the peat stream, however, the median subsurface ammonium concentration was significantly higher in pool locations (196.18 μM) than in run head (40.62 μM, $p = 0.008$) or tail (10.69 μM, $p = 0.001$) locations (Figure 2.8e). Subsurface ammonium concentrations decreased significantly ($p < 0.001$) from June (0.47 μM) to August (0.23 μM) in the alluvial stream (Figure 2.8c). No significant temporal pattern was evident with subsurface ammonium concentrations in the peat stream (Figure 2.8f).

2.3.2.4 Soluble Reactive Phosphorus

Patterns of SRP concentration in the two streams were very similar to those seen for ammonium. Again, there were no significant differences in median SRP concentration with depth in the alluvial subsurface (Figure 2.9a). In the peat stream, however, median SRP concentration increased significantly with depth in the subsurface. It increased significantly from 0.03 μM in the surface water to 0.14 μM in the shallow subsurface ($p = 0.003$) and 0.57 μM in the bottom subsurface ($p = 0.002$) (Figure 2.9a).

In the alluvial stream, subsurface SRP concentration was not significantly different among stream features (Figure 2.9b). In the peat stream, however, median

subsurface SRP concentration was significantly higher in pool locations (0.85 μM) than in run head (0.20 μM, $p = 0.005$) or tail (0.13 μM, $p = 0.003$) locations (Figure 2.9b). There were no significant changes in subsurface SRP concentration over time in either stream type (Figure 2.9c).

2.3.2.5. Dissolved Organic Carbon

In the alluvial stream, there were no significant differences in median DOC concentration with depth in the subsurface (Figure 2.10a). However, in the peat stream, shallow subsurface (467 μM) and bottom subsurface (635 μM) median DOC concentrations were both significantly higher than the surface water median DOC concentration (339 μM) ($p = 0.004$ and $p = 0.003$, respectively) (Figure 2.10a).

In the alluvial stream, there were no significant differences in median DOC concentration with respect to stream feature, but in the peat stream, pool locations had significantly higher median subsurface DOC concentrations (1057 μM) than run heads (535 μM) or tails (469 μM) ($p < 0.001$) (Figure 2.10b). There was a significant increase in median subsurface DOC concentration from June (285 μM) to August (301 μM) in the alluvial subsurface ($p = 0.007$), but no significant differences over time in the peat stream (Figure 2.10c).

2.3.3. Estimates of Nutrient Regeneration Rates

R_{EXCH} was two orders of magnitude higher in the alluvial stream (June: 2.78 L s^{-1}, August: 2.93 L s^{-1}) than in the peat stream (June: 0.0669 L s^{-1}, August: 0.0732 L s^{-1}).

R_{NR} was calculated for NO_3, NH_4 and SRP for each stream reach in June and August. The alluvial hyporheic zone served as a source of ammonium (June: 1.50 μmol m^{-2} h^{-1}, August: 1.32 μmol m^{-2} h^{-1}) and SRP (June: 0.70 μmol m^{-2} h^{-1}, August: 0.39 μmol m^{-2} h^{-1}) to the stream throughout the summer of 2005 and switched from being a sink for nitrate in June (-20.11 μmol m^{-2} h^{-1}) to being a source of nitrate in August (35.84 μmol m^{-2} h^{-1}). The hyporheic zone of the peat stream consistently served as a source of ammonium (June: 3.68 μmol m^{-2} h^{-1}, August: 9.90 μmol m^{-2} h^{-1}) and SRP (June: 0.02 μmol m^{-2} h^{-1}, August: 0.07 μmol m^{-2} h^{-1}) to the stream and as a sink for nitrate (June: -1.48 μmol m^{-2} h^{-1}, August: -1.58 μmol m^{-2} h^{-1}) during the summer of 2005. The alluvial hyporheic zone was a stronger source of SRP than the peat hyporheic zone, but a much weaker source of ammonium than the peat hyporheic zone. Nitrate regeneration rates were much more variable in the alluvial stream than in the peat stream.

2.4. Discussion

2.4.1. Extent of Hyporheic Exchange

According to *Triska et al.* [1989], the hyporheic zone is considered to be any subsurface zone containing at least 10% stream water. By this definition, any subsurface sample that has a P_C >10% can be considered hyporheic. In both streams, P_C decreased exponentially with depth. The median P_C was >10% down to an average depth of approximately 15 cm in the alluvial subsurface and was >10% down to an average depth of 12 cm in the peat subsurface. Beneath those depths, median P_C was <10% in both

stream types. While the median P_C was 7% at medium depths in the alluvial stream, values were highly variable, ranging from 0 to 94%. This indicates that hyporheic exchange is occurring at the medium depths in the alluvial subsurface, but that this exchange is occurring via flow paths that have quite variable residence times (i.e., flow paths that vary in length, flow rate or both). RWT was rarely present at the bottom of the thaw bulb in either stream, indicating a lack of surface-subsurface connection at these depths over the timescale of our tracer experiments. They may be connected to the surface water, however, by flow paths with very long residence times.

In summary, the shallow subsurface of the alluvial stream (depth range: 9-29 cm) was highly connected to the surface water, the medium subsurface (depth range: 39-57 cm) was moderately connected to the surface water and the bottom subsurface (depth range: 81-136 cm) was not connected to the surface water over the time scale of the SIEs in this study. In the peat stream, the top 12 cm of the subsurface was moderately to highly connected to the surface water, but somewhere between 12 and 33 cm depth, the degree of surface-subsurface water connection was greatly diminished, such that at depths $\geq$33 cm, there was a complete lack of exchange over the time scale of the SIEs. Ground penetrating radar data have indicated average thaw depths of 122 cm and 191 cm beneath the alluvial stream in June and August, respectively, and average thaw depths beneath the peat stream of 54 cm and 79 cm in June and August, respectively [T. Brosten, unpublished data, 2006]. Based on these data, active hyporheic exchange does not occupy the entire thaw bulb. Rather, the majority of the surface-subsurface water interaction was limited to the uppermost portions of the thaw bulb in both stream types.

The extent of surface-subsurface exchange appears to be constrained more by hydraulic head gradients established by streambed complexity than by depth of the thaw bulb. Abrupt changes in channel gradient (i.e., bed complexity) elicit hyporheic exchange. The alluvial stream has a higher gradient and more complex streambed topography than the peat stream [*Zarnetske*, 2006] and so we would expect a greater degree of hyporheic exchange there than in the peat stream. The physical differences in these two streams are driven by their different slopes. The greater slope of the alluvial stream creates a faster rate of water flow, which provides the energy to carry fine sediments downstream, leaving boulders, cobbles and sand behind. In contrast, the lesser slope of the peat stream results in a slower water flow rate, which does not wash all fine sediments downstream. Instead, those fine sediments fill in the depressions in the streambed, effectively evening out the terrain and reducing the complexity of streambed topography and creating a fine-grained, organic-rich, peat-lined substrate. In fact, the data from this study show that the alluvial stream has a greater degree of surface-subsurface connection than the peat stream, with significant connection at shallow subsurface locations and moderate connection at medium subsurface locations, whereas all surface-subsurface exchange in the peat stream is limited to the top 12 cm of the streambed sediments (Figure 2.4a).

Riffle heads are known to be a point of downwelling [*Harvey and Bencala*, 1993], so we would also expect to see a higher degree of surface-subsurface connection there than at other stream features, especially pools, which tend not to be very active exchange sites. Again, our data show that riffle head locations in the alluvial subsurface are the

features exhibiting the highest degree of connection to the surface water (Figure 2.4b). Because of the lesser degree of streambed complexity in the peat stream, this pattern is not seen in the peat stream (Figure 2.4b).

2.4.2. Biogeochemical Comparisons between the Two Streams

While there were no significant differences in the biogeochemistry of the surface water of the two stream types, there were significant differences in the biogeochemistry of the subsurface water of the two stream types (Table 2.3). Concentrations of all five constituents measured in the subsurface were significantly different between the two stream types. Thus, while the watershed characteristics that affect the surface water composition of the two streams were comparable, subsurface processes in the two streams were quite different.

The degree of surface-subsurface connection drives most of the biogeochemical patterns seen in the two streams. There was a positive correlation in both streams between P_C and subsurface DO concentration (Figure 2.6). This indicates that subsurface hydrology strongly influences the biogeochemical characteristics that develop there. For instance, the lack of oxygen and nitrate and the exceptionally high concentrations of ammonium and SRP in the bottom of the peat thaw bulb are most likely due to a lack of connection to the surface water. Organic matter mineralization occurs there, yet the mineralized ammonium and SRP are transported back to the surface water at a very slow rate and concentrations build up at these deep, relatively disconnected regions. Ammonium and SRP concentrations are significantly higher in the subsurface peat of the

pool features than in the subsurface of the runs, indicating that they are regions of considerably lower surface-subsurface connection. The lack of oxygen there indicates that DO is not regularly renewed by incoming stream water and that any oxygen that may arrive there is quickly consumed via heterotrophic metabolism. That nitrate is undetectable at the bottom of the peat thaw bulb indicates that any nitrate that may be present there is quickly being consumed by denitrification, dissimilatory nitrate reduction, or other similar nitrate transformation process. With respect to concentrations of all biogeochemical constituents measured in this study, the shallow subsurface region represented an intermediate condition between surface water and deep subsurface conditions. Again, this is likely due to the degree of surface-subsurface connection at the shallow subsurface locations. At a median connection value of 47%, it would be expected that shallow subsurface locations would be more similar to surface water conditions than the deep subsurface locations would be.

In contrast to the peat stream, the data from the alluvial stream show a more gradual decrease in surface-subsurface connection with depth in the subsurface. This can be seen from both the tracer and biogeochemical data. Connection to surface water is very high in the shallow subsurface and lower, but still significant, at medium depths. Along with this gradual decrease in connection there is a gradual decrease in subsurface DO concentration, but DO is maintained at a moderate level throughout the thaw depth. Subsurface ammonium and SRP concentrations are not significantly different at any depth from surface water ammonium and SRP concentrations. This suggests a higher

degree of surface-subsurface connection at all depths, which is a very different pattern than that seen in the subsurface of the peat stream.

The aerobic subsurface environment of the alluvial stream supports the production of nitrate via nitrification. Nitrate concentrations increased with depth in the subsurface of the alluvial stream (Figure 2.7a) and nitrate concentrations are significantly higher at riffle tails than at riffle heads or pools (Figure 2.7b). This suggests that oxygenated water entering the hyporheic zone from the stream at riffle heads undergoes nitrification as it passes through hyporheic flowpaths and becomes enriched with nitrate by the time it reaches the riffle tail and reenters the stream. Subsurface nitrate concentrations increased from June to August in the alluvial stream, while subsurface ammonium concentrations concurrently decreased (Figures 2.7c and 2.8c), which provides further evidence that nitrification is an important process in the alluvial stream and that the rate of nitrification may have increased throughout the summer season.

2.4.3. Estimates of Nutrient Regeneration

In both streams, the subsurface was a source of ammonium and SRP to the surface water in June and August (Figure 2.11). Subsurface regeneration rates of ammonium in the peat stream were three- to ten-fold greater than those in the alluvial stream. Ammonium production increased three-fold in the peat stream from June to August. Subsurface SRP production, however, was an order of magnitude higher in the alluvial stream than in the peat stream. The subsurface of the peat stream consistently served as a net sink for nitrate in both June and August (Figure 2.11). This is likely due

to the anaerobic conditions in the peat subsurface that facilitate denitrification, dissimilatory nitrate reduction or other nitrate consuming processes. In June, the alluvial subsurface appeared to be a net sink for nitrate as well, but by August, it was a source for nitrate to the surface water. Along with this change, net ammonium production rates decreased slightly from June to August in the alluvial stream. The net increase in nitrate production rates along with the net decrease in ammonium production rates supports the conclusion that nitrification is an important process in the alluvial stream and that nitrification rates may be increasing throughout the warm season.

The net nitrate, ammonium and SRP regeneration rates averaged for the two sampling periods in each stream in this study show that the hyporheic zone plays a slightly different role in each of the two stream types, especially with regard to nitrate (Table 2.6). The hyporheic zone in the alluvial stream is a source of all three nutrients to the surface water. The hyporheic zone of the peat stream is a source of ammonium and SRP to the stream and a sink for nitrate. While hyporheic zones in both streams supply the streams with these two nutrients, the alluvial subsurface produces SRP at a much higher rate than the peat subsurface and the peat subsurface produces ammonium at a much higher rate than the alluvial subsurface. Furthermore, it is evident that the alluvial subsurface produces nitrate, while the peat subsurface consumes it. Thus, there is clear evidence that the differences in the geomorphology of the two streams in this study resulted in significant and important differences in the biogeochemistry of these two streams.

Nutrient regeneration rates estimated by *Edwardson et al.* [2003] for the reference reach of the Kuparuk River, Alaska, are similar to those made for the alluvial reach in this study (Table 2.6). The Kuparuk River is in relatively close proximity to the streams sampled in this study. It is a fourth-order, cobble-bottom alluvial reach that is low in productivity and dominated by diatoms. Because it is an alluvial reach, it is most similar to the alluvial reach sampled in this study. *Edwardson et al.* [2003] found that the hyporheic zone of the Kuparuk served as a source of nitrate, ammonium and SRP. However, Kuparuk River estimates of all three nutrients were an order of magnitude higher than the alluvial stream estimates in this study.

The Kuparuk River estimates could be higher than our alluvial stream estimates for several reasons. The studies were carried out in two different summers, using quite different methods to sample the subsurface water and to calculate surface-subsurface exchange rates. *Edwardson et al.* [2003] sampled the subsurface from just one depth (35-55 cm) for nutrient concentrations and assumed that was an accurate representation of the hyporheic zone. In our study, multiple depths were sampled for nutrient concentrations at each subsurface sampling location. Furthermore, each subsurface nutrient concentration was weighted by the degree of connection to surface water at that location (available for each sampling location from RWT tracer test results). With greater subsurface sampling resolution and surface-subsurface connection data for each individual sampling location, our estimates are likely to be more accurate than those put forth by *Edwardson et al.* [2003].

Exchange rate estimates in our study came from MODFLOW and MODPATH modeling [see *Zarnetske*, 2006], while exchange rate estimates in the *Edwardson et al.* [2003] study resulted from OTIS modeling. *Edwardson et al.* [2003] assumed that 50% of the exchange rate represented hyporheic exchange and also assumed that 50% of the OTIS-modeled transient storage zone area (this includes both surface and subsurface transient storage zones) was hyporheic. If the assumed proportion of exchange rate or transient storage area attributed to the hyporheic zone was overestimated, the estimated nutrient regeneration rates from the Kuparuk may have been artificially high. Overestimation may have also resulted from the fact that the proportion of total transient storage area assumed to be hyporheic storage (50% of total transient storage area) was not corrected for porosity. Rather, the entire subsurface storage area was assumed to have exchanged, whereas if this number would have been corrected for the sediment present in this zone, perhaps only 50% of this area would have exchanged. Therefore, if subsurface porosity would have been considered, nutrient regeneration rates would have been half that reported by *Edwardson et al.* [2003]. This would bring them closer to the rates we estimated for the alluvial stream in this study.

2.5. Conclusions

Both tracer and biogeochemical data from our study support the conclusion that the majority of hyporheic exchange occurs in the shallow layers of the subsurface in both arctic tundra stream types studied. They indicate, however, that the patterns of surface-subsurface connection are different in high-gradient, alluvial and lower-gradient, peat-

bottomed streams. Beneath the shallow subsurface region of the peat stream (~10 cm), connection to surface water is distinctly diminished. This is evidenced by the fact that no tracer appeared in any of the bottom piezometers in the peat stream during either SIE and also by the fact that there is such a distinct difference between shallow and bottom locations' concentrations of DO and all nutrients.

While P_C decreases and biogeochemical characteristics change with depth in the alluvial subsurface as well, these changes happen more gradually there than in the peat stream. Some connection is maintained through medium depths and it is not until a depth of about one meter that the connection occurs over too slow a timescale to be detected with our SIEs. This limitation of surface-subsurface connection in the alluvial stream occurs at a depth that is 5 to 10 times deeper than it is in the peat subsurface. The median DO concentration of approximately 4 mg/L at the bottom of the alluvial thaw bulb indicates that, even though there is no surface-subsurface water connection on the timescale of our SIEs, there has to be enough connection to maintain that moderate concentration of DO there. By contrast, the median DO concentration at the bottom depths of the peat subsurface (i.e., at just 33 cm) is 1.0 mg/L.

The results from our study support the hypothesis that two arctic tundra streams of differing slope, bed complexity and resulting hydraulic head gradients exhibit very different patterns of surface-subsurface exchange and transient storage. These differences have in turn created very different biogeochemical patterns in the subsurface waters of the two stream types. These differences can be seen in the spatial variation in

concentrations of nitrate, ammonium and SRP in the two streams and lead to clear differences in estimated net nutrient regeneration rates.

The majority of hyporheic exchange in both streams occurs in the uppermost portion of the thaw bulb. Hyporheic exchange occurs to a deeper depth in the alluvial stream than in the peat stream, but it appears that this difference is related more to stream geomorphology (i.e., streambed complexity and small scale head gradients) than it is to the permafrost constraint. Permafrost may inhibit hyporheic exchange, but only up to the point where deeper thaw no longer results in deeper exchange. At that point, the geomorphology of a stream plays a bigger role in determining the extent of hyporheic exchange. This indicates that, assuming the geomorphology of these two streams remains the same, the depth of hyporheic exchange would not likely increase as a result of an increased thaw bulb depth.

2.6. Implications

Because they are characterized by cold temperatures, ice, snow, permafrost and annual freeze-thaw cycles, arctic ecosystems are likely to be more sensitive to and affected by climate change than temperate ecosystems [*McBean*, 2005]. Air, soil and permafrost temperatures are likely to increase, the thaw season is likely to increase in length and the depth of the permafrost active layer is also likely to increase [*Wrona et al.*, 2005]. A deeper thaw bulb or longer thaw season could allow for a greater magnitude of hyporheic nutrient processing on an annual basis. Therefore, it is particularly important

to understand the current role of the hyporheic zone in arctic streams so that we may also predict how that role might be altered by global climate change.

While the results from our study indicate that extent of hyporheic exchange is not likely to increase with an increase in thaw bulb depth alone, other possible effects of climate change could affect the magnitude of hyporheic biogeochemical processing and nutrient regeneration. If nutrient regeneration rates do not change, but the thaw season increases in length, the magnitude of net nutrient regeneration would be larger on an annual basis due to an increase in the number of days per year that conditions are favorable for hyporheic exchange (i.e., thawed subsurface sediments and increased soil temperatures). A possible increase in sediment temperatures could also increase the annual magnitude of hyporheic biogeochemical processing due to increasing microbial metabolic rates. Alternatively, climate change may result in changes in the geomorphology of streams. This research has shown that geomorphology can significantly affect hyporheic characteristics. Increased sediment inputs from thermokarst activity in the region could cause colmation, a clogging of the interstitial spaces of streambed sediments, which could impede hyporheic exchange and convert a stream from alluvial-type to peat-type characteristics. These inputs would also likely significantly increase external carbon and phosphorus loading, which would disturb the current nutrient and organic matter budgets of these arctic tundra streams. This would clearly affect hyporheic biogeochemical processes. The overall impact of climate change on hyporheic processes in arctic tundra stream ecosystems is currently unknown, but is likely to be important.

LITERATURE CITED

Askew, E.F., and R. Smith (2005), Inorganic nonmetallic constituents, in *Standard Methods for the Examination of Water and Wastewater*, edited by A.D. Eaton, L.S. Clesceri, E.W. Rice and A.E. Greenberg, p.123, Port City Press, Baltimore, Maryland.

Baird, R.B. (2005), Aggregate organic constituents, in *Standard Methods for the Examination of Water and Wastewater*, edited by A.D. Eaton, L.S. Clesceri, E.W. Rice and A.E. Greenberg, p. 23, Port City Press, Baltimore, Maryland.

Baxter, C., F.R. Hauer, and W.W. Woessner (2003), Measuring groundwater-stream water exchange: New techniques for installing minipiezometers and estimating hydraulic conductivity, *Transactions of the American Fisheries Society*, *132*, 493-502.

Bradford, J.H., J.P. McNamara, W.B. Bowden, and M.N. Gooseff (2005), Measuring thaw depth beneath peat-lined arctic streams using ground-penetrating radar, *Hydrological Processes*, *19*, 2689-2699.

Brosten, T.R., J.H. Bradford, J.P. McNamara, J.P. Zarnetske, M.N. Gooseff, and W.B. Bowden (2006), Profiles of temporal thaw depths beneath two arctic stream types using ground-penetrating radar, *Permafrost and Periglacial Processes*, *17*, 341-355.

Craig, P.C., and P.J. McCart (1975), Classification of stream types in Beaufort Sea drainages between Prudhoe Bay, Alaska, and the Mackenzie Delta, N.W.T., Canada, *Arctic and Alpine Research*, *7*, 183-198.

Dent, C.L., N.B. Grimm, and S.G. Fisher (2001), Multiscale effects of surface-subsurface exchange on stream nutrient concentrations, *Journal of the North American Benthological Society, 20,* 162-181.

D'Angelo, D.J., J.R. Webster, S.V. Gregory, and J.L. Meyer (1993), Transient storage in Appalachian and Cascade mountain streams as related to hydraulic characteristics, *Journal of the North American Benthological Society*, *12*, 223-235.

Edwardson, K.J., W.B. Bowden, C. Dahm, and J. Morrice (2003), The hydraulic characteristics and geochemistry of hyporheic and parafluvial zones in Arctic tundra streams, North Slope, Alaska, *Advances in Water Resources*, *26*, 907-923.

Fellows, C.S., H.M. Valett, and C.M. Dahm (2001), Whole-stream metabolism in two montane streams: Contribution of the hyporheic zone, *Limnology and Oceanography, 46*, 523-531

Gooseff, M.N., S.M. Wondzell, R. Haggerty, and J. Anderson (2003), Comparing transient storage modeling and residence time distribution (RTD) analysis in geomorphically varied reaches in the Lookout Creek Basin, Oregon, USA, *Advances in Water Resources*, *26*, 925-937.

Gooseff, M.N., R.O. Hall, and J.L. Tank (2007), Relating transient storage to channel complexity streams of varying land use in Jackson Hole, Wyoming, *Water Resources Research*, *43*, W01417, doi:10.1029/2005WR004626.

Grimm, N.B., and S.G. Fisher (1984), Exchange between interstitial and surface water: Implications for stream metabolism and nutrient cycling, *Hydrobiologia*, *111*, 219-228.

Hach Company (1997), Method 8048: Orthophosphate by colorimetry, in The 1997 Edition of the Hach Water Analysis Handbook, Retrieved 18 April 2007 from National Environmental Methods Index, [http://www.nemi.gov].

Haggerty, R., S.A. McKenna, and L.C. Miegs 2000, On the late-time behavior of tracer test breakthrough curves, *Water Resources Research*, *36*, 3467-3479.

Harvey, J.W., and K.E. Bencala (1993), The effect of streambed topography on surface-subsurface exchange in mountain catchments, *Water Resources Research*, *29*, 89-98.

Harvey, J.W., M.H. Conklin, and R.S. Koelsch (2003), Predicting changes in hydrologic retention in an evolving semi-arid alluvial stream, *Advances in Water Resources*, *26*, 939-950.

Hinzman, L.D., D.L. Kane, R.E. Gieck, and K.R. Everett (1991), Hydrologic and thermal properties of the active layer in the Alaskan Arctic, *Cold Regions Science and Technology, 19*, 95-110.

Hobbie, J.E., B.J. Peterson, N. Bettez, L. Deegan, W.J. O'Brien, G.W. Kling, G.W. Kipphut, W.B. Bowden, and A.E. Hershey (1999), Impact of global change on the biogeochemistry and ecology of an Arctic freshwater system, *Polar Research*, *18*, 207-214.

Holmes, R.M., A. Aminot, R. Kérouel, B.A. Hooker, and B.J. Peterson (1999), A simple and precise method for measuring ammonium in marine and freshwater ecosystems, *Canadian Journal of Fisheries and Aquatic Sciences*, *56*, 1801-1808.

Huryn, A.D., K.A. Slavik, R.L. Lowe, S.M. Parker, D.S. Anderson, and B.J. Peterson (2005), Landscape heterogeneity and the biodiversity of Arctic stream communities: a habitat template analysis, *Canadian Journal of Fisheries and Aquatic Sciences, 62*, 1905-1919.

Kasahara, T., and S.M. Wondzell (2003), Geomorphic controls on hyporheic exchange flow in mountain streams, *Water Resources Research*, *39*(1), 1005, doi:10.1029/2002WR001386.

Kling, G.W., G.W. Kipphut, M.M. Miller, and W.J. O'Brien (2000), Integration of lakes and streams in a landscape perspective: the importance of material processing on spatial patterns and temporal coherence, *Freshwater Biology*, *43*, 477-497.

McKnight, D.M., D.K. Niyogi, A.S. Alger, A. Bomblies, P.A. Conovitz, and C.M. Tate (1999), Dry valley streams in Antarctica: Ecosystems waiting for water, *Bioscience*, *49*, 985-995.

Morrice, J.A., H.M. Valett, C.N. Dahm, and M.E. Campana (1997), Alluvial characteristics, groundwater-surface water exchange and hydrological retention in headwater streams, *Hydrological Processes*, *11*, 253-267.

Naegeli, W.M., and U. Uehlinger (1997), Contribution of the hyporheic zone to ecosystem metabolism in a prealpine gravel-bed river, *Journal of the North American Benthological Society*, *16*, 794-804.

Pepin, D.M., and F.R. Hauer., (2002), Benthic responses to groundwater-surface water exchange in 2 alluvial rivers in northwestern Montana, *Journal of the North American Benthological Society, 21*, 370-383.

Storey, R.G., K.W.F. Howard, and D.D. Williams (2003), Factors controlling riffle-scale exchange flows and their seasonal changes in a gaining stream: A three-dimensional groundwater flow model, *Water Resources Research*, *39*(2), 1034, doi:10.1029/2002WR001367.

Triska, F.T., V.C Kennedy, R.J. Avanzino, G.W. Zellweger, and K.E. Bencala (1989), Retention and transport of nutrients in a third-order stream in northwestern California: Hyporheic processes, *Ecology*, *70*, 1893-1905.

Valett, H.M., S.G. Fisher, N.B. Grimm, and P. Camill (1994), Vertical hydrologic exchange and ecological stability of a desert stream ecosystem, *Ecology*, *75*, 548-560.

Wroblicky, J.R., M.E. Campana, H.M. Valett, and C.M. Dahm (1998), Seasonal variation in surface-subsurface water exchange and lateral hyporheic area of two stream-aquifer systems, *Water Resources Research*, *34*, 317-328.

Zarnetske, J. P. (2006), Headwater hyporheic zones in a warming arctic climate: An assessment of hyporheic dynamics across distinct geomorphic and permafrost conditions, M.S. Thesis, Utah State University, Logan, Utah.

Table 2.1. Location of each of the minipiezometers installed in the alluvial subsurface. The letter indicates the location of the nest along the thalweg of the stream and the number indicates its depth layer beneath the streambed

Minipiezometer ID	Distance downstream from SIE dripper (m)	Depth beneath streambed surface (cm)
aa1	30	29
aa2	30	57
aa3	30	136
a1	45	14
a2	45	44
a3	45	103
b1	73	26
b2	73	53
b3	73	139
c1	81	15
c2	81	45
c3	81	94
d1	86	19
d2	86	49
d3	86	81
e1	104	11
e2	104	41
e3	104	102
f1	122	11
f2	122	40
f3	122	101
g1	128	9
g2	128	39
g3	128	104
h1	132	24
h2	132	54
h3	132	118

Table 2.2. Location of each of the minipiezometers installed in the peat subsurface. The letter indicates the location of the nest along the thalweg of the stream and the number indicates its depth layer beneath the streambed

Minipiezometer ID	Distance downstream from SIE dripper (m)	Depth beneath streambed surface (cm)
a1	57	10
a2	57	30
b1	60	10
b2	60	30
c1	67	10
c2	67	30
d1	76	10
d2	76	30
e1	80	10
e2	80	30
f1	85	20
f2	85	40
g1	126	12
g2	126	42
h1	133	10
h2	133	30
i1	142	15
i2	142	35

Table 2.3. Median concentrations of DO, NO_3, NH_4, SRP and DOC in the surface and subsurface water of the alluvial and peat streams (* indicates statistically significant difference between stream types)

	Parameter	Alluvial Median	Peat Median	Mann-Whitney p-value
Surface	DO (mg/L)	9.7	9.2	0.312
	NO_3 (µM)	5.75	7.49	0.885
	NH_4 (µM)	0.20	0.52	0.194
	SRP (µM)	0.02	0.03	0.312
	DOC (µM)	310	339	0.384
Subsurface	DO (mg/L)	6.7	1.3	<0.001*
	NO_3 (µM)	7.15	0.00	<0.001*
	NH_4 (µM)	0.36	43.76	<0.001*
	SRP (µM)	0.06	0.22	<0.001*
	DOC (µM)	291	538	<0.001*

Table 2.4. The set of p-values resulting from Mann-Whitney comparisons of P_C, DO, NO_3, NH_4, SRP and DOC among subsurface depths, stream features and time in the alluvial stream (* indicates a statistically significant difference for a given comparison; α' = 0.017 for depth and feature and α' = 0.05 for time)

Factor	Comparison	P_C	DO	NO_3	NH_4	SRP	DOC
Depth	Surface v. Shallow	0.067	0.131	0.543	0.735	0.332	0.095
	Surface v. Medium	0.026	0.008*	0.843	0.166	0.052	0.199
	Surface v. Bottom	0.007*	0.003*	0.048	0.373	0.048	0.019
Feature	Head v. Tail	0.098	0.051	0.038	0.888	0.604	0.239
	Head v. Pool	0.006*	0.001*	0.486	0.486	0.664	0.800
	Tail v. Pool	0.211	0.025	0.032	0.491	1.000	0.300
Time	June v. August	1.000	0.026*	0.119	<0.001*	0.191	0.007*

Table 2.5. The set of p-values resulting from Mann-Whitney comparisons of P_C, DO, NO_3, NH_4, SRP and DOC among subsurface depths, stream features and time in the peat stream (* indicates a statistically significant difference for a given comparison; α' = 0.025 for depth; α' = 0.017 for feature; α' = 0.05 for time)

Factor	Comparison	P_C	DO	NO_3	NH_4	SRP	DOC
Depth	Surface v. Shallow	0.027	0.002*	0.008*	0.003*	0.018*	0.004*
	Surface v. Bottom	0.013*	0.002*	<0.001*	0.001*	0.002*	0.003*
Feature	Head v. Tail	0.656	0.489	0.333	0.047	0.317	0.456
	Head v. Pool	0.655	0.661	0.939	0.008*	0.005*	<0.001*
	Tail v. Pool	0.344	0.256	0.440	0.001*	0.003*	<0.001*
Time	June v. August	0.699	0.068	0.166	0.818	0.427	0.217

Table 2.6. Estimated net nutrient regeneration rates for the Kuparuk River, AK [*Edwardson et al.*, 2003] and the alluvial and peat streams in the current study

Nutrient	Kuparuk River, AK [*Edwardson et al.*, 2003]	Alluvial stream [this study]	Peat stream [this study]
NO_3 ($\mu mol\ m^{-2}\ h^{-1}$)	28	7.86	-1.53
NH_4 ($\mu mol\ m^{-2}\ h^{-1}$)	28	1.41	6.79
SRP ($\mu mol\ m^{-2}\ h^{-1}$)	2	0.54	0.05

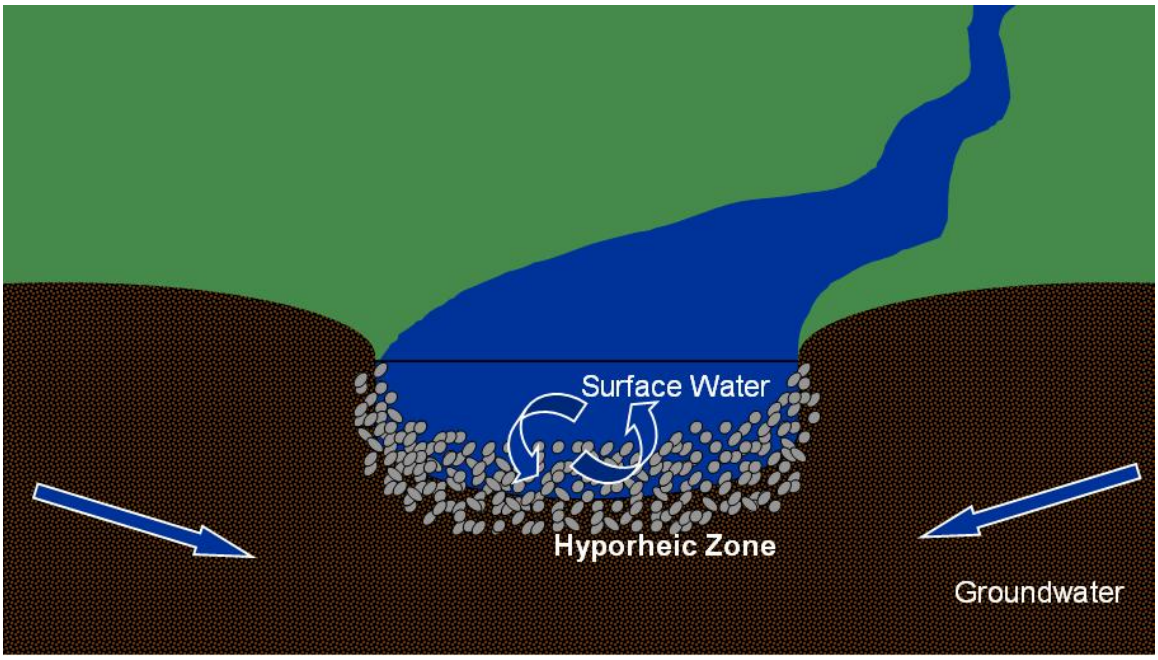

Figure 2.1. A cross-sectional diagram of a typical temperate stream, showing hyporheic exchange and potential groundwater interaction

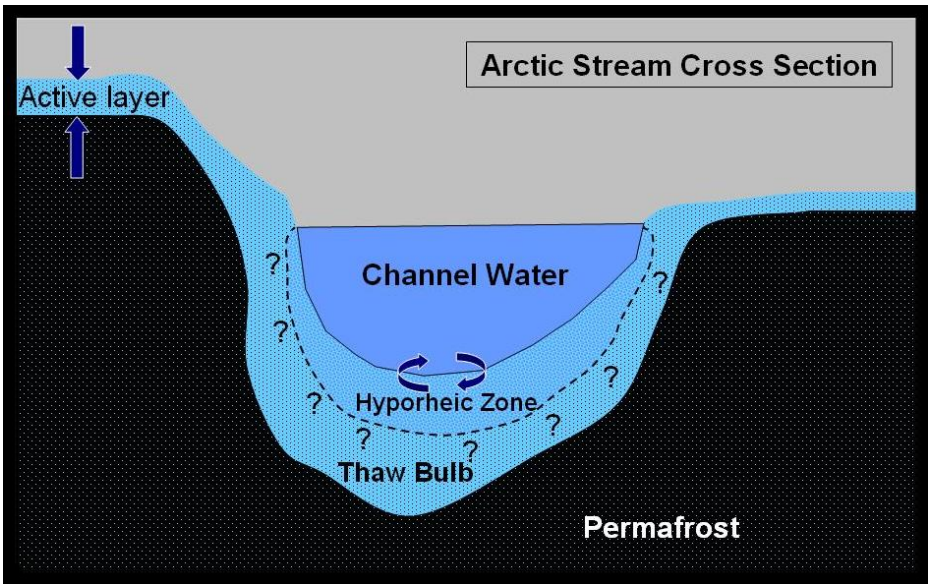

Figure 2.2. Arctic tundra stream cross section showing the active layer and thawbulb within the continuous permafrost. The hyporheic zone exists within the thawbulb.

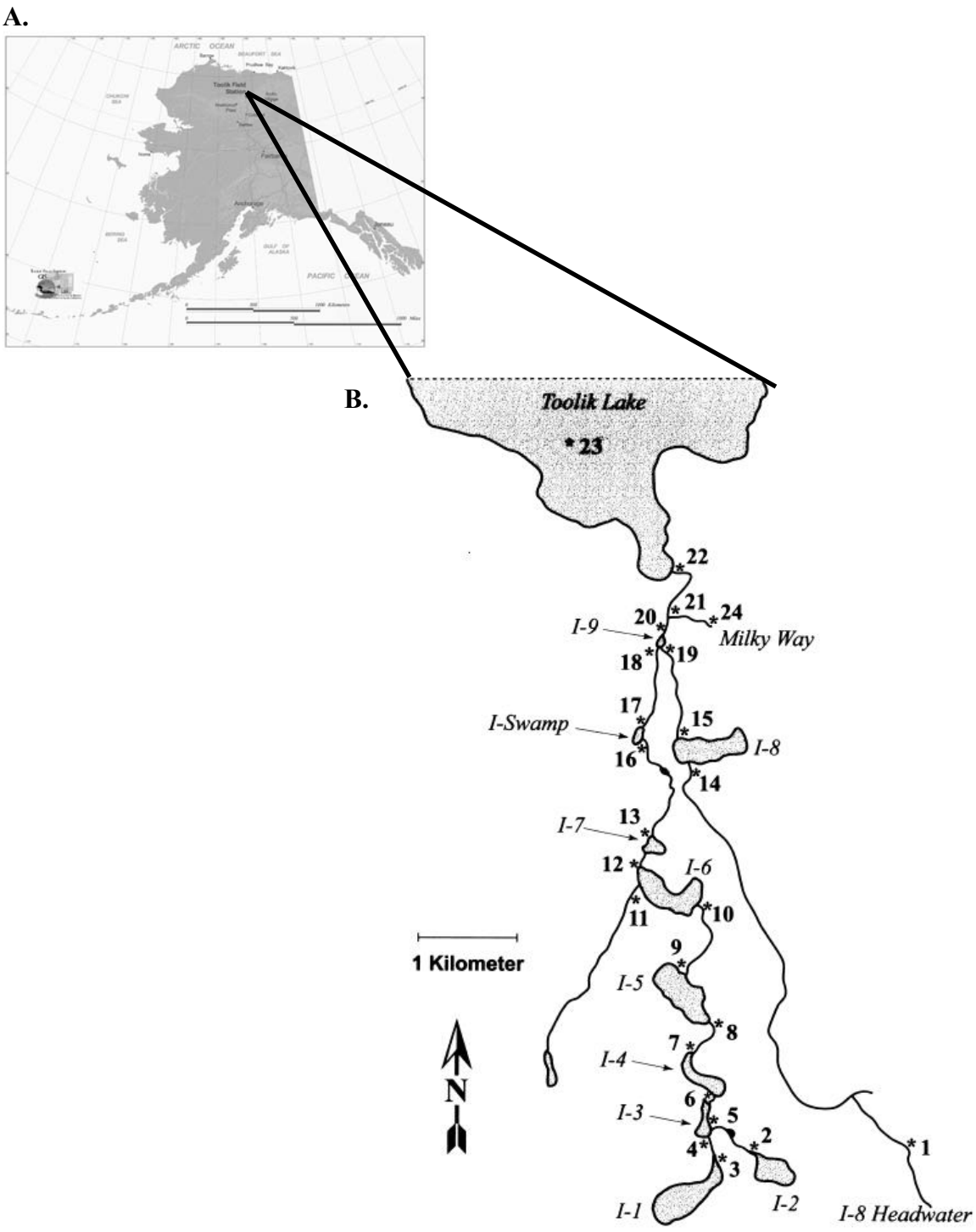

Figure 2.3. (A) Location of the Toolik Field Station on the North Slope of the Brooks Range in Alaska (credit: A. Balser) and (B) an illustration of the Inlet Series to Toolik Lake taken from *Kling et al.* [2000]. The alluvial stream location is indicated by the number 14 on this illustration and the peat stream location is indicated by the number 16.

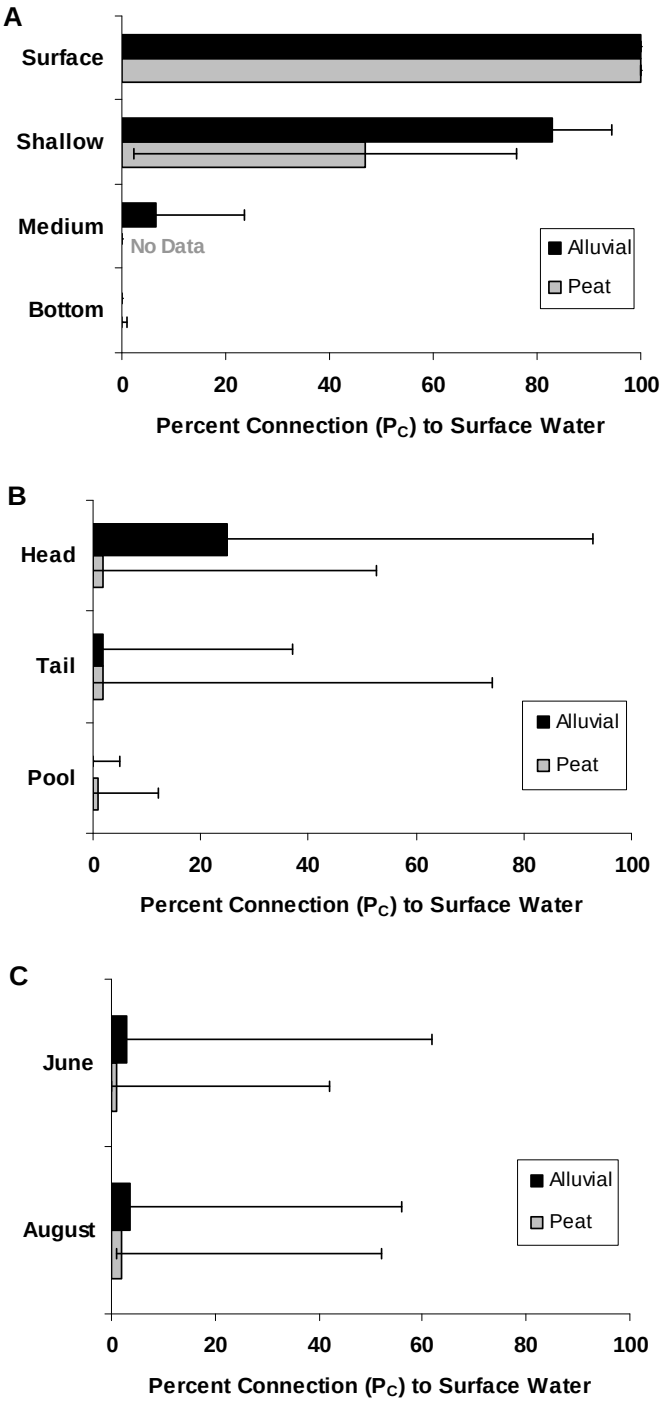

Figure 2.4. Median P_C values at (A) distinct subsurface depths, (B) stream features and (C) two time periods in the alluvial and peat stream types (error bars indicate first and third quartile values)

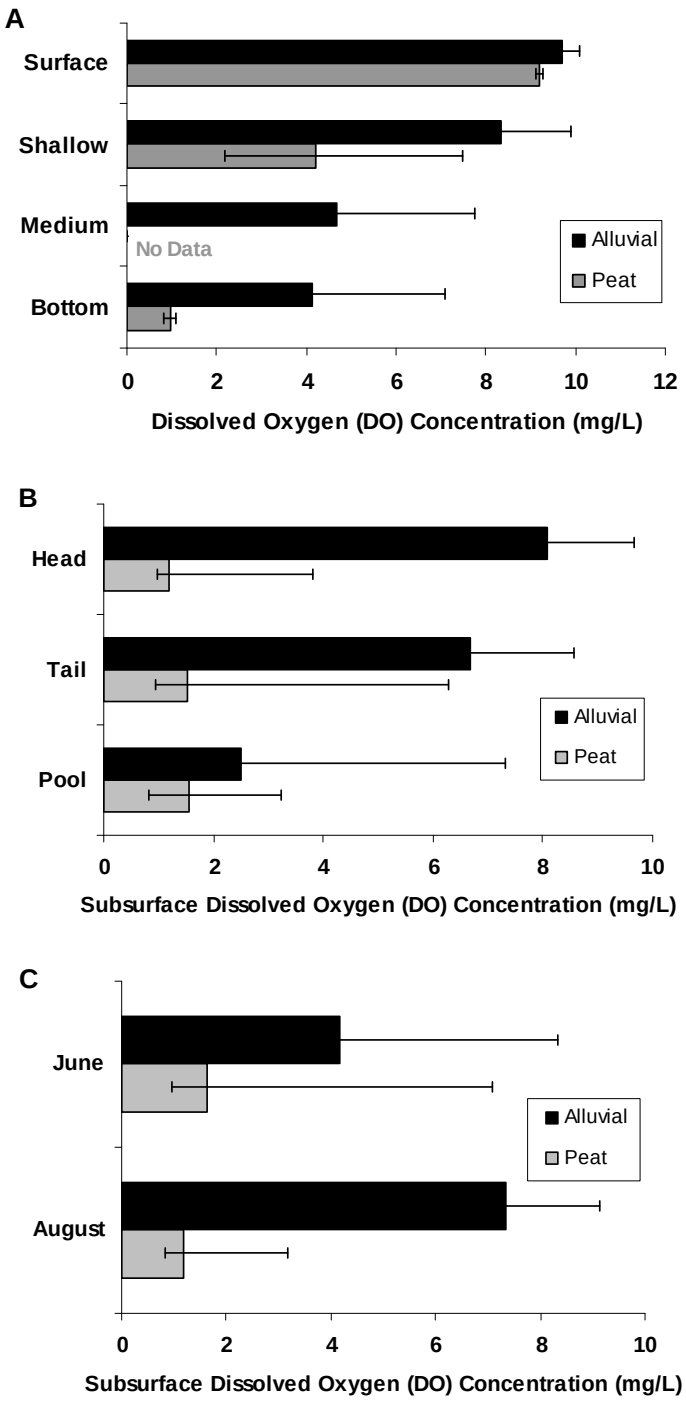

Figure 2.5. Median dissolved oxygen concentration at (A) distinct subsurface depths, (B) stream features and (C) two time periods in the alluvial and peat stream types (error bars indicate first and third quartile values)

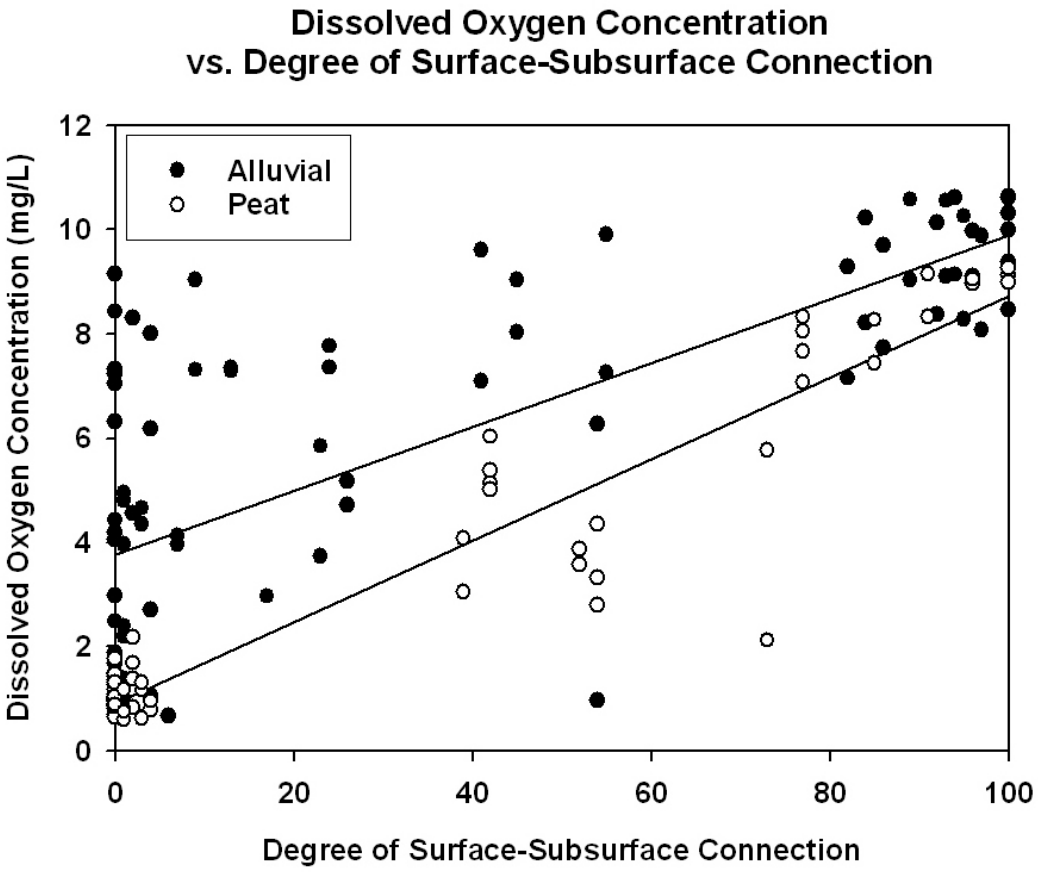

Figure 2.6. Subsurface dissolved oxygen concentration vs. degree of surface-subsurface connection in the alluvial and peat streams. The Spearman's correlation coefficient between the two variables is 0.74 ($p < 0.001$) for the alluvial stream and 0.78 ($p < 0.001$) for the peat stream.

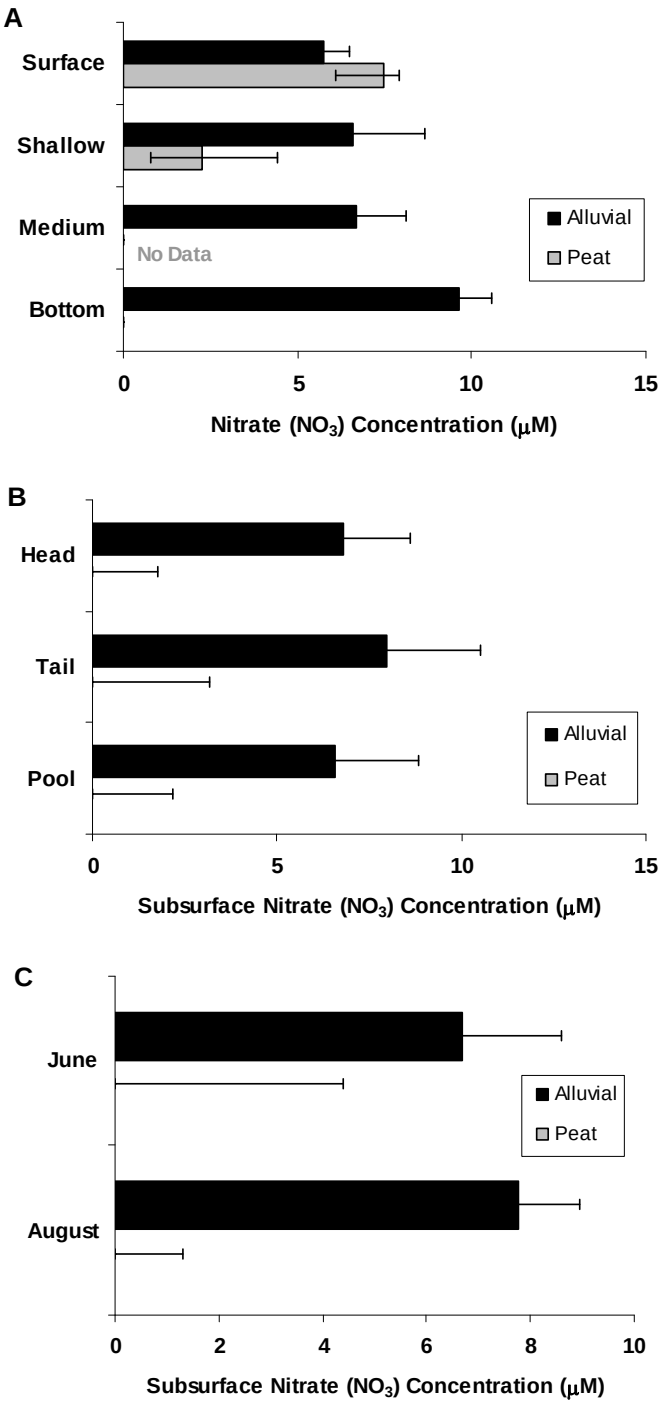

Figure 2.7. Median nitrate concentration at (A) distinct subsurface depths, (B) stream features and (C) two time periods in the alluvial and peat stream types (error bars indicate first and third quartile values)

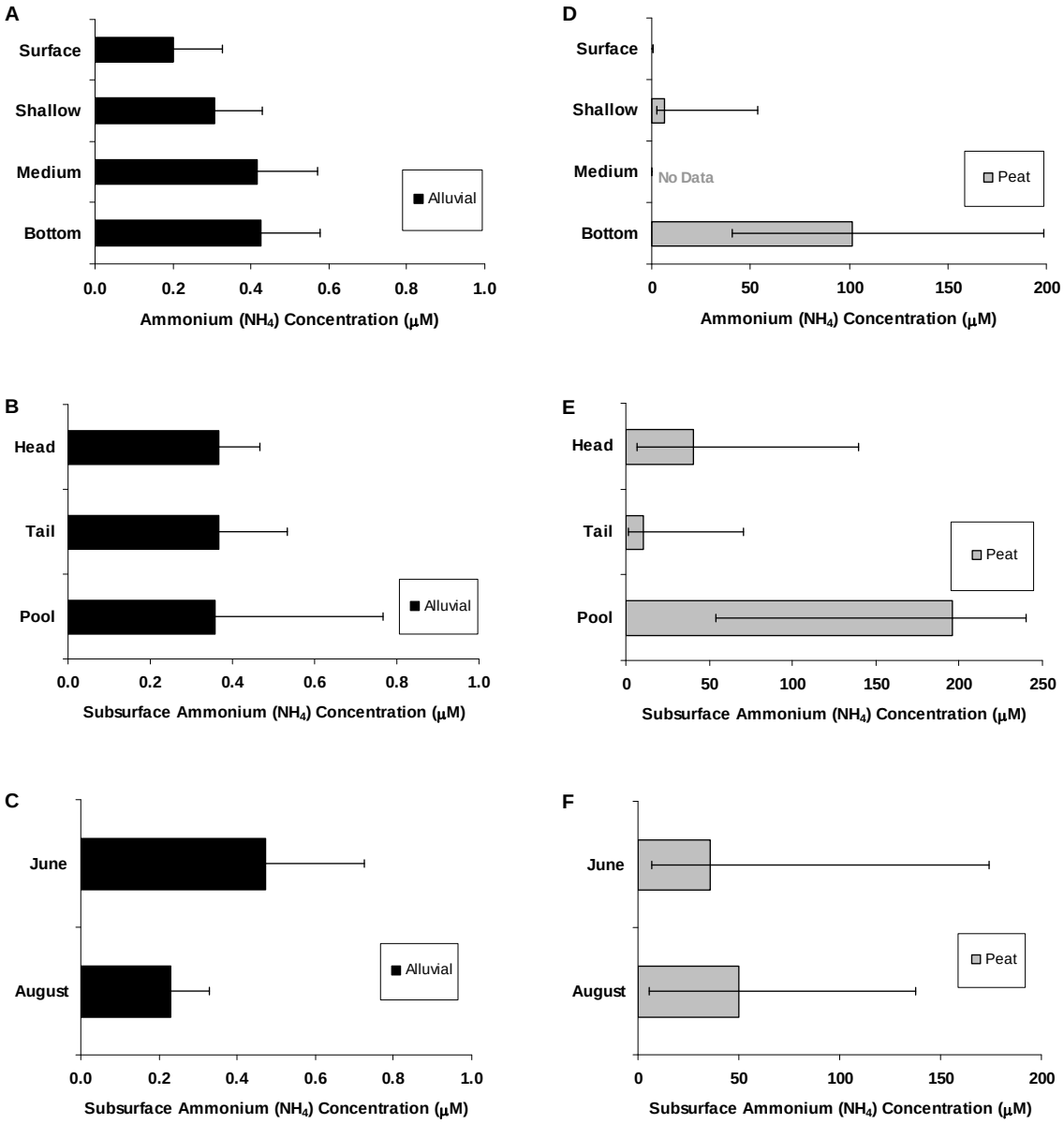

Figure 2.8. Median ammonium concentration at (A) distinct subsurface depths, (B) stream features and (C) two time periods in the alluvial stream and at (D) distinct subsurface depths, (E) stream features and (F) two time periods in the peat stream (error bars indicate first and third quartile values)

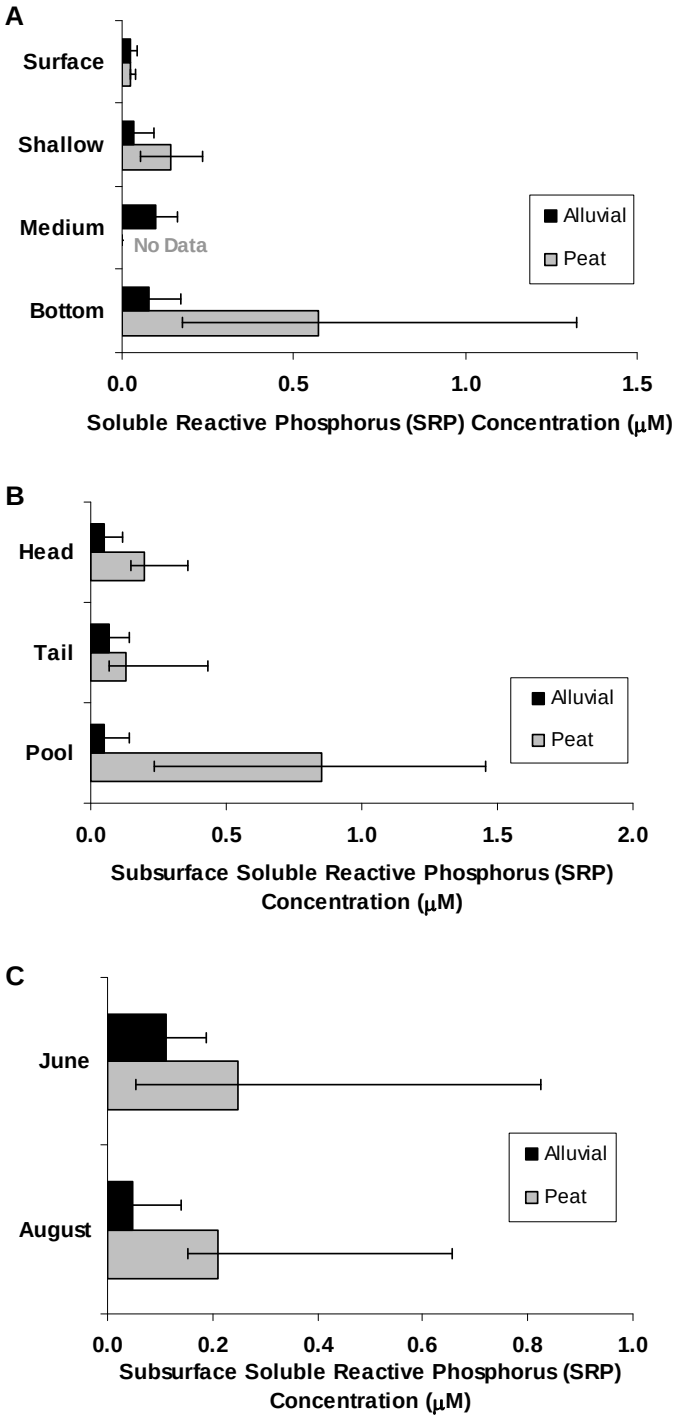

Figure 2.9. Median soluble reactive phosphorus concentration at (A) distinct subsurface depths, (B) stream features and (C) two time periods in the alluvial and peat stream types (error bars indicate first and third quartile values)

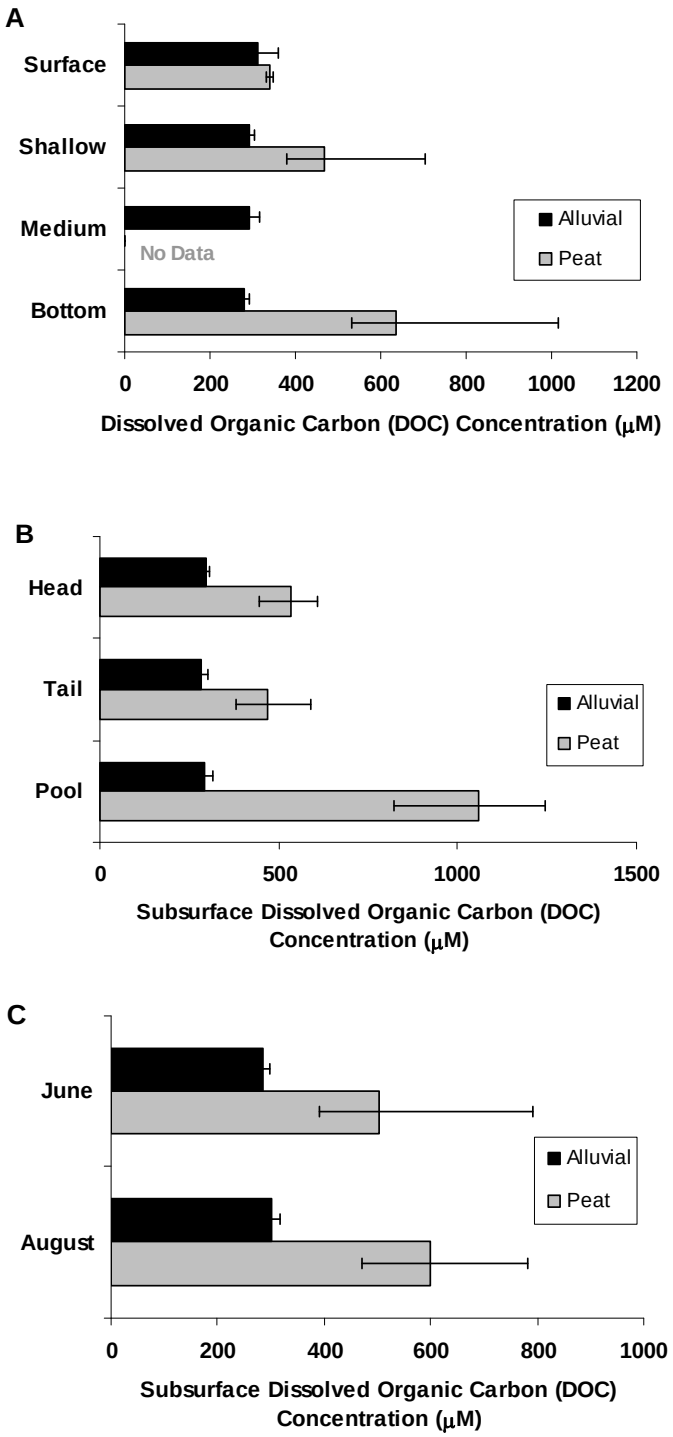

Figure 2.10. Median dissolved organic carbon concentration at (A) distinct subsurface depths, (B) stream features and (C) two time periods in the alluvial and peat stream types (error bars indicate first and third quartile values)

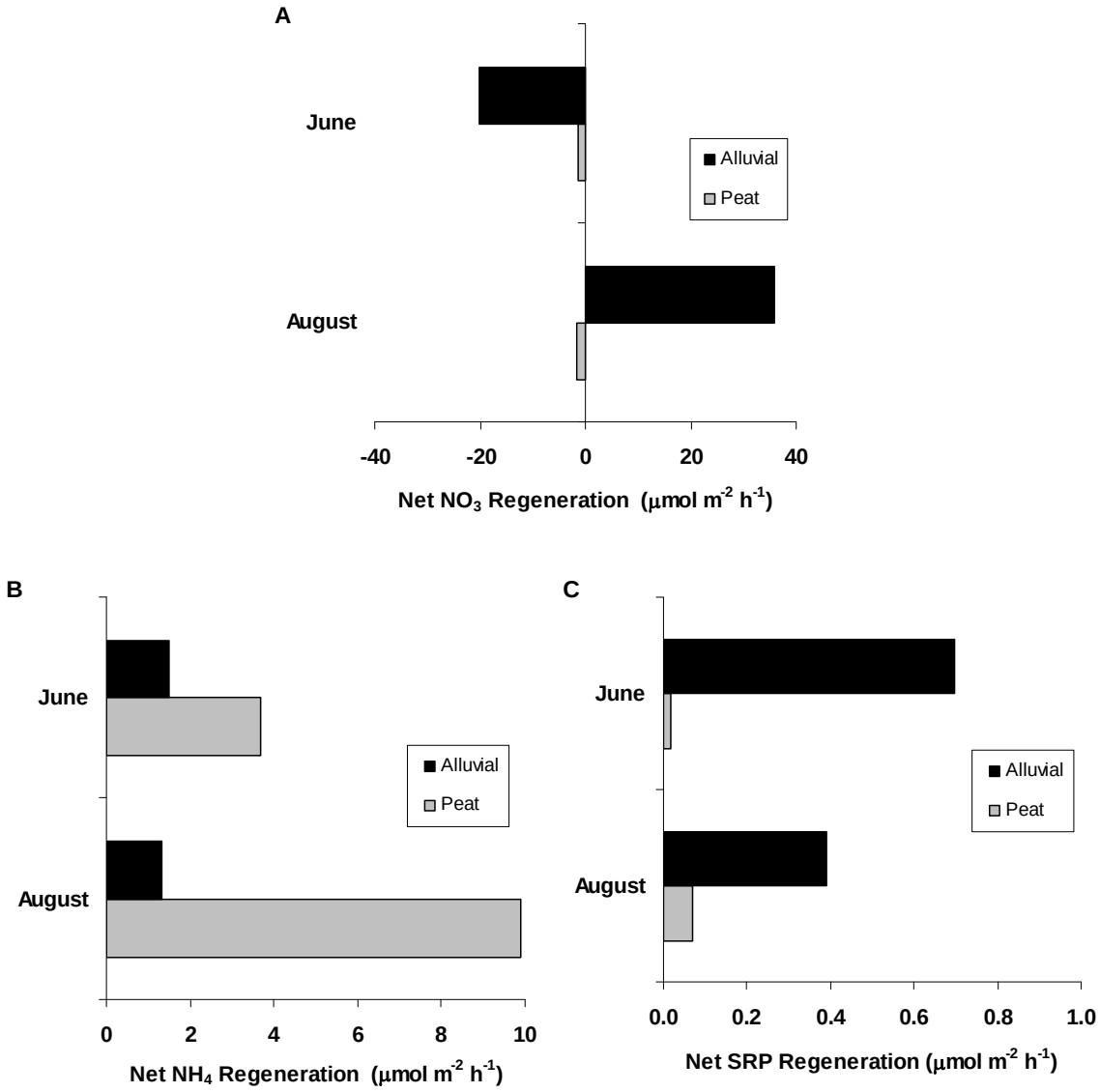

Figure 2.11. Estimated net regeneration rates for (A) nitrate, (B) ammonium and (C) soluble reactive phosphorus in the alluvial and peat stream types; a negative value indicates that the subsurface served as a sink for a given nutrient, while a positive value indicates that the subsurface served as a source for a given nutrient.

CHAPTER 3: HYPORHEIC FLOW AND BIOGEOCHEMICAL PROCESSING IN AN ARCTIC RIVER GRAVEL BAR

ABSTRACT

The hyporheic zone is an important component of transient storage (i.e., delayed downstream transport) in streams. By moving through sediment interstices, water in the hyporheic zone experiences an increased residence time and undergoes important biogeochemical transformations because it is in close contact with microbial biofilms. The hyporheic zone often serves as a site for organic matter decomposition and nutrient regeneration to the surface water. Currently, little is known regarding the biogeochemical processes occurring in the hyporheic zones of arctic streams. It has been difficult to separate transient storage into its surface (e.g., backwaters, eddies) and subsurface (e.g., hyporheic zone) components using tracer tests. However, in this study, a gravel bar located at the confluence of two arctic tundra streams served as a unique setting to study the subsurface component of transient storage alone. The deposition of the gravel bar caused all surface flow from one of the streams to travel through the gravel bar sediments via a network of well-defined flow paths before it emerged at the opposite end of the gravel bar to join the surface water of the other stream. We used a tracer test along with surface and subsurface water sampling to estimate the direction and rate of subsurface flow through the gravel bar sediments and to examine biogeochemical patterns throughout the gravel bar. Ordinary kriging was used to estimate concentrations of the tracer and important biogeochemical constituents across the gravel bar at three distinct subsurface depth layers. Using the flow rates along with the surface and subsurface biogeochemical data, we estimated net nutrient regeneration rates from the gravel bar to the stream water for nitrate, ammonium and soluble reactive phosphorus (SRP). Subsurface flow rates were 19 m h^{-1} on average, ranging from 3 to 29 m h^{-1}. The most utilized subsurface flow paths were located at the middle depth layer (approximately 1 m beneath the surface of the gravel bar). These flow paths exhibited high dissolved oxygen concentrations due to their high degree of connection to the surface water and also tended to have lower concentrations of ammonium and SRP than the less-connected regions, where inorganic nutrient concentrations tend to build up. As a whole, the gravel bar served as a net source of ammonium (18.01 μM m^{-1} d^{-1}) and SRP (0.37 μM m^{-1} d^{-1}) to the surface water and as a net nitrate sink (-0.99 μM m^{-1} d^{-1}).

3.1. Introduction

Hyporheic exchange promotes surface-subsurface water interactions that are important to the overall function of stream ecosystems. When water moves through the interstices of stream sediments, its residence time in contact with sediment biofilms increases. The microorganisms that comprise the biofilm effectively decompose organic matter and recycle nutrients within stream ecosystems.

Although methods have been developed that allow the differentiation between surface water moving through the thalweg and water traveling through transient storage zones, it has been very difficult to separate water moving through subsurface transient storage zones (i.e., hyporheic zones) from that moving through surface water transient storage zones (i.e., eddies and backwaters), let alone distinguishing between different subsurface flow paths. So far, the most successful attempt at characterizing transient storage in a stream has been through plotting residence time distributions of the cumulative transient storage zones in a system [e.g., *Haggerty et al.*, 2002, *Gooseff et al.*, 2003].

In this study, we took advantage of a unique natural system that allowed us to study subsurface flow through exposed alluvium without the added variation of in-channel transient storage and surface-subsurface interactions. We studied subsurface flow through a large gravel bar located at a stream confluence in the headwaters of the Kuparuk River in northern Alaska. This study site was a useful analog for hyporheic flow in a stream channel because it was less complex than a stream system with full hyporheic interactions and in-stream transient storage, but more natural and less disturbed than a laboratory microcosm experiment [*Butturini et al.*, 2000, *Sheibley et al.*, 2003].

Like substream hyporheic zones, gravel bars serve as important regions of biogeochemical transformation, but can be less complex to study than hyporheic zones beneath streams. In a study of subsurface nitrogen fluxes to McRae Creek in the H.J. Andrews Experimental Forest, Oregon, *Wondzell and Swanson* [1996] found that during the summer months, a gravel bar served as an important site for the transformation of dissolved organic nitrogen to ammonium and ultimately to nitrate. It did not serve as a source of nitrate to the stream during the summer months due to a disconnect caused by a low water table. During fall storms, however, the gravel bar served as a strong source of inorganic nitrogen to the stream, as the nitrate and ammonium were flushed out of the gravel bar.

We used conservative tracer additions, subsurface biogeochemical sampling, and geostatistical methods to interpolate subsurface water flow paths and biogeochemical patterns in the gravel bar and to estimate nutrient regeneration rates from the gravel bar. Geostatistical methods such as ordinary kriging make use of the fact that the physical characteristics of locations that are close to one another tend to be more similar to one another than those that are farther away from one another. Ordinary kriging uses semivariograms (referred to as variograms here) to illustrate how data for a given variable are related in space and also to estimate characteristics of nearby unsampled locations based on existing data and their spatial relationships. Geostatistical methods originated in the geological and mining fields [*Journel*, 1978] but have become useful and important tools in the fields of ecology and other natural sciences [*Goovaerts*, 1999]. For more detailed description of geostatistical methods and applications, see *Goovaerts* [1999] and *Isaaks and Srivastava* [1989].

A variogram is a plot of semivariance versus lag distance (i.e., distance between two points being compared). In ordinary kriging, a variogram is created based on existing data and the relationship between semivariance and lag distance is then modeled so that the spatial variance of a given attribute can be described as a mathematical equation. The variogram typically indicates semivariance between points increasing as their distance apart in space increases. Semivariance tends to increase to a certain lag distance at which it levels out and reaches a plateau. At this point, an increase in lag distance will not cause an increase in semivariance. The semivariance at this point is called the sill and the lag distance at this point is called the range. A variogram is modeled in terms of its distribution (e.g., Gaussian, exponential, spherical, linear) and the parameters that create the equation include the sill, range and nugget. The nugget is the semivariance between two values at a lag distance of zero. It essentially accounts for the variance that is not due to separation in space. See *Isaaks and Srivastava* [1989] for more details.

The hypothesis of the current study was that surface water would move from one end of the gravel bar to the other through a network of well-defined subsurface flow paths and that the patterns of subsurface water movement would directly affect the biogeochemical characteristics of the subsurface environment, thus affecting the stream ecosystem through nutrient regeneration. Due to the overall high degree of connection to the surface water, we would expect the gravel bar to serve as an important site of organic matter decomposition and nutrient regeneration to the stream. In this study, we employed a solute injection experiment (SIE) in conjunction with ordinary kriging to elucidate the major subsurface flow network through the gravel bar and also conducted surface and

subsurface biogeochemical sampling to examine the influence of flow patterns on subsurface biogeochemical gradients and transformations. We used the flow path information obtained from the SIE along with the surface and subsurface biogeochemical data to estimate nutrient regeneration rates from the subsurface to the surface water.

3.2. Methods

3.2.1. Study Site

This study took place at the confluence of two headwater streams draining the North Slope of the Brooks Range in Arctic Alaska. The site (68º 31'N, 149º 13'W) is located about 15 miles southeast of the Toolik Lake Field Station (Figure 3.1). Just past the confluence, the stream becomes the inlet to Green Cabin Lake and then feeds the Kuparuk River, which continues to flow north for about 180 km to the Arctic Ocean.

The two stream types coming together at this confluence were a low gradient, peat-bottomed stream and a higher gradient alluvial stream. A few years prior to this study (~2002), a gravel bar was formed at this confluence as the result of a large sediment deposition event (Figure 3.2). At the time of this study (2005), the elevation of the gravel bar surface was higher than the elevation of the water surface of the peat stream flowing into the confluence. Consequently, in periods of low to moderate flow, all of the surface water coming from the peat stream abruptly became subsurface flow when it reached the gravel bar. It moved through the gravel bar via subsurface flow paths until it rejoined the surface flow of the alluvial stream at the bar's northwest end.

3.2.2. Solute Injection Experiments

We performed initial exploratory tracer tests, which allowed us to determine the general direction of subsurface flow through the gravel bar and to gain rough estimates of travel time through the gravel bar sediments. These initial tracer tests involved adding a slug of Rhodamine WT (RWT) into shallow pits that were dug on the surface of the gravel bar. Within minutes to hours, the tracer dye began to appear on the opposite, downstream side of the gravel bar.

To better understand the subsurface flow path network, we carried out a more extensive solute injection experiment (SIE) on 6-August 2005. The gravel bar was outfitted with 14 multi-depth minipiezometer nests that allowed us to sample subsurface water during the SIE (Table 3.1). In the peat channel, at a distance upstream from the gravel bar that would allow for adequate mixing in the channel (approximately 40 m), RWT (stock concentration: 3.5 g/L) was dripped at a rate of 25 ml/min for 4 hours to obtain a target plateau concentration of 100 μg/L in the channel. At approximately 20-minute intervals throughout the duration of the drip, water samples were taken from the inflowing surface water, the outflowing surface water, and from all of the multidepth minipiezometers across the gravel bar. A background sample was taken at each sampling location before the SIE and an additional sample was taken 45 minutes after the dripper was turned off to observe the end of the tracer pulse moving through the flow system. A tracer breakthrough curve (RWT concentration versus time) was generated for each sampling location for the length of the SIE (Figure 3.3).

3.2.3 Subsurface Water Sampling Technique

Subsurface water samples were obtained from inexpensive, lightweight minipiezometers inserted into the gravel bar to known depths. Each minipiezometer was constructed from a 1.5-meter long tube of rigid Delrin plastic with a 6.3-mm outer diameter and 3.2-mm inner diameter. Five holes were drilled into the walls of each minipiezometer over the bottom 10 cm of its length and the bottom hole of each tube was left open (total open area: 68 mm^2). The drilled ends of the piezometers were covered with a geotextile sleeve to prevent sediment clogging.

The minipiezometers were bundled in sets of two or three so that the screened ends of the piezometers of a multi-depth bundle were a known distance apart. The installation of each bundle then provided 2 to 3 distinct sampling depths at one location on the gravel bar. There were 14 total minipiezometer bundles installed across the gravel bar surface. The minipiezometer bundles were arranged so that the deepest minipiezometer was installed at the deepest accessible point (i.e., depth of refusal). The deepest group of piezometers (n=7) was installed to an average of 1.3 m beneath the gravel bar surface. The shallow (n=11) and medium (n=10) minipiezometer groups were installed at an average depth of 0.6 m and 1.0 m, respectively, beneath the gravel bar surface.

The nested bundles were installed into the gravel bar using a steel installation tool consisting of a hardened steel rod (19.0 mm diameter, 240 cm length) within a hardened steel tube (25.4 mm inner diameter, 235 cm length) similar to that described by *Baxter et al.* [2003]. The inner rod and sleeve were pounded into the streambed to the depth of refusal using a fencepost driver. The inner rod was removed from the sleeve and the

minipiezometer bundle was inserted into the sleeve. The sleeve was then carefully removed, allowing the sediment to collapse around the minipiezometer bundle, securing its position within the sediment matrix. Fourteen multi-depth bundles (28 total minipiezometers) were installed across the gravel bar to cover a swath of area between the inflowing stream and the where the RWT plume entered the surface water in the initial exploratory solute test.

To take a subsurface water sample, a 60-ml disposable syringe (Becton-Dickenson, Franklin Lakes, NJ) was attached to each minipiezometer via a 3-way disposable syringe stopcock (Cole-Parmer, Vernon Hills, IL). A small volume of water (5-10 ml) was drawn into the syringe to clear the minipiezometer and was discarded via the open port of the 3-way stopcock without detaching the syringe from the minipiezometer. Fresh sample water was then drawn into the syringe and processed for analysis as described in the following sections. Between sampling events the syringes were removed from the minipiezometers, but the 3-way stopcocks were left in place in the off position, such that the minipiezometer was closed to the atmosphere.

3.2.4. Geostatistical Methods

Ordinary kriging methods were used to interpolate the subsurface tracer concentrations across the entire gravel bar at four distinct time points during the SIE. The four time points were chosen to include two points during the period of rapidly increasing RWT concentration, the plateau period, and the decrease of RWT concentration after the tracer dripper was turned off (Figure 3.3). Four separate variograms (i.e., one for each time period of interest) were created using the RWT

concentrations and lag distances between all possible pairs of sampling locations. The equation used to calculate the semivariance for each lag distance (h) was:

$$\lambda = \frac{1}{2n} \sum_{i=1}^{n} (x_i - y_i)^2 \qquad \text{Eqn. 3.1}$$

where x and y are the pair of values being compared and n is the total number of sampled pairs at that specified lag distance (h) [*Isaaks and Srivastava*, 1989].

Two large matrices of data were generated, one of all possible lag distances (h) and on of the associated semivariances (λ) at those lag distances. To work with a more manageable subset of the data, the data were binned so that each bin contained a roughly equal number of data points. For each bin, a mean lag distance and a mean semivariance was calculated. From this, a plot of mean semivariance versus mean lag distance was created. The distribution of the variogram was modeled and an equation explaining the semivariance (λ) in terms of lag distance (d), nugget (n), sill (s) and range (r) was obtained for each variogram.

Estimates of RWT concentration across each subsurface layer of the gravel bar were made by creating a grid of 1 m squares and estimating the RWT concentration at every meter across the gravel bar. The entire estimated area was a 22 m by 22 m grid, which results in 484 estimate points for each layer of the subsurface. To estimate the concentration at an unsampled location, a weighted linear combination of available concentrations from nearby sampled locations at a particular time was used. For each estimated concentration, an error variance value was calculated to determine the degree of certainty for each estimate. Finally, estimated RWT concentrations across the entire

gravel bar were plotted (Matlab version 7.0.4, The MathWorks, Inc.) for the three subsurface layers, for each of the four time points of interest. A linear interpolation algorithm within Matlab was used to interpolate the concentrations and error variances between each of the estimated locations and to create a smoothed graphical transition between each of the estimated points.

3.2.5. Biogeochemical Sampling and Analysis

To couple the physical water movement data with the biogeochemical processes occurring in the gravel bar, samples were taken from all sampling locations for analysis of dissolved oxygen (DO), dissolved organic carbon (DOC) and nutrient concentrations, including nitrate, ammonium and soluble reactive phosphorus (SRP). These samples were taken via the minipiezometers on the same day as the SIE was conducted, prior to the start of the injection.

DO was measured in the field (directly in the sampling syringe after carefully removing the plunger) with a WTW Oxi 340i handheld dissolved oxygen meter. The reported accuracy for this dissolved oxygen meter is $\pm$0.01 mg/L (WTW, Weilheim, Germany). However, due to our modified use of the equipment (measuring concentration of water in syringe pulled from the subsurface), we estimated an accuracy of $\pm$0.1 mg/L. All other biogeochemical samples were filtered through a 0.45 µm, 25 mm diameter, cellulose acetate syringe filter and kept on ice for transport to the laboratory.

Ammonium and SRP analyses were done within 24-48 h at the Toolik Field Station. Ammonium analysis was performed using the orthophthaldialdehyde (OPA) method [*Holmes et al.*, 1999]. The minimum detection limit of Protocol A of the OPA

Method is 0.03 μM and the relationship is linear up to a concentration of 6.2 μM [*Holmes et al.*, 1999]. SRP analysis was performed using the colorimetric molybdate blue method [*Hach Company*, 1997]. The reported minimum detection limit for this method is 0.004 mg/L and the reported precision is 1 RSD. Nitrate samples were immediately frozen at the field station then transported to the University of Vermont's Rubenstein Ecosystem Science Laboratory in Burlington, VT where they were analyzed within 6 months by the cadmium reduction technique [*Askew and Smith*, 2005, p. 123]. The cadmium reduction method has a reported detection limit of 0.01 mg NO_3-N/L. Reported standard deviations for standards at four concentrations (0.04 mg/L, 0.24 mg/L, 0.55 mg/L and 1.04 mg/L) were $\pm$0.005, $\pm$0.004, $\pm$0.005 and $\pm$0.01, respectively [*Askew and Smith*, 2005, p. 123]. DOC samples were preserved with 6N hydrochloric acid to a pH of 2, transported to the Ecosystems Center in Woods Hole, MA and analyzed by the persulfate-ultraviolet method within 6 months [*Baird*, 2005, p. 23]. The reported minimum detection limit for this method is 0.01 mg/L and the reported single-operator precision (P) for a concentration range of 0.1 – 4000 mg/L is expressed as $P = 0.04x + 0.1$, where x = DOC concentration [*Baird*, 2005, p. 23]. All of the above analyses were based on standard calibration curves built each day before an analytical run. These response vs. concentration curves were fitted via linear regressions and r^2 values of $\geq$ 0.99 were ensured. In all analytical runs, check standards of a known, mid-range concentration were analyzed to ensure congruence with the day's standard calibration curve.

In the same manner that RWT concentrations were estimated for each of the three subsurface layers of the gravel bar for each time period of the SIE, concentrations of DO, nitrate, ammonium, SRP and DOC were estimated for each of the three subsurface layers

of the gravel bar. One variogram was created for each constituent rather than four separate temporal variograms, because the concentrations of the biogeochemical variables did not change as rapidly as the RWT concentrations during the SIE. Estimates were created for each variable for each of the three subsurface layers of the gravel bar.

Lastly, to examine how the flow paths through the gravel bar subsurface influenced the biogeochemistry of the water moving through them, linear regressions were performed for each of the biogeochemical constituents against the RWT concentrations at the 2.63-hour mark of the SIE. The 2.63-hour mark was chosen because it was during the plateau period of the SIE. Nutrient regeneration rates were also estimated for each of the subsurface sampling locations based on the average travel time of RWT from the head of the bar to a given sampling location beneath the bar. To arrive at an estimated nutrient regeneration rate for a given subsurface sampling location, the change in nutrient concentration (μM) from the inflowing surface water to that subsurface sampling location was divided by the average flow rate (m/s) of water from the inflowing surface water to that subsurface sampling location. The average flow rate was calculated as the most direct distance (m) from the head of the gravel bar to the subsurface sampling location divided by the average RWT arrival time at that location. A net nutrient regeneration rate was estimated for each sampling location in the gravel bar subsurface and those values were averaged across the gravel bar to estimate the net regeneration rate for each nutrient for the entire bar. A negative value would indicate that the gravel bar served as a sink for a particular nutrient, while a positive value would indicate that it served as a nutrient source.

3.3. Results

3.3.1. Tracer Concentration Estimates

A separate variogram was developed for each of four representative time periods during the SIE (0.45 h, 0.70 h, 2.63 h and 4.45 h) (Figure 3.4). The optimal model fit for each of the variograms was linear with a set of specific model parameters (i.e., sill, range and nugget) for each variogram model (Table 3.2). The models were used in conjuction with known RWT concentrations at the sampled locations to estimate RWT concentrations across the gravel bar at three subsurface layers for each of the four time periods of interest (Figure 3.5).

Having the estimated RWT concentrations for the four snapshots in time during the SIE allowed us to see the progression of water movement through the subsurface. RWT moved through the shallow layer (average depth: 0.6 m) from southeast to northwest, staying confined to the center of the sampled zone. RWT was most concentrated in the middle depth layer (average depth: 1.0 m) and the pattern of water movement in that layer was less confined than what was seen in the shallow layer. The water moved directly from the south end of the gravel bar to the northwest within this layer, showing much less confinement. Of the three layers, RWT moved through the deepest layer (average depth: 1.3 m) at the lowest concentrations and was confined to the westernmost edge of the gravel bar subsurface. The average subsurface flow rate through the gravel bar was 19 m h^{-1} and flow rates ranged from 3 to 29 m h^{-1}.

3.3.2. Biogeochemical Concentration Estimates

A variogram was developed for each of the biogeochemical parameters sampled (NO_3, NH_4, SRP, DO and DOC). Again, the variogram models indicated that semivariance increased linearly with increasing lag distance for each of the five biogeochemical variables (Figure 3.6). Each had specific nugget, sill and range values (Table 3.2). DO concentrations were highest overall in the middle depth layer, but also through the center of the shallow depth layer (Figure 3.7). The mean DO concentration of 7.3 mg/L across all subsurface locations indicates that the subsurface was generally well-supplied with oxygen from the surface water, thus there was generally a high degree of hydrologic connectivity between the surface and subsurface. There were a few isolated locations, however, of very low DO concentrations in the northeast region of the gravel bar and this transcended all depth layers. There was a similar hypoxic region in the northwest region of the gravel bar, but it existed only in the shallow and deep layers. The low DO regions corresponded spatially to areas of relatively high ammonium (Figure 3.9), SRP (Figure 3.10) and DOC (Figure 3.11) concentrations. Average subsurface concentrations of ammonium, SRP and DOC were 7.3 μM, 0.2 μM, and 526 μM, respectively. Nitrate concentrations were very low (~1 μM) across all subsurface locations of the gravel bar (Figure 3.8) except for one shallow location that was very high (7.32 μM). This point was removed from analysis because it was an extreme outlier.

There was a significant positive relationship ($R^2 = 0.948$, $p < 0.001$) between estimated RWT concentrations at the SIE plateau and DO concentrations across the gravel bar (Figure 3.12, Table 3.3). There were significant negative relationships between estimated RWT concentrations at the SIE plateau and estimated ammonium (R^2

= 0.653, $p < 0.001$), SRP ($R^2 = 0.575$, $p < 0.001$), and DOC ($R^2 = 0.328$, $p = 0.001$) concentrations. There was no significant relationship between RWT concentration estimates at SIE plateau and nitrate concentration estimates ($p = 0.158$). This did not change with the removal of the high nitrate point ($p = 0.146$). Net nutrient regeneration rates for the gravel bar were estimated at 18.01 μM m^{-1} d^{-1} for ammonium, 0.37 μM m^{-1} d^{-1} for SRP and -0.99 μM m^{-1} d^{-1} for nitrate (Table 3.4).

3.4. Discussion

3.4.1. Tracer Concentration Estimates

The estimated tracer concentration plots indicate that water generally moved in a northwesterly direction (Figure 3.5). This confirmed what was seen from the initial tracer slug tests. The advantage of the longer-term tracer additions employed in conjunction with subsurface water sampling and geostatistical interpolation is seen in the level of detail that is shown for each distinct subsurface depth throughout the course of the SIE. The most utilized subsurface flow paths moved through the medium depth layer and were oriented in a north-northwesterly direction (Figure 3.5). Since the elevation of the gravel bar surface was roughly 0.5 to 1.0 m higher than the surface of the stream water flowing into the head of the gravel bar, the medium depth subsurface layer was at an elevation roughly equal to the surface water level, which was the source of the tracer-laden water. In fact, some of the minipiezometers installed in the shallow layer of the gravel bar subsurface could not be used because sampling efforts resulted in obtaining air from the sediment interstices rather than water (i.e., the water table within the gravel bar subsurface was not high enough to obtain water samples there). The medium subsurface

layer likely received most of the flow from the stream and RWT seen at higher or lower flowpaths may have migrated up or down in the subsurface from the medium layer. However, the flow paths in the deep layer indicated that water came directly from the south and very low concentrations of RWT were seen in the eastern half of the gravel bar at that layer. This indicates that perhaps there was also a relatively deeper subsurface connection between the stream and the gravel bar that occurred within the thawed sediments surrounding the inflow stream. In other words, the visible surface water flowing into the head of the gravel bar was likely not the only entry point to the gravel bar subsurface. There was probably a deeper subsurface connection to the gravel bar sediments as well.

RWT concentrations in the shallow layer were highest in the central zone of the flow paths as there are distinct points of lower RWT concentration toward the lateral edges of the subsurface flow zone. There were some constriction points on these outer edges of the shallow layer that restricted flow there and kept it channeled toward the center of the gravel bar. These constriction points were also identifiable in the other two depth layers. We suspect that these areas may be peat deposits that were laid down at the time of the gravel bar formation. This hypothesis is supported by the fact that those sampling locations exhibited relatively low DO concentrations and relatively high ammonium, SRP and DOC concentrations, indicating a higher rate of organic matter decomposition and/or a lower hydraulic conductivity. We also noted an increase in the degree of resistance while pounding the insertion tool into the substrate to install the minipiezometers at those locations.

3.4.2. Biogeochemical Concentration Estimates

There is a striking similarity between the spatial patterns of DO concentrations and the RWT concentrations at SIE plateau (Figures 3.5 and 3.7). Given this relationship, DO concentration could be used as a surrogate to predict flow paths (i.e., faster flow paths tend to show higher DO concentrations and vice versa). This hypothesis is supported by the results of the linear regression between DO and RWT concentrations (Figure 3.12A, $R^2 = 0.948$, p-value < 0.001). The concentration of RWT at SIE plateau, which is a surrogate for rate of water movement through the system, is highly positively correlated to subsurface DO concentrations.

Dissolved oxygen is an important variable that controls biogeochemical patterns in subsurface environments [*Baker et al.*, 2000]. As metabolism occurs, DO is consumed. If a location is not sufficiently connected to a source of high DO water (e.g., the surface stream flow), it will become hypoxic or anoxic. DO gradients that develop in the subsurface control many other important microbially-mediated biogeochemical reactions that influence the concentration of nutrients available to ecosystem primary producers. Redox potential is a key driver influencing the type of microbial metabolism that will occur [*Stumm and Morgan,* 1996]. For instance, the first process to occur when dissolved oxygen is depleted is denitrification.

Nitrate concentrations were consistently low across all subsurface locations (~1 μM). Because of the similarity in sediment structure, we would have expected nitrate concentrations in the gravel bar subsurface to be comparable to those seen in the hyporheic zone of the alluvial stream studied in Chapter 2 (5-10 μM). Perhaps this difference in nitrate concentration was due to differences in lithology or glaciation history

between the two sites. Based on the results in the study in Chapter 2, we also would have expected to see nitrate concentrations positively correlated with DO concentrations. However, in some cases nitrate was undetectable, regardless of the DO concentration at that site. In general, stream concentrations of nitrate were higher than those in the gravel bar subsurface, indicating that the gravel bar is serving as a nitrate sink. In fact, the estimated net nitrate regeneration rate for the gravel bar was -0.99 $\mu M\ m^{-1}\ d^{-1}$.

The relationships between the concentration of RWT at SIE plateau and concentrations of ammonium and SRP were linear and negative (Table 3.3). Concentrations of ammonium, SRP and DOC were typically inversely related to concentrations of DO in the subsurface (Figures 3.10, 3.11 and 3.12). Where lower DO conditions were present (in the regions of peat deposits, for instance), concentrations of ammonium and SRP were higher than average for the gravel bar. DOC concentrations are higher in these areas due to the presence of peat. Based on the relationship between DO and flow paths, we can predict that these regions of low DO concentration indicate slower flow paths. This also makes sense because we know that the hydraulic conductivity of peat is relatively low. In these areas, it is likely that organic matter decomposition and the production of ammonium and SRP are occurring, but that since they are relatively disconnected from the surface water, they are both limited in their oxygen supply and also limited in their capacity to have ammonium and SRP carried away. These nutrients tend to build up to higher concentrations before they are regenerated to the surface water. In general, ammonium and SRP concentrations were higher in the gravel bar subsurface than in the stream water. The net regeneration rates

for ammonium and SRP (18.01 μM m^{-1} $d^{-1}$and 0.37 μM m^{-1} d^{-1}, respectively) indicated that the gravel bar served as a source of these nutrients to the stream.

3.4.3 Conclusions

This study has shown that ordinary kriging is a useful tool for determining the major flow paths through the subsurface of a gravel bar feature. The most heavily utilized flow paths through the subsurface occurred at an elevation similar to the inflowing surface water. We also found a high positive correlation between DO concentration and the degree of surface-subsurface connection. Conversely, we found high negative correlations between ammonium, SRP and DOC concentrations and the degree of surface-subsurface connection. Nitrate concentrations were low and variable throughout the gravel bar subsurface and no patterns were able to be detected with respect to DO or RWT concentration. The gravel bar served as a net source of ammonium and SRP to the stream water and as a net sink of nitrate in the system.

The gravel bar study was a unique opportunity to look at just the subsurface component of transient storage in a system and to examine the biogeochemical dynamics of a subsurface environment that had a high degree of connection to the surrounding surface water. Unlike a study of the hyporheic zone with overlying stream water present, the biogeochemical transformations observed could be attributed specifically to subsurface flow paths. Overall, this study shows that surface-subsurface interactions are important to the biogeochemistry of arctic stream ecosystems and that the subsurface

environment serves as an important site for the decomposition of organic matter and the regeneration of nutrients to the stream ecosystem.

LITERATURE CITED

Askew, E.F., and R. Smith (2005), Inorganic nonmetallic constituents, in *Standard Methods for the Examination of Water and Wastewater*, edited by A.D. Eaton, L.S. Clesceri, E.W. Rice and A.E. Greenberg, p. 123, Port City Press, Baltimore, Maryland.

Baird, R.B. (2005), Aggregate organic constituents, in *Standard Methods for the Examination of Water and Wastewater*, edited by A.D. Eaton, L.S. Clesceri, E.W. Rice and A.E. Greenberg, p. 23, Port City Press, Baltimore, Maryland.

Baker, M.A., C.N. Dahm, and H.M. Valett, (2000), Anoxia, anaerobic metabolism, and biogeochemistry of the stream-water-ground-water interface, in *Streams and Groundwaters*, edited by J.B. Jones, and P.J. Mulholland, p. 259, Academic Press, San Diego, California.

Baxter, C., F.R. Hauer, and W.W. Woessner (2003), Measuring groundwater-stream water exchange: New techniques for installing minipiezometers and estimating hydraulic conductivity, *Transactions of the American Fisheries Society*, *132*, 493-502.

Butturini, A., T.J. Battin, and F. Sabater (2000), Nitrification in stream sediment biofilms: The role of ammonium concentration and DOC quality, *Water Research, 34,* 629-639.

Gooseff, M.N., S.M. Wondzell, R. Haggerty, and J. Anderson (2003), Comparing transient storage modeling and residence time distribution (RTD) analysis in geomorphically varied reaches in the Lookout Creek Basin, Oregon, USA, *Advances in Water Resources*, *26*, 925-937.

Goovaerts, P. (1999), Geostatistics in soil science: state-of-the-art and perspectives, *Geoderma*, *89*, 1-45.

Hach Company (1997), Method 8048: Orthophosphate by colorimetry, in The 1997 Edition of the Hach Water Analysis Handbook, Retrieved 18 April 2007 from National Environmental Methods Index, [http://www.nemi.gov].

Haggerty R., S.M. Wondzell, and M.A. Johnson (2002), Power-law residence time distribution in the hyporheic zone of a 2nd order mountain stream, *Geophysical Research Letters*, *29*(13), doi:10.1029/2002GL014743.

Holmes, R.M., A. Aminot, R. Kérouel, B.A. Hooker, and B.J. Peterson (1999), A simple and precise method for measuring ammonium in marine and freshwater ecosystems, *Canadian Journal of Fisheries and Aquatic Sciences*, *56*, 1801-1808.

Isaaks, E.H., and R.M. Srivastava (1989), *An introduction of applied geostatistics*, Oxford University Press, New York, New York.

Journel, A. G., and C. Huijbregts (1978), *Mining Geostatistics*, Academic Press, New York, NY.

Sheibley, R.W., J.H. Duff, A.P. Jackman, and F.J. Triska (2003), Inorganic nitrogen transformations in the bed of the Shingobee River, Minnesota, USA: Integrating hydrologic and biological processes using sediment perfusion cores, *Limnology and Oceanography*, *48*, 1129-1140.

Stumm, W., and J.J. Morgan (1996), *Aquatic chemistry: Chemical equilibria and rates in natural waters*, John Wiley & Sons, Inc., New York, New York.

Wondzell, S.M., and F.J. Swanson (1996), Seasonal and storm dynamics of the hyporheic zone of a 4th-order mountain stream. II: Nitrogen cycling, *Journal of the North American Benthological Society*, *15*, 20-34.

Table 3.1. Location of each of the mini-piezometers installed in the gravel bar. The letter in the mini-piezometer identification indicates its position on the bar and the number indicates its subsurface depth layer.

Minipiezometer ID	Distance from head of gravel bar (m)	Depth beneath gravel bar surface (m)
a1	4	0.4
a2	4	0.9
b2	8	0.8
b3	8	1.3
d2	14	1.1
e2	19	0.8
e3	19	1.3
f1	18	0.7
f2	18	1.0
f3	18	1.3
g1	21	0.7
g2	21	1.0
g3	21	1.3
i1	9	0.7
i2	9	1.0
i3	9	1.3
j1	14	0.8
j2	14	1.1
k1	11	0.8
k2	11	1.1
k3	11	1.4
l1	14	0.3
m1	3	0.4
n1	20	0.4
o1	5	0.7
p1	18	0.8
p2	18	1.1
p3	18	1.4

Table 3.2. Variogram model parameters (nugget, sill and range) for each of the linear models created for the RWT concentrations at four separate time periods and the biogeochemical concentrations.

	Nugget	Sill	Range
$RWT_{0.45\ h}$	0	1000	23
$RWT_{0.75\ h}$	300	1000	15
$RWT_{2.63\ h}$	1200	1400	20
$RWT_{4.45\ h}$	500	650	20
DO	9	12	20
NO_3	1	2.5	20
NH_4	75	250	20
SRP	0.01	0.07	20
DOC	10000	28000	20

Table 3.3. Linear regression results for dissolved oxygen, nitrate, ammonium, soluble reactive phosphorus and dissolved organic carbon against RWT concentration at SIE Plateau (2.63-hour mark). R-squared values, linear equations and p-values are given for each parameter.

Linear Equation	R-sq	p-value
$[DO] = 1.22 + 0.0907 * [RWT]$	0.95	<0.001
$[NO_3] = 1.79 - 0.0106 * [RWT]$	0.07	0.158
$[NH_4] = 27.4 - 0.310 * [RWT]$	0.65	<0.001
$[SRP] = 0.453 - 0.0045 * [RWT]$	0.58	<0.001
$[DOC] = 673 - 2.29 * [RWT]$	0.33	0.001

Table 3.4. Estimated net NO_3, NH_4 and SRP regeneration rates for the gravel bar.

Nutrient	Estimated Net Regeneration Rate ($\mu M\ m^{-1}\ d^{-1}$)
NO_3	-0.99
NH_4	18.01
SRP	0.37

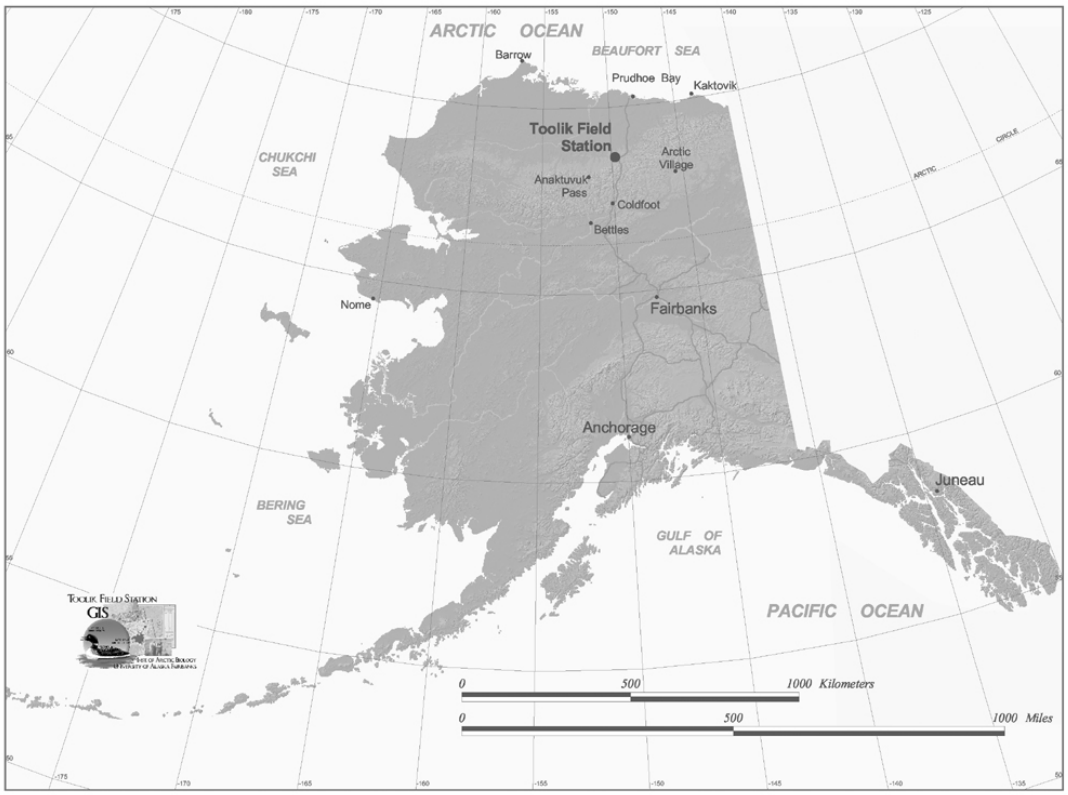

Figure 3.1. Location of the Toolik Field Station on the North Slope of Alaska's Brooks Range. Credit: A. Balser (2004)

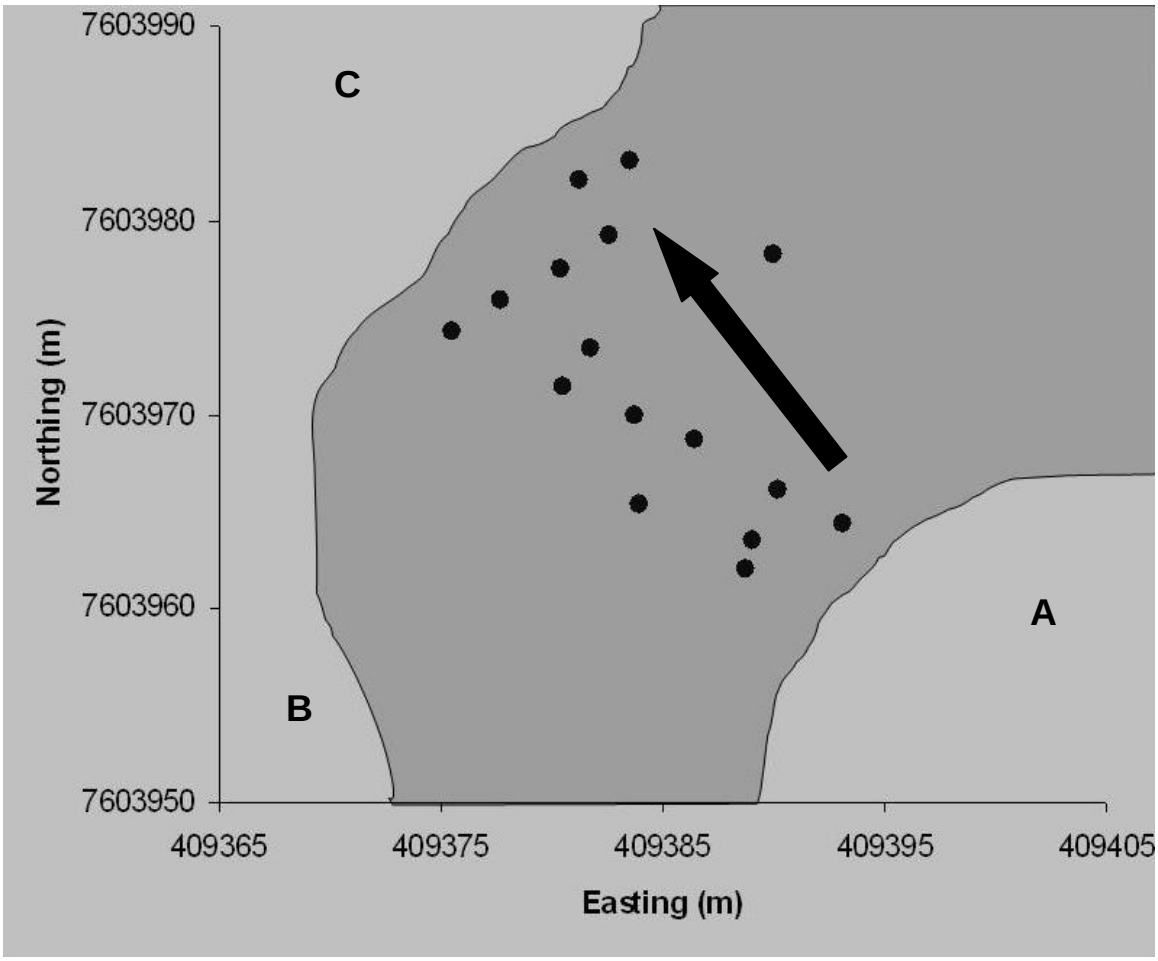

Figure 3.2. A representation of the gravel bar (shown in dark grey) with all subsurface sampling locations marked to scale (as solid black dots). Arrow indicates general direction of subsurface flow through the bar. Note that channels A (peat) and B (alluvial) used to come together to form channel C, but channel A has been truncated by the deposit of the gravel so that all of its flow became subsurface when it reached the gravel bar.

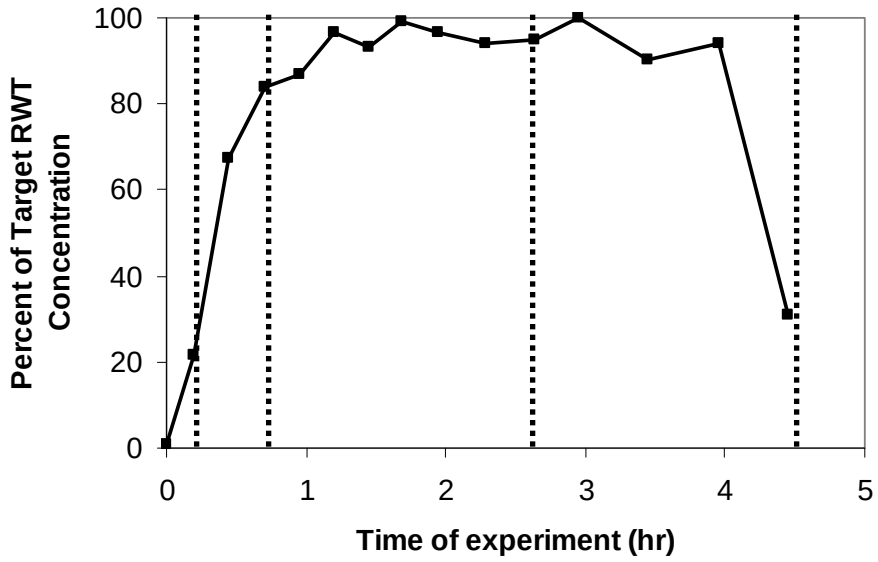

Figure 3.3. Example of a tracer breakthrough curve from the gravel bar SIE. Tracer dripper was started at 0 h and stopped at 4 h. Dotted lines indicate the four time periods for which variograms were constructed and [RWT] estimates were made.

A.

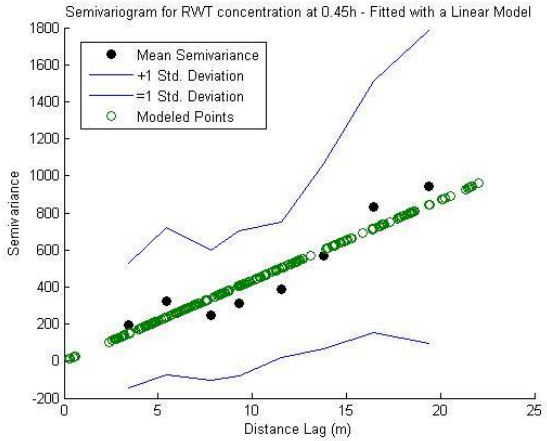

B.

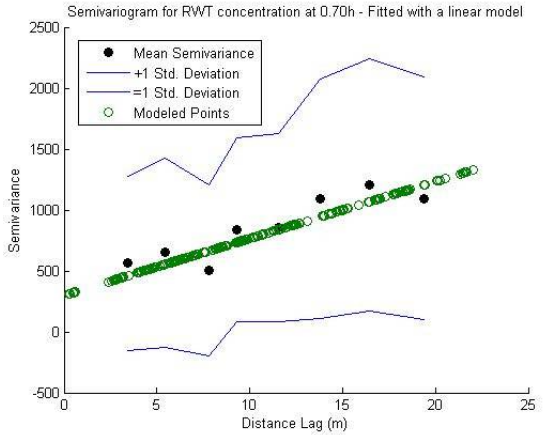

C.

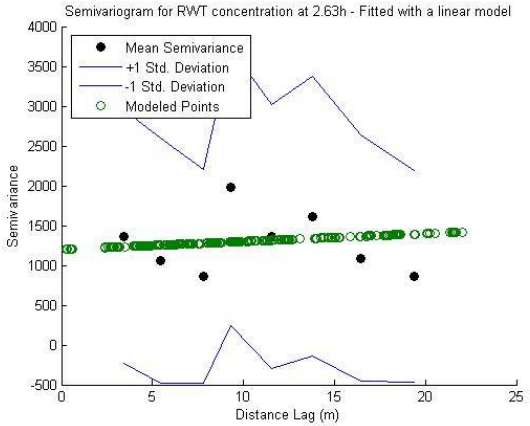

D.

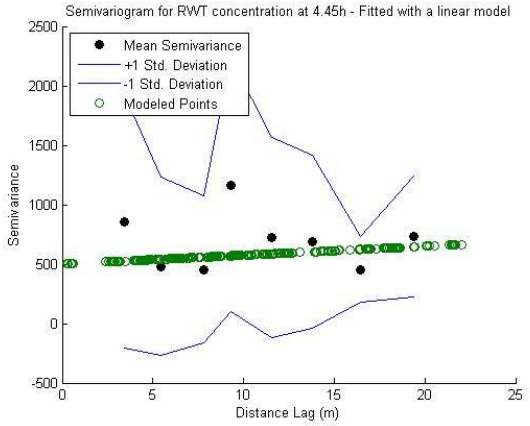

Figure 3.4. Variograms developed for the four SIE time points chosen (A-D). Solid dots represent the mean semivariance for mean lag distances. Open dots represent the model chosen to fit the data. Solid lines represent $\pm$ 1 standard deviation around the plotted means.

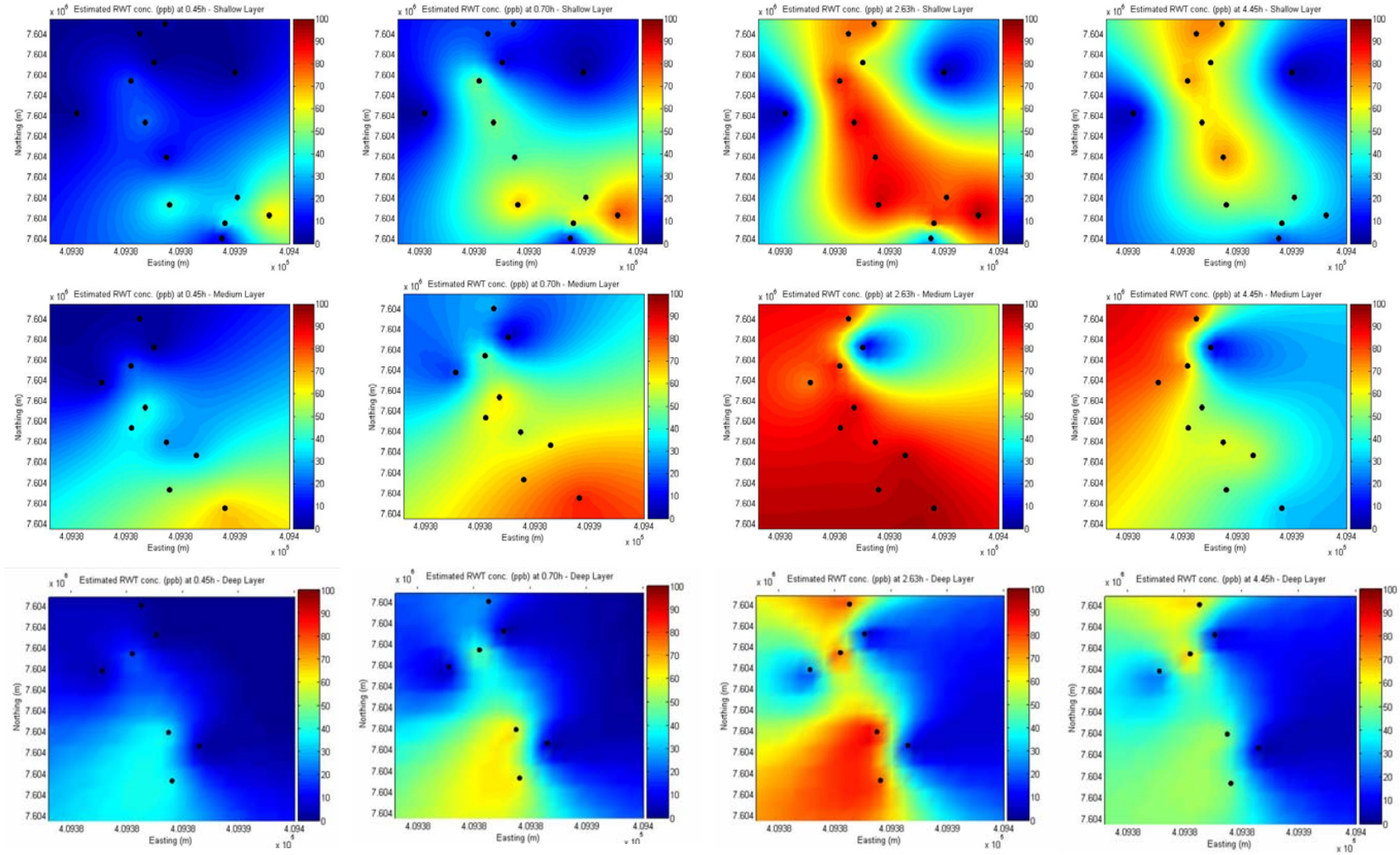

Figure 3.5. Estimated RWT concentrations over the gravel bar throughout the SIE. Plots from top to bottom show the concentrations in the shallow, medium and deep layers of the subsurface. Plots from left to right show the movement of RWT through the gravel bar at each of the four time points during the SIE. Black points represent sampling locations.

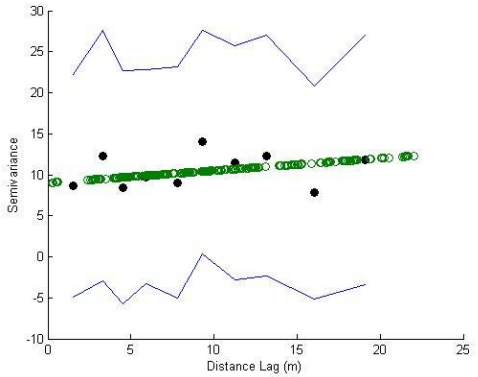

A. DO Variogram

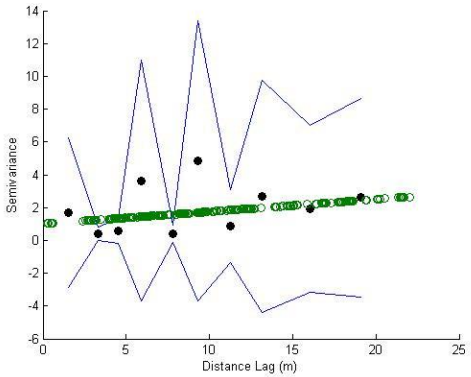

B. NO_3 Variogram

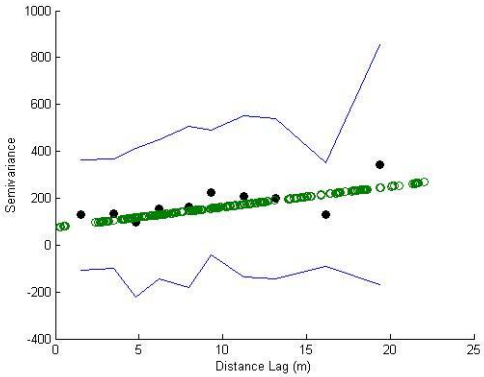

C. NH_4 Variogram

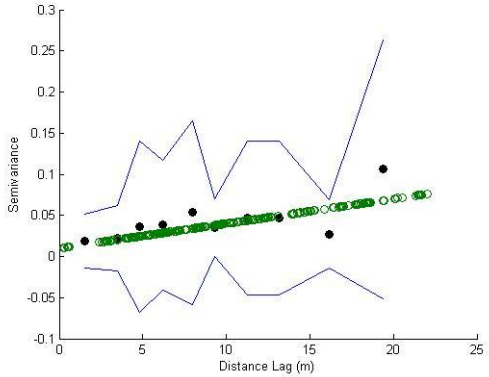

D. SRP Variogram

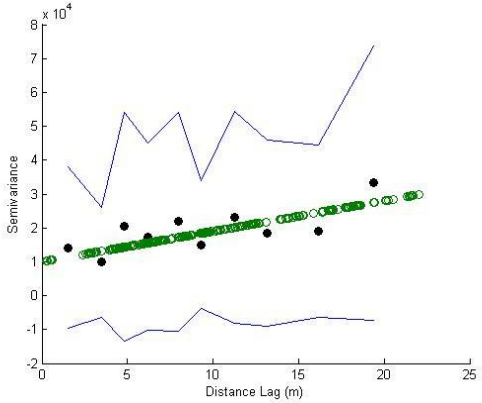

E. DOC Variogram

Figure 3.6. Variograms developed for each of the biogeochemical parameters (A-E). Solid dots represent mean lag distances and semivariances for binned data. Lines represent $\pm$ 1 standard deviation around the plotted means. Open circles represent the linear model chosen to fit the data.

A

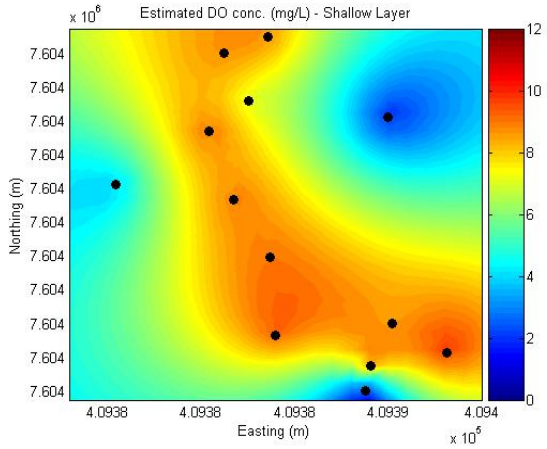

B

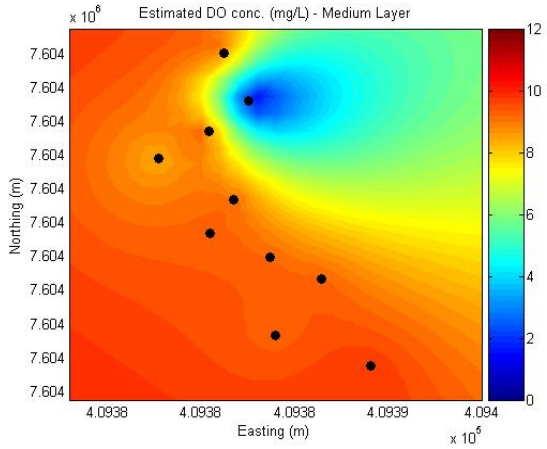

C

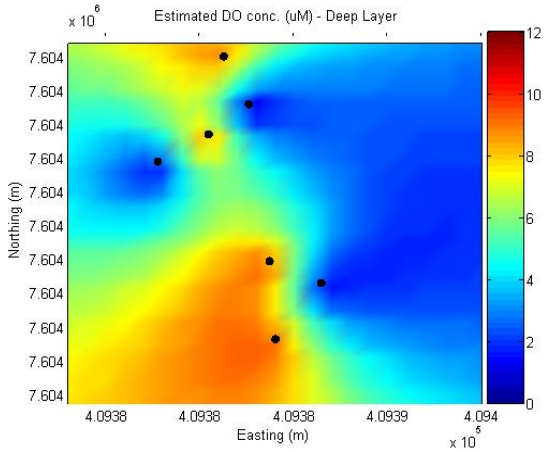

Figure 3.7. Estimated dissolved oxygen (DO) concentrations for the (A) shallow, (B) medium and (C) deep layers of the gravel bar subsurface. Black dots represent actual sampling locations for each layer.

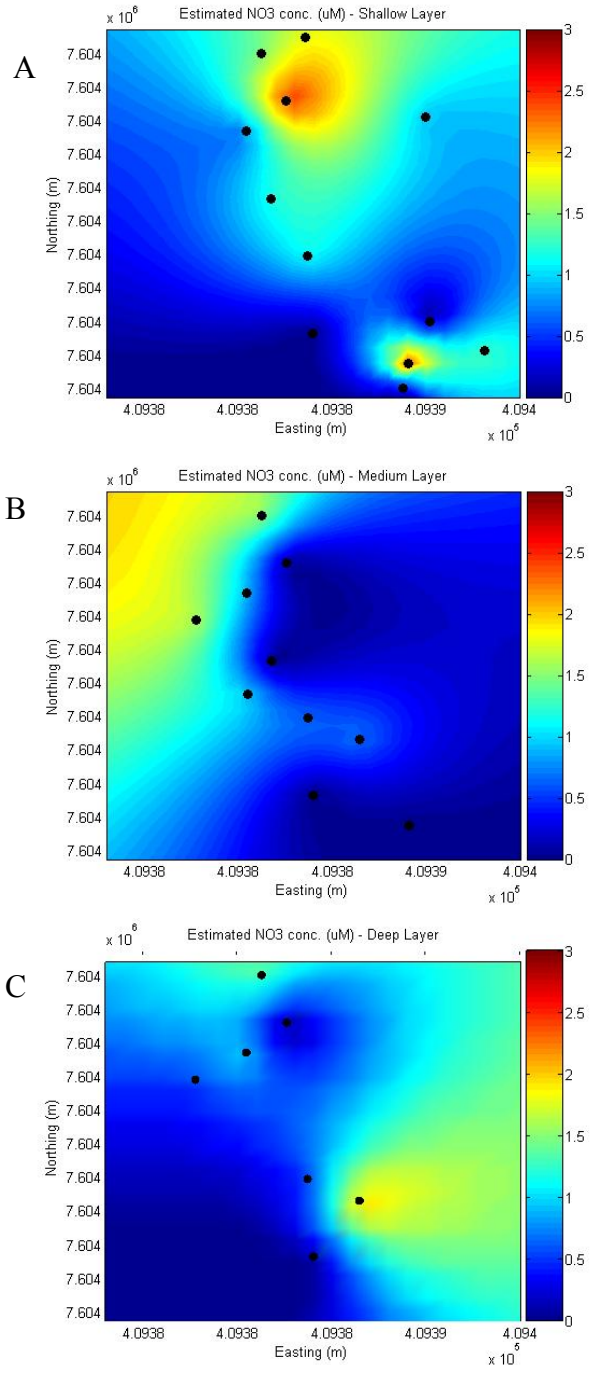

Figure 3.8. Estimated nitrate concentrations for the (A) shallow, (B) medium and (C) deep layers of the gravel bar subsurface. Black dots represent actual sampling locations for each layer.

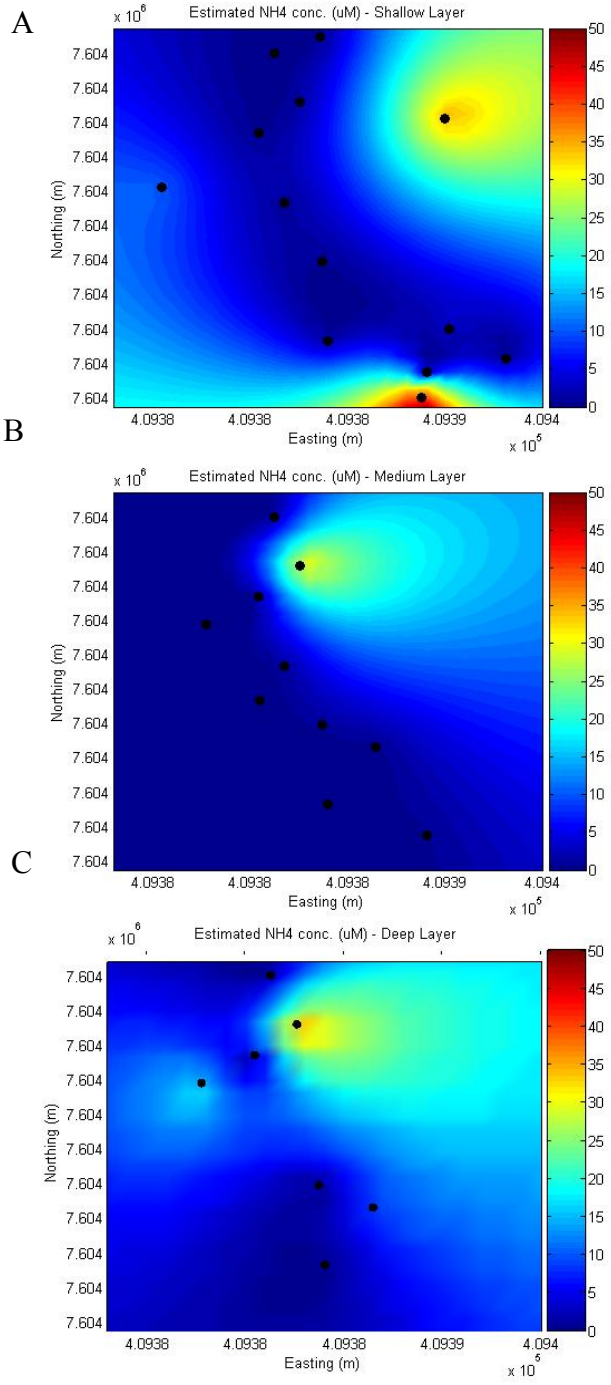

Figure 3.9. Estimated ammonium concentrations for the (A) shallow, (B) medium and (C) deep layers of the gravel bar subsurface. Black dots represent actual sampling locations for each layer.

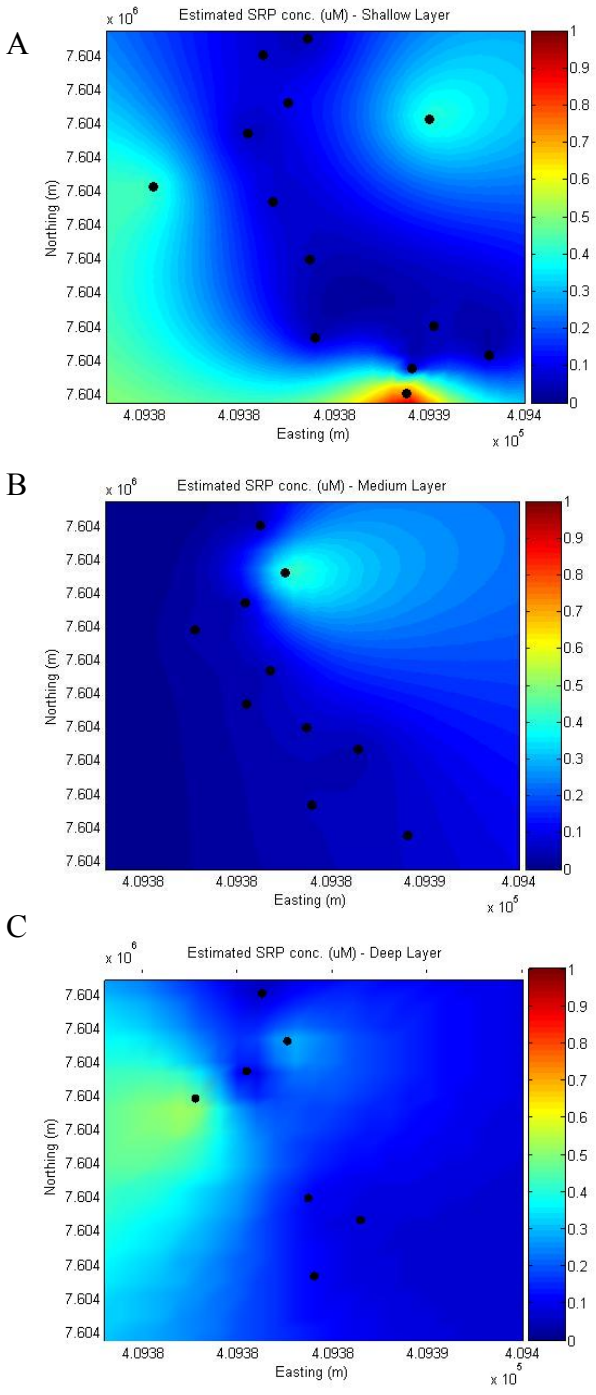

Figure 3.10. Estimated soluble reactive phosphorus concentrations for the (A) shallow, (B) medium and (C) deep layers of the gravel bar subsurface. Black dots represent actual sampling locations for each layer.

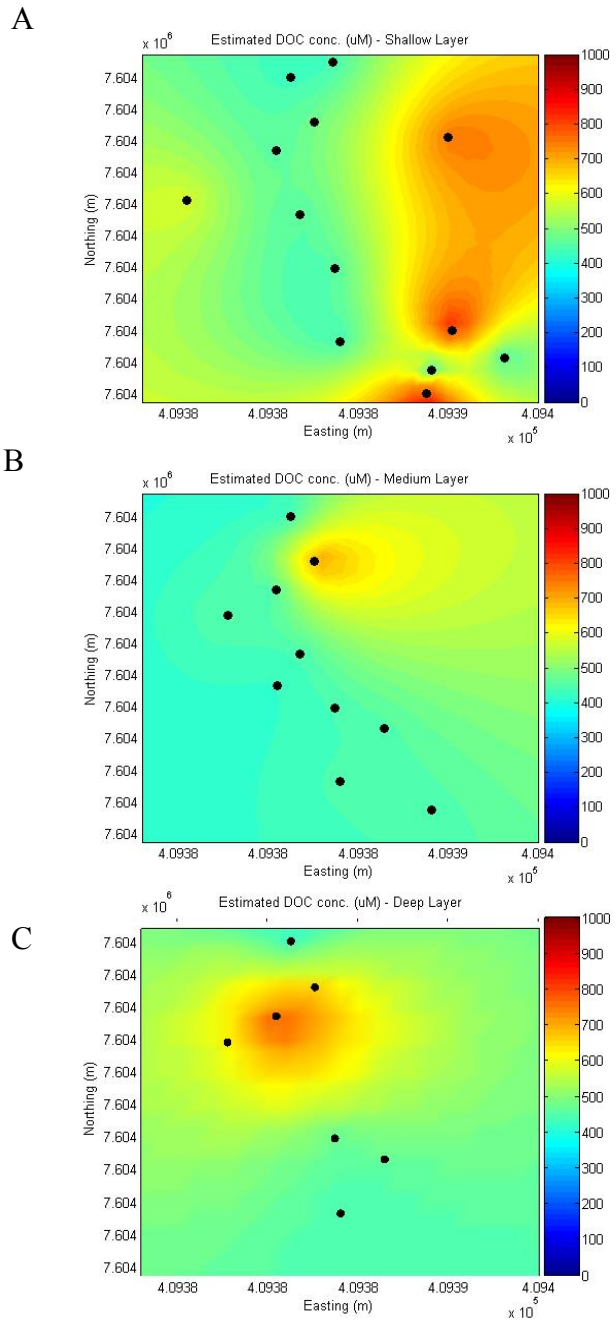

Figure 3.11. Estimated dissolved organic carbon (DOC) concentrations for the (A) shallow, (B) medium and (C) deep layers of the gravel bar subsurface. Black dots represent actual sampling locations for each layer.

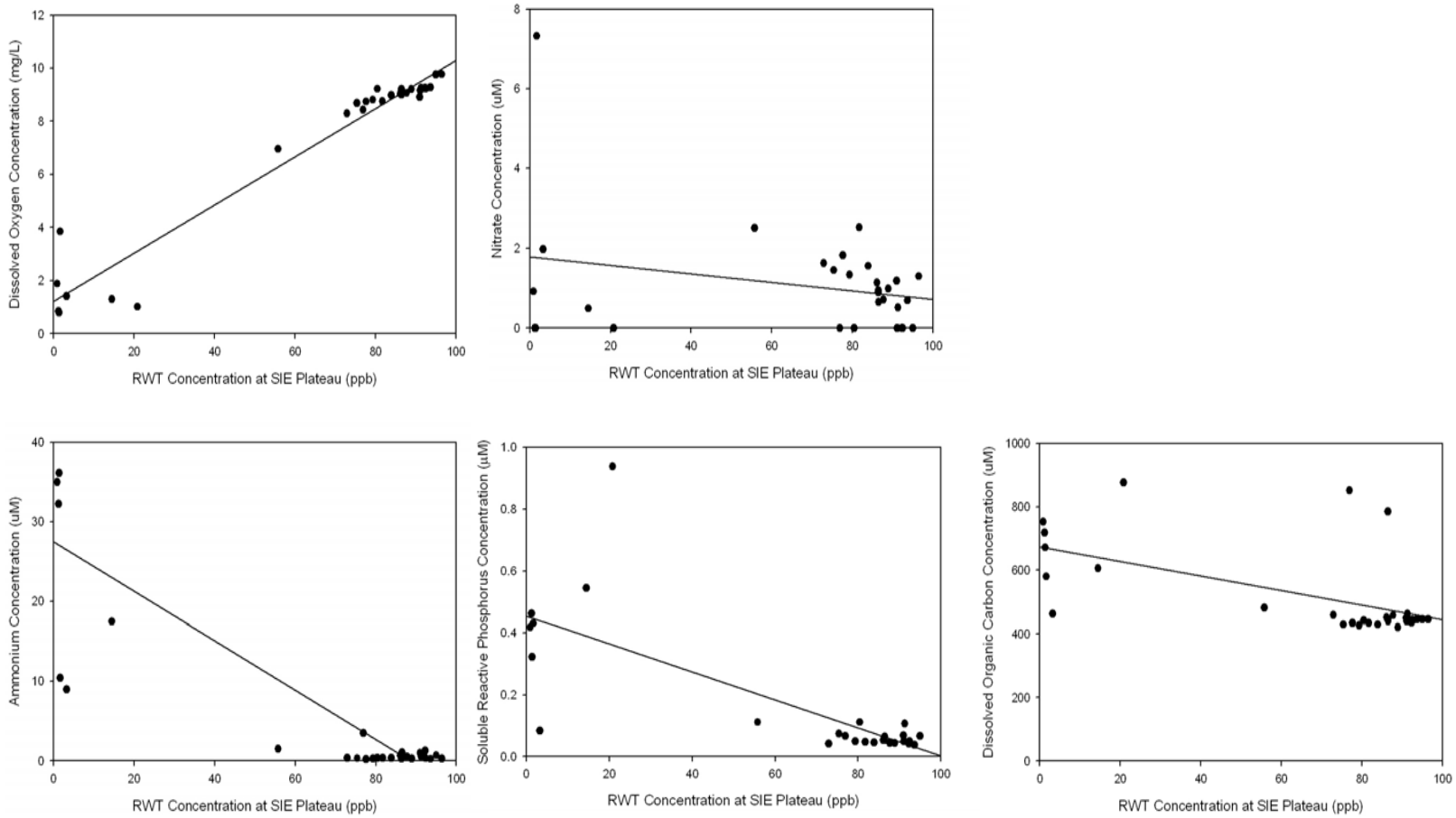

Figure 3.12. Linear regressions for (A) dissolved oxygen, (B) nitrate, (C) ammonium, (D) soluble reactive phosphorus and (E) dissolved organic carbon against RWT concentration at SIE Plateau (2.63-hour mark).

COMPREHENSIVE LITERATURE CITED

Askew, E.F., and R. Smith (2005), Inorganic nonmetallic constituents, in *Standard Methods for the Examination of Water and Wastewater*, edited by A.D. Eaton, L.S. Clesceri, E.W. Rice and A.E. Greenberg, p. 123, Port City Press, Baltimore, Maryland.

Baird, R.B. (2005), Aggregate organic constituents, in *Standard Methods for the Examination of Water and Wastewater*, edited by A.D. Eaton, L.S. Clesceri, E.W. Rice and A.E. Greenberg, p. 23, Port City Press, Baltimore, Maryland.

Baker, M.A., C.N. Dahm, and H.M. Valett, (2000), Anoxia, anaerobic metabolism, and biogeochemistry of the stream-water-ground-water interface, in *Streams and Groundwaters*, edited by J.B. Jones, and P.J. Mulholland, p. 259, Academic Press, San Diego, California.

Battin, T.J., L.A. Kaplan, J.D. Newbold, and C.M.E. Hansen (2003), Contributions of microbial biofilms to ecosystem processes in stream mesocosms, *Nature*, *426*, 439-442.

Baxter, C., F.R. Hauer, and W.W. Woessner (2003), Measuring groundwater-stream water exchange: New techniques for installing minipiezometers and estimating hydraulic conductivity, *Transactions of the American Fisheries Society*, *132*, 493-502.

Bencala, K.E., and R.A. Walters (1983), Simulation of solute transport in a mountain pool-and-riffle stream: A transient storage model, *Water Resources Research*, *19*, 718-724.

Bernhardt, E.M., R.O. Hall, and G.E. Likens (2002), Whole-system estimates of nitrification and nitrate uptake in streams of the Hubbard Brook Experimental Forest, *Ecosystems*, *5*, 419-430.

Boulton, A.J., S. Findlay, P. Marmonier, E.H. Stanley, and H.M. Valett, (1998), The functional significance of the hyporheic zone in streams and rivers, *Annual Review of Ecology and Systematics*, *29*, 59-81.

Bradford, J.H., J.P. McNamara, W.B. Bowden, and M.N. Gooseff (2005), Measuring thaw depth beneath peat-lined arctic streams using ground-penetrating radar, *Hydrological Processes*, *19*, 2689-2699.

Brosten, T.R., J.H. Bradford, J.P. McNamara, J.P. Zarnetske, M.N. Gooseff, and W.B. Bowden (2006), Profiles of temporal thaw depths beneath two arctic stream types using ground-penetrating radar, *Permafrost and Periglacial Processes*, *17*, 341-355.

Bunnell, F.L., S.F. Maclean, Jr., and J. Brown (1975), Barrow, Alaska, USA., in *Structure and function of tundra ecosystems, Ecol. Bull., 20, 73-124,* edited by T. Rosswall, and O.W. Heal, Stockholm: Swedish Natural Science Research Council.

Butturini, A., T.J. Battin, and F. Sabater (2000), Nitrification in stream sediment biofilms: The role of ammonium concentration and DOC quality, *Water Research, 34,* 629-639.

Callaghan, T.V. (2005), Arctic tundra and polar desert ecosystems, in *Arctic Climate Impact Assessment*, Cambridge University Press, New York, New York.

Carlyle, G.C., and A.R. Hill (2001), Groundwater phosphate dynamics in a river riparian zone: Effects of hydrologic flowpaths, lithology and redox chemistry, *Journal of Hydrology*, *247*, 151-168.

Choi, J., J.W. Harvey, and M.H.Conklin (2000), Characterizing multiple timescales of stream and storage zone interaction that affect solute fate and transport in streams, *Water Resources Research*, *36*, 1511-1518.

Craig, P.C., and P.J. McCart (1975), Classification of stream types in Beaufort Sea drainages between Prudhoe Bay, Alaska, and the Mackenzie Delta, N.W.T., Canada, *Arctic and Alpine Research*, *7*, 183-198.

Cushing, C.E., and J.D. Allan (2001), *Streams: Their ecology and life*, Academic Press, San Diego, California.

D'Angelo, D.J., J.R. Webster, S.V. Gregory, and J.L. Meyer (1993), Transient storage in Appalachian and Cascade mountain streams as related to hydraulic characteristics, *Journal of the North American Benthological Society*, *12*, 223-235.

De Wiest, R.J.M. (1969), *Flow through porous media*, Academic Press, New York, New York.

Dent, C.L., J.D Schade, N.B. Grimm, and S.G. Fisher (2000), *Subsurface influences on surface biology*, in *Streams and Groundwaters*, edited by J.B. Jones, and P.J. Mulholland, p. 381, Academic Press, San Diego, California.

Dent, C.L., N.B. Grimm, and S.G. Fisher (2001), Multiscale effects of surface-subsurface exchange on stream nutrient concentrations, *Journal of the North American Benthological Society, 20,* 162-181.

Duff, J.H., and F.J. Triska (2000), Nitrogen biogeochemistry and surface-subsurface exchange in streams, in *Streams and Groundwaters*, edited by J.B. Jones, and P.J. Mulholland, pp. 197-220, Academic Press, San Diego, California.

Edwardson, K.J., W.B. Bowden, C. Dahm, and J. Morrice (2003), The hydraulic characteristics and geochemistry of hyporheic and parafluvial zones in Arctic tundra streams, North Slope, Alaska, *Advances in Water Resources*, *26*, 907-923.

Fellows, C.S., H.M. Valett, and C.M. Dahm (2001), Whole-stream metabolism in two montane streams: Contribution of the hyporheic zone, *Limnology and Oceanography, 46*, 523-531.

Findlay, S., D. Strayer, C. Goumbala, and K. Gould (1993), Metabolism of streamwater dissolved organic carbon in the shallow hyporheic zone, *Limnology and Oceanography, 38*, 1493-1499.

Findlay, S. (1995) Importance of surface-subsurface exchange in stream ecosystems: The hyporheic zone, *Limnology and Oceanography*, *40*, 159-164.

Findlay, S., and W.V. Sobczak (2000), Microbial communities in hyporheic sediments, in *Streams and Groundwaters*, edited by J.B. Jones, and P.J. Mulholland, p. 287, Academic Press, San Diego, California.

Gooseff, M.N., S.M. Wondzell, R. Haggerty, and J. Anderson (2003), Comparing transient storage modeling and residence time distribution (RTD) analysis in geomorphically varied reaches in the Lookout Creek Basin, Oregon, USA, *Advances in Water Resources*, *26*, 925-937.

Gooseff, M.N., R.O. Hall, and J.L. Tank (2007), Relating transient storage to channel complexity streams of varying land use in Jackson Hole, Wyoming, *Water Resources Research*, *43*, W01417, doi:10.1029/2005WR004626.

Goovaerts, P. (1999), Geostatistics in soil science: state-of-the-art and perspectives, *Geoderma*, *89*, 1-45.

Grimm, N.B., and S.G. Fisher (1984), Exchange between interstitial and surface water: Implications for stream metabolism and nutrient cycling, *Hydrobiologia*, *111*, 219-228.

Gücker, B., and I.G. Boëchat (2004), Stream morphology controls ammonium retention in tropical headwaters, *Ecology*, *85*, 2818-2827.

Hach Company (1997), Method 8048: Orthophosphate by colorimetry, in The 1997 Edition of the Hach Water Analysis Handbook, Retrieved 18 April 2007 from National Environmental Methods Index, [http://www.nemi.gov].

Haggerty, R., S.A. McKenna, and L.C. Miegs 2000, On the late-time behavior of tracer test breakthrough curves, *Water Resources Research*, *36*, 3467-3479.

Haggerty R., S.M. Wondzell, and M.A. Johnson (2002), Power-law residence time distribution in the hyporheic zone of a 2nd order mountain stream, *Geophysical Research Letters*, *29*(13), doi:10.1029/2002GL014743.

Harvey, J.W., and K.E. Bencala (1993), The effect of streambed topography on surface-subsurface exchange in mountain catchments, *Water Resources Research*, *29*, 89-98.

Harvey, J.W., B.J. Wagner, and K.E. Bencala (1996), Evaluating the reliability of the stream tracer approach to characterize stream-subsurface water exchange, *Water Resources Research, 32*, 2441-2451.

Harvey, J.W., and B.J. Wagner (2000), Quantifying hydrologic interactions between streams and their subsurface hyporheic zones, in *Streams and Groundwaters*, edited by J.B. Jones, and P.J. Mulholland, p. 41, Academic Press, San Diego, California.

Harvey, J.W., M.H. Conklin, and R.S. Koelsch (2003), Predicting changes in hydrologic retention in an evolving semi-arid alluvial stream, *Advances in Water Resources*, *26*, 939-950.

Hendricks, S.P., and D.S. White (2000), Stream and groundwater influences on phosphorus biogeochemistry, in *Streams and Groundwaters*, edited by J.B. Jones, and P.J. Mulholland, p. 221, Academic Press, San Diego, California.

Henry, K.S., H.M. Valett, J.A. Morrice, C.N. Dahm, G.J. Wroblicky, M.A. Santistevan, and M.E. Campana (1994), Ground water – surface water exchange in two headwater streams, in *Proceedings of the Second International Conference on Groundwater Ecology*, *AWRA*, pp 319-328.

Hinzman, L.D., D.L. Kane, R.E. Gieck, and K.R. Everett (1991), Hydrologic and thermal properties of the active layer in the Alaskan Arctic, *Cold Regions Science and Technology, 19*, 95-110.

Hobbie, J.E., B.J. Peterson, N. Bettez, L. Deegan, W.J. O'Brien, G.W. Kling, G.W. Kipphut, W.B. Bowden, and A.E. Hershey (1999), Impact of global change on the biogeochemistry and ecology of an Arctic freshwater system, *Polar Research*, *18*, 207-214.

Holmes, R.M., S.G. Fisher, N.B. Grimm, and B.J. Harper (1998), The impact of flash floods on microbial distribution and biogeochemistry in the parafluvial zone of a desert stream, *Freshwater Biology*, *40*, 641-654.

Holmes, R.M., A. Aminot, R. Kérouel, B.A. Hooker, and B.J. Peterson (1999), A simple and precise method for measuring ammonium in marine and freshwater ecosystems, *Canadian Journal of Fisheries and Aquatic Sciences*, *56*, 1801-1808.

Huryn, A.D., K.A. Slavik, R.L. Lowe, S.M. Parker, D.S. Anderson, and B.J. Peterson (2005), Landscape heterogeneity and the biodiversity of Arctic stream communities: a habitat template analysis, *Canadian Journal of Fisheries and Aquatic Sciences, 62*, 1905-1919.

Isaaks, E.H., and R.M. Srivastava (1989), *An introduction of applied geostatistics*, Oxford University Press, New York, New York.

Jones, J.B., S.G. Fisher, and N.B. Grimm (1995a), Nitrification in the hyporheic zone of a desert stream ecosystem, *Journal of the North American Benthological Society*, *14*, 249-258.

Jones, J.B., S.G. Fisher, and N.B. Grimm (1995b), Vertical hydrologic exchange and ecosystem metabolism in a Sonoran Desert stream, *Ecology*, *76*, 942-952.

Jones, J.B. (1995), Factors controlling hyporheic respiration in a desert stream, *Freshwater Biology*, *34*, 91-99.

Jones, J.B., and R.M. Holmes (1996), Surface-subsurface interactions in stream ecosystems, *Trends in Ecology and Evolution*, *11*, 239-242.

Journel, A. G., and C. Huijbregts (1978), *Mining Geostatistics*, Academic Press, New York, NY.

Kasahara, T., and S.M. Wondzell (2003), Geomorphic controls on hyporheic exchange flow in mountain streams, *Water Resources Research*, *39*(1), 1005, doi:10.1029/2002WR001386.

Kling, G.W., G.W. Kipphut, M.M. Miller, and W.J. O'Brien (2000), Integration of lakes and streams in a landscape perspective: the importance of material processing on spatial patterns and temporal coherence, *Freshwater Biology*, *43*, 477-497.

Martin, L.A., P.J. Mulholland, J.R. Webster, and H.M. Valett (2001), Denitrification potential in sediments of headwater streams in the southern Appalachian Mountains, USA, *Journal of the North American Benthological Society*, *20*, 505-519.

McBean, G. (2005), Arctic climate: Past and present, in *Arctic Climate Impact Assessment*, Cambridge University Press, New York, New York.

McKnight, D.M., D.K. Niyogi, A.S. Alger, A. Bomblies, P.A. Conovitz, and C.M. Tate (1999), Dry valley streams in Antarctica: Ecosystems waiting for water, *Bioscience*, *49*, 985-995.

McNamara, J.P., D.L. Kane, and L.D. Hinzman (1998), An analysis of stream flow hydrology in an Arctic drainage basin: a nested watershed approach, *Journal of Hydrology*, *206*, 39-57.

Morrice, J.A., H.M. Valett, C.N. Dahm, and M.E. Campana (1997), Alluvial characteristics, groundwater-surface water exchange and hydrological retention in headwater streams, *Hydrological Processes*, *11*, 253-267.

Mulholland, P.J., E.R. Marzoff, J.R. Webster, D.R. Hart, and S.P. Hendricks (1997), Evidence that hyporheic zones increase heterotrophic metabolism and phosphorus uptake in forest streams, *Limnology and Oceanography*, *42*, 443-451.

Naegeli, W.M., and U. Uehlinger (1997), Contribution of the hyporheic zone to ecosystem metabolism in a prealpine gravel-bed river, *Journal of the North American Benthological Society*, *16*, 794-804.

Packman, A.I. and K.E. Bencala (2000), Modeling surface-subsuface hydrological interactions, in *Streams and Groundwaters*, edited by J.B. Jones, and P.J. Mulholland, p. 45, Academic Press, San Diego, California.

Pepin, D.M., and F.R. Hauer., (2002), Benthic responses to groundwater-surface water exchange in 2 alluvial rivers in northwestern Montana, *Journal of the North American Benthological Society, 21*, 370-383.

Peterson, B.J., W.M. Wollheim, P.J. Mulholland, J.R. Webster, J.L. Meyer, J.L. Tank, E. Marti, W.B. Bowden, H.M. Valett, A.E. Hershey, W.H. McDowell, W.K. Dodds, S.K. Hamilton, S. Gregory, and D.D. Morrall (2001), Control of nitrogen export from watersheds by headwater streams, *Science*, *292*, 86-90.

Rouse, W.R., M.S.V. Douglas, R.E. Hecky, A.E. Hershey, G.W. Kling, L. Lesack, P. Marsh, M. McDonald, B.J. Nicholson, N.T. Roulet, and J.P. Smol (1997), Effects of climate change on the freshwaters of Arctic and Subarctic North America, *Hydrological Processes*, *11*, 873-902.

Runkel, R.L. (1998), One-dimensional transport with inflow and storage (OTIS) - A solute transport model for streams and rivers, in U.S. *Geological Survey Water-Resources Investigations Report 98–4018*, 73 pp.

Runkel, R.L. (2000), Using OTIS to model solute transport in streams and rivers, in *U.S. Geological Survey Fact Sheet FS-138-99*. 4 pp.

Schlesinger, W.H. (1997), *Biogeochemistry: An analysis of global change*, Academic Press, San Diego, California.

Sheibley, R.W., J.H. Duff, A.P. Jackman, and F.J. Triska (2003), Inorganic nitrogen transformations in the bed of the Shingobee River, Minnesota, USA: Integrating hydrologic and biological processes using sediment perfusion cores, *Limnology and Oceanography*, *48*, 1129-1140.

Sterner, R.W., and J.J. Elser (2002), *Ecological Stoichiometry: The biology of elements from molecules to the biosphere*, Princeton University Press, New Jersey.

Storey, R.G., K.W.F. Howard, and D.D. Williams (2003), Factors controlling riffle-scale exchange flows and their seasonal changes in a gaining stream: A three-dimensional groundwater flow model, *Water Resources Research*, *39*(2), 1034, doi:10.1029/2002WR001367.

Strauss, E.A., and G.A. Lamberti (2000), Regulation of nitrification in aquatic sediments by organic carbon, *Limnology and Oceanography*, *45*, 1854-1859.

Stream Solute Workshop (1990), Concepts and methods for assessing solute dynamics in stream ecosystems, *Journal of the North American Benthological Society*, *9*, 95-119.

Stumm, W., and J.J. Morgan (1996), *Aquatic chemistry: Chemical equilibria and rates in natural waters*, John Wiley & Sons, Inc., New York, New York.

Triska, F.T., V.C Kennedy, R.J. Avanzino, G.W. Zellweger, and K.E. Bencala (1989), Retention and transport of nutrients in a third-order stream in northwestern California: Hyporheic processes, *Ecology*, *70*, 1893-1905.

Valett, H.M., S.G. Fisher, and E.H. Stanley (1990), Physical and chemical characteristics of the hyporheic zone of a Sonoran Desert stream, *Journal of the North American Benthological Society*, *9*, 210-215.

Valett, H.M., S.G. Fisher, N.B. Grimm, and P. Camill (1994), Vertical hydrologic exchange and ecological stability of a desert stream ecosystem, *Ecology*, *75*, 548-560.

Valett, H.M., J.A. Morrice, C.N. Dahm, and M.E. Campana (1996), Parent lithology, surface-groundwater exchange, and nitrate retention in headwater streams, *Limnology and Oceanography, 41*, 333-345.

Verhagen, F.J.M., and H.J. Laanbroek (1991), Competition for ammonium between nitrifying and heterotrophic bacteria in dual energy-limited chemostats, *Applied and Environmental Microbiology*, *57*, 3255-3263.

Walsh, J.E. (2005), Cryosphere and hydrology, in *Arctic Climate Impact Assessment,* Cambridge University Press, New York, New York.

Wondzell, S.M., and F.J. Swanson (1996), Seasonal and storm dynamics of the hyporheic zone of a 4th-order mountain stream. II: Nitrogen cycling, *Journal of the North American Benthological Society*, *15*, 20-34.

Wroblicky, J.R., M.E. Campana, H.M. Valett, and C.M. Dahm (1998), Seasonal variation in surface-subsurface water exchange and lateral hyporheic area of two stream-aquifer systems, *Water Resources Research*, *34*, 317-328.

Wrona, F.J., T.D. Prowse, and J.D. Reist (2005), Freshwater ecosystems and fisheries, in *Arctic Climate Impact Assessment*, Cambridge University Press, New York, New York.

Zarnetske, J. P. (2006), Headwater hyporheic zones in a warming arctic climate: An assessment of hyporheic dynamics across distinct geomorphic and permafrost conditions, M.S. Thesis, Utah State University, Logan, Utah.